

THESIS ON NATURAL AND EXACT SCIENCES B138

**Validation of critical factors for the
quantitative characterization of
bacterial physiology in accelerostat
cultures**

RANNO NAHKU

TUT
PRESS

TALLINN UNIVERSITY OF TECHNOLOGY

Faculty of Science
Department of Chemistry

**This dissertation was accepted for the defense of the degree of Doctor of
Philosophy (Chemistry) on June 13th, 2012.**

- Supervisor:** Senior Scientist Kaarel Adamberg,
Department of Food Processing,
Tallinn University of Technology (TUT)
- Co-supervisor:** Professor Raivo Vilu,
Department of Chemistry,
Tallinn University of Technology (TUT)
- Opponents:** Professor Emeritus Sven-Olof Enfors,
School of Biotechnology,
Royal Institute of Technology, Sweden
- Professor Uldis Kalnenieks,
Institute of Microbiology and Biotechnology,
University of Latvia, Latvia

Defense of the thesis: November 7th, 2012

DECLARATION: I hereby declare that this doctoral thesis, submitted for the doctoral degree at TUT, is my original investigation and achievement and has not been submitted for the defense of any academic degree elsewhere.

Ranno Nahku

COPYRIGHT: Ranno Nahku, 2012. Licensed under the Creative Commons Attribution-NonCommercial-NoDerivs 3.0 Unported License.

COLOPHON: This thesis was typeset with L^AT_EX 2_ε using André Miede's *classicthesis* style with modifications by Ardo Illaste and David W. Schryer to conform with TUT style guidelines. The main font is Libertine. ZapfChancery is used for Latin text. Biolinum is used for *sans serif* text.

ISSN 1406-4723
ISBN 978-9949-23-371-7 (publication)
ISBN 978-9949-23-372-4 (PDF)



LOODUS - JA TÄPPISTEADUSED B138

**Kriitiliste faktorite valideerimine
bakterite füsioloogia uurimiseks
akselerostaatsetes
kultiveerimiseksperimentides**

RANNO NAHKU

TTÜ
KIRJASTUS

CONTENTS

ABSTRACT – KOKKUVÕTE	vii
LIST OF PUBLICATIONS	x
LIST OF CONFERENCE PRESENTATIONS	xi
ACKNOWLEDGMENTS	xii
ACRONYMS	xiii
THESIS	17
1 INTRODUCTION	19
1.1 Continuous cultivation	19
1.1.1 Changestat cultivation	20
1.1.2 Choice of acceleration of dilution in A-stat cultivation	20
1.1.3 Comparing the cellular state in A-stat and chemostat experiments	22
1.1.4 Genome stability of <i>E. coli</i> in continuous culture	23
2 AIMS OF THIS DISSERTATION	27
3 MATERIALS AND METHODS	29
3.1 Strains used	29
3.2 Media and cultivation conditions	29
3.2.1 <i>E. coli</i> K-12	29
3.2.2 <i>Lactococcus lactis</i> subsp. <i>lactis</i> IL1403	29
3.3 Analytical methods	30
3.4 Gene expression profiling	30
3.5 Simulation of A-stat and chemostat data	30
3.6 Mutation analysis (Publication IV)	32
3.6.1 Genomic DNA extraction	32
3.6.2 Illumina whole genome re-sequencing	32
3.6.3 Genome sequence data analysis	32
3.6.4 Mutation validation with Sanger sequencing	33
4 RESULTS AND DISCUSSION	35
4.1 Experiments with <i>Escherichia coli</i> K-12	35
4.2 Experiments with <i>L. lactis</i>	38
4.3 Comparison of accelerostat with chemostat (Publication II and Publication III)	40
4.3.1 Comparison using <i>E. coli</i> K-12	40
4.3.2 Comparison using <i>L. lactis</i> Il1403	44

CONTENTS

4.4	Culture adaptation in change-stat cultures (Publication IV and Publication V)	46
4.4.1	Culture hysteresis in D-stat (Publication IV)	46
4.4.2	Investigation of possible evolution in A-stat culture (Publication V)	47
4.4.3	Mismatches in different stock cultures from <i>E. coli</i> K-12 MG1655 reference genome	47
4.4.4	Evolution did not take place during A-stat cultivation	49
4.4.5	Heterogeneity of stock culture	50
	SUMMARY	53
5	CONCLUSIONS	55
	BIBLIOGRAPHY	57
	CURRICULUM VITAE	64
	APPENDICES	69
	SUPPLEMENTAL TABLE S1	71
	PUBLICATION I	73
	PUBLICATION II	81
	PUBLICATION III	97
	PUBLICATION IV	111
	PUBLICATION V	123
	DISSERTATIONS DEFENDED AT TUT IN NATURAL AND EXACT SCIENCES	133

ABSTRACT

CONTINUOUS CULTIVATION METHODS maintain constant environmental conditions so that cells grow in a strictly defined physiological state at a desired specific growth rate (μ). Chemostat, accelerostat (A-stat), and dilution stat (D-stat) experiments provide quantitative steady state data useful for metabolic modeling. An A-stat experiment starts as a chemostat, but after reaching steady state, a steady change of dilution rate (D) is applied. D is changed slowly (0.01 h^{-2} - 0.005 h^{-2}), to allow cells to adapt to the changing conditions while maintaining a stable physiological state. This dissertation presents a critical assessment of A-stat and D-stat cultivation techniques and contains recommendations useful for all who practice continuous cultivation. We demonstrate the reproducibility of this cultivation technique in a series of glucose-limited A-stat experiments with *Escherichia coli* K-12 MG1655 (Publication I and Publication II). Similar glucose-limited experiments with *Lactococcus lactis* IL1403 (Publication III) show that A-stat data can be directly compared with a series of chemostat experiments over the same range of μ , including transcriptome and proteome data, along with rates and profiles of product formation and substrate utilization. However, choosing the rate of change of D (α_d) in A-stat experiments requires careful consideration. Smaller α_d values increase the residence time in the fermenter which makes it more difficult to remove fermentation products thus increasing the fermentation time. However, the rate of evolutionary adaptation places a limit on the length of time continuous cultivation (*e.g.*, A-stat) can be performed (Ferenci, 2008). For *E. coli* K-12 MG1655 we show that α_d should be around 0.01 h^{-2} to obtain a reliable comparison between the biomass and fermentation product yields, as well as transcriptome and proteome results. Chemostat experiments with *L. lactis* IL1403 at $\mu = 0.45 \text{ h}^{-1}$ compare well with A-stat experiments when $\alpha_d = 0.005 \text{ h}^{-2}$. The optimal choice of α_d is thus species dependent. We observed hysteresis in culture characteristics at the level of biomass yield, product yields and gene expression in a D-stat experiment with 60 generations of *L. lactis* (Publication IV), an effect likely caused by the evolution of mutant strains. To test how long genetic homogeneity can be maintained in changestat experiments we applied high throughput gene sequencing in short-term (20 generations) glucose-limited A-stat experiments with *E. coli* K-12 MG1655 (Publication V). We sequenced samples from the A-stat experiment along with its stock culture made with only 10 generations of cultivation from stab-agar colonies ordered from a stock culture center. We did not detect any new mutations during the A-stat experiment, however, the stock culture contained a significant amount of heterogeneity. 31% of the culture contained different mutants, and all of these mutant populations were detected in the A-stat samples. Thus, all mutations were already present in the stab-agar culture. Even if the A-stat experiments had been initiated from single colonies, there would have been a large chance of picking a mutant clone. This surprising heterogeneity shows the importance of sequencing the genome of a culture at the start of a microbial physiology study, especially if phenotypic data from the experiment are to be used in comparisons between different research groups or for metabolic modeling.

KOKKUVÕTE

SUBSTRAAT-LIMITEERITUD PIDEVKULTIVEERIMIST on kasutatud mikroorganismide füsioloogia uurimiseks juba üle 60 aasta [1, 2]. Peamine pidevkultiveerimise (näiteks kemostaat) eelis perioodilise kultiveerimise ees (batch) on tõsiasi, et pidevkultiveerimisel on võimalik hoida konstantseid keskkonnatingimusi ja sellest tulenevalt sundida rakke kasvama soovitud kasvuerikiirusel. See võimaldab koguda metaboolseks mudeldamiseks kvantitatiivseid andmeid steady state tingimustes. Kiirendusstaat (A-staat) võimaldab koguda ühe eksperimendiga suurel hulgal kvantitatiivseid andmeid laias kasvuerikiiruste vahemikus [3]. A-staatne eksperiment algab kemostaadiga, kuid pärast steady state'i saavutamist rakendatakse sujuv läbivoolukiiruse (D) muutus. Tavaliselt on läbivoolukiiruse muutus suhteliselt aeglane ($\alpha_d = 0.01 \text{ h}^{-2} - 0.005 \text{ h}^{-2}$), mis võimaldab rakkudel kohaneda muutuvate tingimustega ja säilitada stabiilne füsioloogiline seisund, mis vastab steady state'le – quasi-steady state. Iseenesest mõistetavalt on A-staadi meetodi reprodutseeritavus kriitiline faktor, mida tuleb valideerida. Probleemi uurimiseks viidi läbi glükoos-limiteeritud *Escherichia coli* K-12 MG1655 A-staatsed eksperimendid (Artiklid I ja II). Tulemused näitavad head reprodutseeritavust – katsetevahelised suhtelised standardhälbed on enamikel juhtudel tunduvalt alla 10%. Sarnased tulemused saadi ka glükoos-limiteeritud *Lactococcus lactis* IL1403 katsetes (Artikkel III). Lisaks selgus, et A-staadi reprodutseeritavus on sarnane kemostaadiga, mis näitab, et muutuv läbivoolukiirus ei põhjustanud suuremat katsetevahelist varieeruvust. Kõik see lubab meil järeldada, et A-staat on hästi reprodutseeritav.

Järgmine kriitiline faktor A-staatsetes eksperimentides on läbivoolukiiruse muutuse valik (läbivoolukiirendus, α_d). Kuna läbivoolukultiveerimisel toimub pidev suhteliselt aeglane kultuuri lahjendamine, siis võtab uue statsionaarse seisundi saavutamine kaua aega, kui selleks tuleb eemaldada kasvu kõrvalproduktid, mis tekkisid varasematel kultiveerimistingimustel. Sellest tulenevalt on selge, et mida aeglasemalt lahjenduskiirust muudetakse, seda sarnasemad on quasi-steady state (A-staat) andmed steady state kemostaadiga. Samas, väga aeglaste läbivoolukiirenduste kasutamine muudab A-staadi eksperimendid väga pikaks ning võib toimuda kultuuri evolutsiooniline adapteerumine [4]. Järelikult tuleb läbivoolukiirendust A-staatsetes eksperimentides valida hoolikalt. Head kokkulangevust A-staadi ($\alpha_d = 0.01 \text{ h}^{-2}$) ja kemostaadi vahel täheldati *E. coli* K-12 MG1655 eksperimentides Y_{xs} , O_{ace} , O_{CO_2} , O_{cAMP} tasemel. On oluline märkida, et esimest korda näidati A-staadi ja kemostaadi sarnasust ka transkriptoomi ja proteoomi tasemel (Artikkel II). *L. lactis* IL1403 kemostaadi ja A-staadi ($\alpha_d = 0.005 \text{ h}^{-2}$) andmete (Y_{xs} , Y_{Lg} , aminohapete tarbimised ja produktide saagised) võrdlus kasvuerikiirusel 0.45 h^{-1} näitas, et A-staat ja kemostaat on väga sarnased (Artikkel III). Kõik see lubab meil järeldada, et läbivoolukiirenduste $\alpha_d = 0.01 \text{ h}^{-2} - 0.005 \text{ h}^{-2}$ kasutamine on sobilik, et saada *E. coli* K-12 MG1655 ja *L. lactis* IL1403 puhul steady state'le vastavaid andmeid. Samas, kuna evolutsiooni kiirus on sõltuv uuritavast liigist ning kasvukeskkonnast, tuleb iga liiki ja keskkonnatingimusi valideerida eraldi.

Kemostaadi meetod loodi algselt, et uurida evolutsiooni konstantsetes kasvutingimustes ning on teada, et mõningatel juhtudel vahetavad mutandid välja algse tüve [5, 6]. See toob kaasa kontrollimata faktori, mis vähendab kvantitatiivsete steady state andmete usaldusväärsust. Hüsteresi nähtus ilmselt ka meie eksperimentides biomassis saagises, produktide erisaagistes ja geeni ekspressioonis suhteliselt pikkades (60 generatsiooni) *L. lactise* D-staatsetes eksperimentides (Artikkel IV). Hüsteresi on arvatavasti tingitud mainitud paremini adapteerunud mutantide esilekerkimisest. See tekitab küsimuse, kui kaua on võimalik läbivoolukultiveerimise eksperimente sooritada ilma geneetilise heterogeensuse tekkimiseta? Nimetatud probleemile otsiti vastust uurides *E. coli* K-12 MG1655 genoomi stabiilsust glükoos-limiteeritud A-staatsetes katsetes (20 generatsiooni) kasutades kõrge läbilaskevõimega sekveneerimist (Artikkel V). Uuriti heterogeensuse esinemist kahes A-staadi proovis ning alustus-kultuuris (stokk-kultuuris), millega eksperimente alustati. Heterogeensuse analüüsi käigus ei tuvastatud ühtegi mutatsiooni, mis oleks tekkinud katse käigus, mis lubab meil järeldada, et 20 generatsiooni pikkune glükoos-limiteeritud *E. coli* K-12 MG1655 A-staatne eksperiment on piisavalt lühike, et vältida mutantsete tüvede esilekerkimist. Samas, alustus- kultuuri analüüs võimaldas tuvastada suhteliselt suure heterogeensuse, nimelt, 31% kultuurist olid erinevad mutandid, mis leidsid ka A-staadi proovides. On oluline märkida, et uuritud alustus-kultuur valmistati DSMZ kultuurikollektsioonist pärit pistekülvkolooniast ainult 10 generatsioonilise perioodilise (batch) kultiveerimisega. See viitab, et nähtud heterogeensus esines juba kollektsioonist saadud kultuurikoloonias. Suhteliselt suur täheldatud heterogeensus viitab vajadusele sekveneerida uuritava tüve genoom enne raku füsioloogia uuringu algust, eriti, kui saadud andmeid soovitakse kasutada laboritevahelistes võrdlustes või metabolismi mudeldamiseks.

LIST OF PUBLICATIONS

The following publications form the basis of this dissertation and are reproduced in the appendices with permission from the publishers.

- I [Nahku R](#), Valgepea K, Lahtvee PJ, Erm S, Abner K, Adamberg K, Vilu R **Specific growth rate dependent transcriptome profiling of *Escherichia coli* K12 MG1655 in accelerostat cultures.** *Journal of Biotechnology*, 145(1):60-65 (2010)
- II Valgepea K, Adamberg K, [Nahku R](#), Lahtvee PJ, Arike L, Vilu R **Systems biology approach reveals that overflow metabolism of acetate in *Escherichia coli* is triggered by carbon catabolite repression of acetyl-CoA synthetase.** *BMC Systems Biology*, 4:166 (2010)
- III Lahtvee PJ, Adamberg K, Arike L, [Nahku R](#), Aller K, Vilu R **Multi-omics approach to study the growth efficiency and amino acid metabolism in *Lactococcus lactis* at various specific growth rates.** *Microbial Cell Factories*, 10:12 (2011)
- IV Lahtvee PJ, Valgepea K, [Nahku R](#), Abner K, Adamberg K, Vilu R **Steady state growth space study of *Lactococcus lactis* in D-stat cultures.** *Antonie Van Leeuwenhoek*, 96(4):487-96 (2009)
- V [Nahku R](#), Peebo K, Valgepea K, Barrick JE, Adamberg K, Vilu R **Stock culture heterogeneity rather than new mutational variation complicates short-term cell physiology studies of *Escherichia coli* K-12 MG1655 in continuous culture.** *Microbiology 2011*, 157:2604-2610 (2010)

SUMMARY OF AUTHOR'S CONTRIBUTION

The author led the establishment of transcriptomics methods at the Competence Center of Food and Fermentation Technologies (CCFFT) and supervised the introduction of genetic engineering methods for bacterial strain development. In addition, the author introduced genomic and subpopulation analysis with HT DNA sequencing and actively studies acetate overflow in *E. coli* K-12 using both genetic engineering and growth media development.

- I In [Publication I](#), the author the author designed and helped to perform the experimental work, analyzed and interpreted the data, and wrote the manuscript.
- II In [Publication II](#), the author participated in designing and performing the experiments. The author was responsible for carrying out the transcriptomic analysis.
- III In [Publication III](#), the author carried out the transcriptomic analysis.
- IV In [Publication IV](#), the author carried out the transcriptomic analysis.
- V In [Publication V](#), the author designed and helped to perform the experimental work, analyzed and interpreted the data, and wrote the manuscript.

LIST OF PRESENTATIONS

- I Nahku R, Erm S, Lahtvee PJ, Valgepea K, Adamberg K, Vilu R
Simulating fluctuations in environmental parameters using small scale continuous cultivations
Poster presentation at: Inhomogenities in large-scale bioreactors,
24-27 November, 2009, Berlin, Germany
- II Nahku R, Valgepea K, Lahtvee PJ, Arike L, Adamberg K, Vilu R
Overflow Metabolism in *Escherichia coli* is triggered by decrease of acetate assimilation capabilities in the PTA-ACS Node
Poster presentation at: Systems Biology of Microorganisms,
21-25 March, 2010, Paris, France
- III Nahku R, Peebo K, Valgepea K, Barrick JE, Adamberg K, Vilu R
High-throughput sequencing proves heterogeneity of stock cultures and no evolution in short term continuous cultures
Poster presentation at FEBS-SystemsX-SysBio2011: From Molecules To Function,
26 February – 3 March, 2011, Innsbruck, Austria

ACKNOWLEDGMENTS

CHANGESTAT CULTIVATION EXPERIMENTS are relatively time consuming and laborious. It is often necessary to collect samples and perform culture density measurements for 50 or even 100 hours with an interval of one or two hours. Performing these kinds of experiments requires good team work. Measurements have to be consistent and difference between people minimized. This is only possible to achieve with proper training. I am lucky to be part of our fermentation team – young enthusiasts and fans of continuous cultivation.

Firstly, I would like to thank Kaspar Valgepea, Petri-Jaan Lahtvee, Sten Erm and Liisa Arike for excellent co-operations during my PhD studies. I have also had privilege to work with Karl Peebo who has played major part in *E. coli* mutation analysis. I would also like to thank all my other colleagues in CCFET for creating a good working environment. I would like to express my gratitude to my supervisors Kaarel Adamberg and Raivo Vilu for their patience and support during my studies. Special thanks go also to Jeffrey E Barrick for his help in HT DNA sequencing data analysis.

I would like to thank my opponents Sven-Olof Enfors and Uldis Kalnenieks for finding time for finding time for reviewing my thesis.

My family has helped me a lot by creating peaceful home environment. Special thanks to my wife Joanna for understanding that during fermentation experiments it is necessary to work overtime.

This research was supported by EU project EU22704 and EU29994, Estonian targeted and science foundation projects SF0140090s08 and G8165 as well as European Social Fund's Doctoral Studies and Internationalisation Programme DoRa, which is carried out by Foundation Archimedes.

ACRONYMS

A-stat	accelerostat cultivation
ABC	ATP-binding cassette transporter
CDM	chemically defined media
cDTA	comparative dynamic transcriptome analysis
cDNA	complementary DNA
DCW	dry cellular weight
DSMZ	Deutsche Sammlung von Mikroorganismen und Zellkulturen GmbH, Germany
D-stat	dilutionstat cultivation
GEO	NCBI Gene Expression Omnibus
HT	high throughput
INRA	Institut national de la recherche agronomique
IS	insertion sequence
KEGG	Kyoto encyclopedia of genes and genomes
mRNA	messenger RNA
PCR	polymerase chain reaction
RNA	ribonucleic acid
SNP	single-nucleotide polymorphism
SRA	NCBI Sequence Read Archive
SSI	Statens Serum Institute, Denmark
subsp.	subspecies

CULTIVATION PARAMETERS

α_d	acceleration of dilution (D)
D	dilution rate, F divided with V
F	pumping rate
μ	specific growth rate (h^{-1})
μ_{\max}	maximum specific growth rate when culture wash-out occurs
μ_{critical}	specific growth rate where acetate production starts
D_{critical}	dilution rate at the onset of aerobic fermentation
V	culture volume, L
Y_{xs}	biomass yield, ($\text{g}_{\text{DCW}} \cdot \text{g}_{\text{glucose}}^{-1}$)
Y_{Lg}	produced lactate per consumed glucose, $\text{g}_{\text{lactate}} \cdot \text{g}_{\text{glucose}}^{-1}$
S_o	concentration of glucose in the medium, $\text{g} \cdot \text{L}^{-1}$
O_{acetate}	acetate production normalized to biomass, $\text{mmol} \cdot \text{g}_{\text{DCW}}^{-1}$
O_{cAMP}	cAMP production normalized to biomass, $\text{mmol} \cdot \text{g}_{\text{DCW}}^{-1}$
O_{CO_2}	CO_2 production normalized to biomass, $\mu\text{mol} \cdot \text{g}_{\text{DCW}}^{-1}$
O_{protein}	protein production normalized to biomass, $\text{mmol} \cdot \text{g}_{\text{DCW}}^{-1}$
O_{lactate}	lactate production normalized to biomass, $\text{mmol} \cdot \text{g}_{\text{DCW}}^{-1}$
I_{glucose}	consumption rate of glucose, $\text{g}_{\text{glucose}} \cdot \text{h}^{-1}$
I_{AA}	total amount of amino acids consumed normalized to biomass, $\text{g}_{\text{amino acids}} \cdot \text{g}_{\text{DCW}}^{-1}$
I_{acetate}	consumption rate of acetate, $\text{g}_{\text{acetate}} \cdot \text{h}^{-1}$
I_x	biomass production rate, $\text{g}_{\text{DCW}} \cdot \text{h}^{-1}$
I_{protein}	number of protein molecules synthesized per minute
k_{protein}	protein degradation rate ($\frac{\ln(2)}{\text{average protein half-life in hours}}$)
C_{acetate}	concentration of acetate, $\text{mmol} \cdot \text{L}^{-1}$
C_{protein}	concentration of protein, $\text{molecules} \cdot \text{L}^{-1}$
C_{protein_o}	initial concentration of protein, $\text{molecules} \cdot \text{L}^{-1}$
C_{acetate_o}	initial concentration of acetate, $\text{mmol} \cdot \text{L}^{-1}$

CHEMICALS AND ENZYMES

<i>allD</i>	ureidoglycolate dehydrogenase, <i>E.coli.</i> : b0517
<i>cAMP</i>	adenosine-3',5'-cyclic phosphate, KEGG: C00575
<i>arcA</i>	arginine deiminase, <i>L.lactis.</i> : L0329
<i>arcC1</i>	carbamate kinase, <i>L.lactis.</i> : L93826
<i>arcC2</i>	carbamate kinase, <i>L.lactis.</i> : L92850
<i>arcD1</i>	arginine/ornithine antiporter, <i>L.lactis.</i> : L94890
<i>argE</i>	acetylornithine deacetylase, <i>L.lactis.</i> : L0115
<i>argR</i>	arginine catabolic regulator, <i>L.lactis.</i> : L0110
ATP	adenosine-5'-triphosphate, KEGG: C00002
<i>betA</i>	choline dehydrogenase, a flavoprotein, <i>E.coli.</i> : b0311
<i>citC</i>	acetate-SH-citrate lyase ligase, <i>L.lactis.</i> : L0038
<i>citD</i>	citrate lyase subunit gamma, <i>L.lactis.</i> : L0039
<i>CspA</i>	RNA chaperone and anti-terminator, cold-inducible product, <i>E.coli.</i> : b3556
<i>cspG</i>	cold shock protein homolog, cold-inducible, <i>E.coli.</i> : b0990
<i>cspH</i>	stress protein, member of the CspA-family, <i>E.coli.</i> : b0989
DEPC	diethyl pyrocarbonate, PubChem: 3051
DNA	deoxyribonucleic acid, PubChem: 44135672
<i>dppD</i>	dipeptide/heme transporter, <i>E.coli.</i> : b3541
<i>flhD</i>	DNA-binding transcriptional dual regulator with FlhC, <i>E.coli.</i> : b1892
FlhD	DNA-binding transcriptional dual regulator with FlhC product, <i>E.coli.</i> : b1892
<i>gltP</i>	glutamate/aspartate proton symporter, <i>E.coli.</i> : b4077
<i>glyA</i>	serine hydroxymethyltransferase, <i>E.coli.</i> : b2551
<i>lamB</i>	maltose outer membrane porin, <i>E.coli.</i> : b4036
<i>malKFG</i>	maltose ABC transporter
<i>malT</i>	DNA-binding transcriptional activator for the mal regulon and maltotriose-ATP-binding protein, <i>E.coli.</i> : b3418
<i>mgID</i>	DNA-binding transcriptional repressor (galS in KEGG), <i>E.coli.</i> : b2151
<i>mlc</i>	Global DNA-binding transcriptional repressor (dgsA in KEGG), <i>E.coli.</i> : b1594
<i>ppiC</i>	peptidyl-prolyl cis-trans isomerase C (rotamase C), <i>E.coli.</i> : b3775
<i>ptsG</i>	fused glucose-specific PTS enzymes IIB component/IIC component, <i>E.coli.</i> : b1101
<i>recB</i>	exonuclease V (RecBCD complex), β subunit, <i>E.coli.</i> : b2820
<i>rpoS</i>	RNA polymerase, sigma S (sigma 38) factor, <i>E.coli.</i> : b2741
<i>rrlD</i>	23S ribosomal RNA of <i>rrnD</i> operon, <i>E.coli.</i> : b3275
<i>uspC</i>	universal stress protein, <i>E.coli.</i> : b1895
<i>yahE</i>	predicted protein, <i>E.coli.</i> : b0319
<i>yadL</i>	predicted fimbrial-like adhesin protein, <i>E.coli.</i> : b0137
<i>yhdJ</i>	DNA adenine methyltransferase, SAM-dependent, <i>E.coli.</i> : b3262
<i>yhdU</i>	predicted membrane protein, <i>E.coli.</i> : b3263
<i>yifO</i>	conserved protein (not in KEGG), <i>E.coli.</i> : b3776
<i>yjcO</i>	conserved protein, <i>E.coli.</i> : b4078
<i>ylbE</i>	pseudogene, <i>E.coli.</i> : b4572

THESIS

INTRODUCTION

MICROORGANISMS HAVE THE ABILITY TO ADOPT THEIR METABOLISM to best make use of changes in environmental conditions. They do so by regulating gene and protein expression, controlling enzymatic activity, and adjusting colony formation, among others. Interpreting the influence of all of these effects is challenging, and environmental conditions should be controlled as much as possible during cell physiology experiments. Shake flask or microtiter plate batch cultivations are effective for relatively fast screening of multiple environmental conditions for μ_{\max} or cell yield, but have serious limitations when quantitative data for metabolic modeling is desired. One reason for this is that batch cultivation often results in rapidly changing conditions due to a rapid increase in biomass and concurrent accumulation of metabolic by-products. Continuous cultivation can be employed to alleviate this problem.

1.1 CONTINUOUS CULTIVATION

The core principle of continuous cultivation methods is that fresh medium is continuously pumped into the bioreactor while spent medium with biomass and fermentation products is pumped out. Several types of continuous cultivation methods have been developed, but the most widely used is the chemostat method [1, 2]. In chemostat, microorganisms are cultivated under conditions of substrate limitation and the pumping rate (F) of the growth limiting substrate defines the specific growth rate (μ). Under steady state conditions, F divided with the culture volume (V), *i. e.* dilution rate (D), is equal to μ . Various growth limiting conditions can be utilized such as carbon and nitrogen limitation, and numerous stable growth conditions can be established and maintained [7–9].

Another type of continuous cultivation technique is auxostat where one growth parameter is kept constant by automatic adjustment of the dilution rate. The most well known example of auxostat is turbidostat where the amount of biomass in the bioreactor is kept constant [10]. In a turbidostat, cells are grown in an excess of substrates at maximal specific growth rate, and this method can be used for physiology studies in place of batch cultivation. Several other continuous cultivation techniques have been developed, including gradostat [11] and adaptostat [12].

Continuous cultivation makes it possible to define constant environmental conditions that often allow cells to acquire and function in a state where the production and outflow of metabolic products is steady. It is often assumed that the metabolic fluxes are constant

in this state and the majority of cells are performing the same function. If one is interested in modeling this state, chemostat cultivation is a suitable method for obtaining quantitative data. However, if one is interested in determining how the growth changes over a range of steady states, chemostat cultivation lacks throughput; It takes a relatively long time and numerous experiments to screen the growth rate dependent metabolism of a microorganism. To overcome this drawback, changestat cultivation techniques were developed.

1.1.1 *Changestat cultivation*

Changestat experiments begin their life as a chemostat experiment. After reaching steady state, one environmental condition is steadily changed. The most commonly used changestat method is accelerostat (*A-stat*) which allows one to measure multiple cellular states in one experiment [3]. After reaching steady state, an *A-stat* experiment introduces a steady change in *D*, termed acceleration of dilution (α_d).

Another example of changestat cultivation is dilution rate stat (*D-stat*), where *D* is kept constant and another environmental parameter, *e.g.* temperature or pH, is slowly changed [13]. In a *D-stat* experiment we observe hysteresis in culture characteristics at the level of biomass yield, product yields, and gene expression in an experiment with 60 generations of *Lactococcus lactis* (Publication IV). We attributed this effect to the evolution of mutant strains; An effect common to all forms of continuous cultivation where the cells reproduce.

In principle, if steady state growing cells encounter a very slow change of an environmental parameter, the cells should be able to adapt to changing conditions and maintain a physiological state similar to steady state. We term this quasi-steady state. The concordance between steady states, as measured in a chemostat, and quasi-steady states, measured in changestat cultivation, depend on the rate of environmental change employed in the changestat experiment.

1.1.2 *Choice of acceleration of dilution in A-stat cultivation*

The choice of acceleration of dilution in *A-stat* depends on numerous factors; the main factor is the nature (strain) of the microorganism studied, and peculiarities of its metabolism. Generally, the faster the cells are able to react to changing environmental conditions, more correspondence is seen between comparable *A-stat* and chemostat experiments. Indeed, parameters like transcription and translation rates and also the degradation rates of proteins play an important role in the adaptations that take place.

These parameters have been studied in yeast. Lately, Sun *et al.* used comparative dynamic transcriptome analysis (cDTA) to determine transcription and mRNA degradation rates. The authors found that the half life of mRNA in the medium was 12 minutes for *Saccharomyces cerevisiae* and 59 minutes for *Schizosaccharomyces pombe*. In contrast to the relatively short half lives of mRNA, proteins are much more stable [14]. Helbig *et al.* used nitrogen-limited chemostats at a dilution rate of 0.1 h^{-1} and a medium switch from ^{14}N ammonium sulphate to ^{15}N containing salt. Both, ^{14}N and ^{15}N peptides of the biomass

were quantified to determine the changing $\frac{^{14}\text{N}}{^{15}\text{N}}$ peptide ratios induced by the label switch. It was calculated that the protein half life for *S. cerevisiae* was 10.8 h. It has been estimated that the peptide elongation rate in *S. cerevisiae* depends on the specific growth rate and increases from 2.8 to 10 amino acid per second if the doubling time changes from 486 to 96 minutes [15]. Considering that an average protein molecule contains 300 amino acids it takes 107 or 30 seconds, respectively, to synthesize an average protein molecule at the doubling times mentioned. These times (107 or 30 seconds) are good indicators of how long it takes to synthesize an average protein, and therefore to establish a new protein expression pattern. From all the previously mentioned *S. cerevisiae* cellular parameters it seems that the cells are able to regulate metabolism at the transcriptomic level rather fast. The situation is different looking from the point of view of proteome synthesis and degradation rates. A median protein half-life of 10.8 h indicates that for *S. cerevisiae* it would take a rather long time to remove proteins that are no longer required.

In *Escherichia coli* it has been shown that the mRNA half-life varies between 2.1 to 6 minutes in various mutants at doubling times between 73-85 minutes [16]. These are considerably faster mRNA degradation rates than those observed in *S. cerevisiae*. In contrast, the mRNA synthesis rate was around 10 mRNAs per cell and per cell cycle time, a value around 5 times smaller compared with *S. cerevisiae*. This is expected if we take into account that *E. coli* cells are considerably smaller and have less total RNA in the cell compared with yeast. It has been shown that the peptide elongation rate in *E. coli* also depends on the specific growth rate, as in *S. cerevisiae*, but increases faster from 13 to 20 amino acids per second between doubling times of 100 min and 24 min [17]. Protein half-lives of *E. coli* were recently determined in our laboratory with median values of 3 h (unpublished data). Similar to mRNA half-lives, the protein half-lives were considerably shorter in *E. coli* compared with *S. cerevisiae*. The latter indicates that *E. coli* is likely able to regulate its metabolism faster than *S. cerevisiae* and, therefore, it may be possible to apply a faster dilution rate increase in A-stat experiments to maintain quasi-steady growth of *E. coli*.

It seems that to achieve similar cellular protein concentrations in chemostat and A-stat experiments depends on how rapidly and how much cells need to regulate protein expression as the dilution rate is changed. Moreover, it seems that removal of proteins is the slowest process in adaptation. Therefore, it is important to know by how much protein expression is adjusted when dilution rate is changed. Unfortunately, relatively few experiments have been performed in chemostat with proteome analysis at various dilution rates. Mehmeti studied the proteome of *Enterococcus faecalis* in chemostat at dilution rates 0.05 h^{-1} , 0.15 h^{-1} , and 0.4 h^{-1} [18]. It was found that expression of only a few proteins changing by around two times if dilution rate was increased from 0.05 h^{-1} to 0.15 h^{-1} . Similarly, Dressaire *et al.* investigated the proteome of *L. lactis* at dilution rates of 0.09 h^{-1} , 0.24 h^{-1} , and 0.47 h^{-1} [19]. It was found that only six proteins out of 173 had expression levels more than two times higher as dilution rates increased from 0.09 h^{-1} to 0.24 h^{-1} . When dilution rate increases from 0.09 h^{-1} to 0.47 h^{-1} , 25 out of 173 proteins had expression levels more than two times higher [19]. In *E. coli* it was found that expression of more proteins change between dilution rates 0.4 h^{-1} and 0.5 h^{-1} than between 0.4 h^{-1} and 0.1 h^{-1} , illustrating that more profound changes occur

at higher dilution rates in this organism [20]. The latter study found that the protein expression increases by around 2 times when dilution rate is increased by 0.1 h^{-1} .

Glucose pulse experiments have revealed important information regarding the adaptation of cells in changing environments. Sunya *et al.* applied glucose pulses of different intensities in steady-state *E. coli* chemostat experiments at a dilution rate of 0.15 h^{-1} . They observed a very rapid increase in specific growth rate. Firstly, the specific growth rate reached its maximum in batch cultivation within 15 seconds. Secondly, the specific growth rate stabilized at a value about 70% from its maximum 90 seconds after the glucose pulse [21]. Similar behavior was also observed by Taymaz-Nikerel *et al.* at a dilution rate of 0.1 h^{-1} in *E. coli* glucose pulse experiments [22]. Furthermore, *E. coli* has the ability to react to sudden increases in glucose availability, and this is specific growth rate dependent [23]. Taken together, glucose pulse experiments with *E. coli* show that these cells have the ability to increase growth rate very rapidly. This suggests that enzyme concentrations may not be tightly regulated at many growth rates.

1.1.3 Comparing the cellular state in *A-stat* and chemostat experiments

The most accurate way of comparing *A-stat* and chemostat experiments is direct comparison of quantitative data acquired from both methods. The choice of acceleration of dilution and *A-stat* concordance with chemostat has been studied before. Van der Sluis *et al.* studied glucose-limited cultures of *Zygosaccharomyces rouxii* CBS 4021 in *A-stat* cultivation with α_d values of 0.1, 0.01 and 0.001 h^{-2} and compared various cultivation parameters measured in these experiments (glucose, biomass, and ethanol concentrations, specific growth rate, yield of biomass on glucose) with the same parameters measured in chemostat experiments [24]. Models were used to analyze the differences between the two data sets collected in *A-stat* and chemostat experiments and the authors concluded that 0.001 h^{-2} was the only acceleration of dilution that allowed for direct comparison. Unfortunately, poor reproducibility of biomass and ethanol concentrations at a dilution rate 0.1 h^{-1} between different experiments reduces the reliability of the cultivation experiments.

In another study, various *S. cerevisiae* strains (CBS8066, BAY.17, X2180 and CEN.PK122) were cultivated in glucose-limited accelerostat cultures with an acceleration of dilution of 0.01 h^{-2} and displayed differences in the dilution rate at the onset of aerobic fermentation when ethanol production begins (D_{critical}) [25]. It was noted that the D_{critical} values determined from the accelerostat experiments did not match with chemostat experiments, with the exception being strain CBS8066. It was also reported that deviations in D_{critical} values in the replicate experiments was less than 5% [25]. The differences observed in the behavior of the strains was likely caused by the higher ability of strain CBS8066 to adapt to changing environments because the same acceleration of dilution was applied in all strains.

Relatively good agreement of glucose-limited accelerostat and chemostat cultures was found in experiments with the yeast *Hanseniaspora guilliermondii* NCYC 2380 despite the use of a relatively high acceleration of dilution (0.02 h^{-2}) [26]. It was observed that ethanol first appeared in the bioreactor at a dilution rate of 0.27 h^{-1} in accelerostat, while in chemostat, ethanol first appeared at 0.25 h^{-1} . The most significant difference between

A-stat and chemostat experiments in this study was the significantly higher acetate concentration in accelerostat culture. This is likely caused by applying too rapid α_d .

Accelerostat cultures with different acceleration of dilution values and chemostat cultures of the microalgae *Dunaliella tertiolecta* CCAP 19/6B were studied under light-limited conditions. Various acceleration of dilution values, 0.00809, 0.001, 0.00107, 0.0001, 0.00016, 0.00029 and 0.00001 h^{-2} were tested [27, 28] and concordance with chemostat was observed in measurements of biomass and chlorophyll concentration, average light intensity inside the reactor, and absorption coefficient. It was concluded that the fastest possible acceleration of dilution that resulted in data comparable with chemostat culture is 0.00029 h^{-2} . One might note that slow acceleration of dilution values were applied in these microalgae studies. This illustrates that one of the key factors in cultivation is the ability of cells to adapt to changing environments. It is clear that adaptation mechanisms and rates are species dependent, and may also vary between strains [25].

Besides the studies involving eukaryotic species, *A*-stat and chemostat cultivation has also been compared in bacterial studies. In glucose-limited continuous cultivation of *E. coli* K-12 W3350, large differences were found in the specific growth rate when acetate production starts (μ_{critical}) and when culture wash-out occurs (μ_{max}) comparing *A*-stat experiments ($\alpha_d = 0.015 \text{ h}^{-2}$) and chemostat experiments. In chemostat, μ_{critical} was found to be around 0.3 h^{-1} and μ_{max} 0.38 h^{-1} , while in accelerostat these μ values were 0.47 and 0.57 h^{-1} , respectively [3]. These experiments illustrate that the method of increasing the growth rate is important in determining the response of the culture. Abrupt changes of the dilution rates in chemostat could lead to the overflow of acetate at lower growth rates in comparison with *A*-stat cultivation. In contrast, good concordance between *A*-stat ($\alpha_d = 0.01 \text{ h}^{-2}$) and chemostat cultivation results were observed in fructose-limited experiments with *Corynebacterium glutamicum* ATCC 13745, with comparable biomass concentrations, residual concentrations of demeton-S-methyl (pesticide), and μ_{max} values [29].

Considering all of these experiments, it is clear that the choice of acceleration of dilution depends on both the cultivation conditions and species under investigation. Therefore, one must validate each cultivation condition and organism separately. It is clear that a slower acceleration of dilution provides more similar quantitative data when comparing *A*-stat and chemostat cultivation data. However, applying slow acceleration of dilution results in relatively long experiments, where culture adaptation due to genome mutations often occurs.

1.1.4 Genome stability of *E. coli* in continuous culture

Quantitative data collected from continuous cultivation methods is often used for metabolic modeling. Because DNA sequences encode the metabolic network of the cell, it is essential to know if and when the genomes of cells are changing during these experiments. In fact, chemostat experiments were initially introduced to study evolution and selection in a constant environment. Fitter clones are known to rapidly arise in some cases [5, 6], introducing an uncontrolled dynamic factor that reduces the quantitative reliability of the steady state data collected in chemostat and other cultivation experiments. There-

fore, to avoid genetic heterogeneity interfering with the interpretation of steady state physiology measurements, it is important to check the stability of the genome of the cells being cultured by monitoring the entire genetic homogeneity of population over time.

Flaws in stock culture handling are one possible source of genetic heterogeneity in cell physiology studies. Indeed, heterogeneity in stab agar cultures has been reported during long-term storage of *E. coli* K-12 W3110 at room temperature [30–32]. Considerably fewer mutations are expected when cell cultures are stored in a frozen state where no metabolic activity is possible. Nevertheless, genetic differences including loss of genes and variation in growth phenotype on various carbon sources have been detected in *E. coli* K-12 MG1655 strains acquired from different stock centers and laboratories [33]. Furthermore, variation in motility has been observed between *E. coli* K-12 strain derivatives (including MG1655) where an increase motility was found to be caused by insertion sequence (IS)-mediated activation of *flhD*, a regulator of flagellar gene transcription [34]. Presumably, periodic sub-culturing steps can contribute to this heterogeneity.

Genetic heterogeneity may also arise during continuous cultivation experiments as the result of spontaneous mutations. Information about which genes are possible targets for beneficial mutations is available from continuous cultivation experiments that are much longer than “routine” cell physiology studies. Long-term evolution of *E. coli* under glucose-limited chemostat cultivation has been studied quite intensively during the last decade [4, 35]. As one might expect, mutations that increase glucose transport are common in glucose-limited chemostat experiments [5, 36–38]. Namely, mutations in *mglD* (a DNA-binding transcriptional dual regulator) and *mgl* operator resulting in higher gene expression of *mglBAC* (galactose ABC transporter) has been found in aerobic cultures growing on glucose [39, 40]. Under the same conditions, mutations in *mlc* (a DNA-binding transcriptional repressor) and *malT* (a DNA-binding transcriptional activator) were also observed [40]. These mutations up-regulate *ptsG* (the glucose specific phosphotransferase system permease), *lamB* (the maltose high-affinity receptor) and *malKFG* (the maltose ABC transporter) [39, 40]. Because there is more than one mutation which could lead to increased glucose transport, multiple lineages with different mutations typically arise and compete during prolonged chemostat experiments and often there is not a single dominant genotype [39, 40]. Long-term evolution in glucose-limited chemostats can also result in the formation of a stable consortia of acetate-utilizing specialists that coexist with the main population [41]. Another important fact is that *E. coli*'s capacity to diversify is specific growth rate dependent; Considerably higher mutational heterogeneity was found at a dilution rate of 0.1 h^{-1} compared to 0.6 h^{-1} [42].

These phenomena are observed in prolonged continuous cultivation experiments exceeding the number of generations necessary for cell physiology studies by at least one order of magnitude. Therefore, for studying cell physiology using continuous cultures, it is important to find out how long a genetically uniform culture can be maintained. Generally, pumping through five working volumes in a chemostat experiment is assumed to be enough to reach steady state (50 h and 7 generations at $D = 0.1 \text{ h}^{-1}$). The maintenance of actual steady state has been questioned due to how rapidly fitter clones may arise [4]. Indeed, mutations in the stress-induced sigma factor *rpoS* have been detected in *E. coli* K-12 BW2952 cultures growing in glucose-limited chemostat experiments at $D = 0.1$

h^{-1} after only 24-72 h (3-10 generations) of cultivation [43]. On the other hand, the appearance of *rpoS* mutations is strain dependent. For example, no mutations were detected in an *E. coli* K-12 MG1655 strain within 96 h (14 generations) of cultivation at $D = 0.1 \text{ h}^{-1}$ [44]. The fact that different *E. coli* K-12 strains acquire *rpoS* mutations at different rates under similar cultivation conditions [44] makes it difficult to generalize about how long a genetically uniform culture of *E. coli* K-12 MG1655 could be maintained. Moreover, it is plausible that the latter strain acquires mutations other than *rpoS* during glucose-limited continuous cultivation experiments.

To assess the genetic stability of a strain and monitor possible genetic heterogeneities that might evolve during a cell physiology study in continuous culture, a method capable of detecting all mutations should be used. Recent advances in DNA sequencing technologies [45] have made it possible to routinely determine the full genome sequences of microorganisms and to generate high-coverage data sets for analysing genetic diversity within communities. For example, it was possible to monitor the frequencies of *E. coli* sub-populations that evolved during a long-term batch transfer experiment with 50 times genome coverage [46].

Similarly to the concordance between *A-stat* and chemostat it seems that the mechanisms that induce genetic changes are also strain dependent. Therefore, high throughput (HT) DNA sequencing was applied in this dissertation to examine the stability of the genome and characterize genetic heterogeneity during a short-term continuous cultivation experiment (*A-stat*, 20 generations of continuous cultivation) of *E. coli* K-12 MG1655.

AIMS OF THIS DISSERTATION

THE AIM OF THIS STUDY is to investigate the phenomena that may interfere with quantitative steady state analysis of *E. coli* K-12 and *L. lactis* IL1403 using continuous accelerostat (A-stat) cultivation. The following two main topics were investigated:

- I Investigation into the reproducibility of A-stat cultivation data, including a critical evaluation and comparison with data collected in chemostat cultivation experiments at the same specific growth rates.
- II Investigation into the source of genetic heterogeneity that is observed in continuous cultivation. This involves using HT sequencing to verify genetic stability in A-stat cultivation experiments.

MATERIALS AND METHODS

MORE DETAILED DESCRIPTIONS OF THE materials and methods applied are available in the publications. The following sections are provided to make this material more accessible.

3.1 STRAINS USED

- I *E. coli* K-12 MG1655 (λ -, F-, rph-1, Fnr+; Deutsche Sammlung von Mikroorganismen und Zellkulturen (DSMZ), DSM No.18039) was used in [Publication II](#) and [Publication V](#).
- II *E. coli* K-12 MG1655 strain (λ -, F-, rph-1, Fnr+; Statens Serum Institute (SSI), Reference number: C 438-01) was used in [Publication I](#) and [Publication V](#).
- III *L. lactis* subsp. *lactis* IL1403 was kindly provided by Dr. Ogier from INRA (Jouy-en-Josas, France) and used in [Publication III](#) and [Publication IV](#).

3.2 MEDIA AND CULTIVATION CONDITIONS

3.2.1 *E. coli* K-12

Defined minimal medium with 10 g·L⁻¹ ([Publication I](#)) and 4.5 g·L⁻¹ ([Publication II](#) and [Publication V](#)) α -(D)-glucose, temperature 37°C, pH 7 and aerobic conditions were used in all experiments. In all *A-stat* experiments with *E. coli* K-12, $\alpha_d = 0.01$ h⁻² was used after the chemostat stabilization phase. The chemostat phases were carried out at different dilution rates: 0.3 h⁻¹ in [Publication I](#), 0.1 h⁻¹ and 0.2 h⁻¹ in [Publication II](#) and [Publication V](#).

3.2.2 *L. lactis* subsp. *lactis* IL1403

In [Publication III](#) and [Publication IV](#) we used chemically defined media (CDM) with 3.5 g·L⁻¹ and 5 g·L⁻¹ of α -(D)-glucose, respectfully. In addition, the medium used in [Publication III](#) contained 70% GIBCOTMF-12 Nutrient Mixture (Invitrogen Corporation, Carlsbad, CA) and 30% modified CDM with a composition matching the one used in [Publication IV](#). In addition to glucose the CDM used in [Publication IV](#) contained amino acids, vitamins, minerals and nitrogen-bases. Cultivation experiments were carried out under

anaerobic conditions (N^2 -environment) with an agitation speed of 300 rpm at 34°C and pH 6.4. In all *A-stat* experiments with *L. lactis* IL1403, an acceleration of dilution of 0.005 h^{-2} was applied after the stabilization phase in chemostat at $D = 0.1 \text{ h}^{-1}$ (Publication III). In *D-stat* experiments, dilution rate was constantly 0.2 h^{-1} and different ramps of pH and/or temperature were applied (see Publication IV for details).

3.3 ANALYTICAL METHODS

Glucose and organic acids in the culture media were measured using high pressure liquid chromatography (Alliance 2795 system, Waters Corp., Milford, MA), using a BioRad HPX-87H column (Hercules, CA) with isocratic elution of 5 mM H_2SO_4 at a flow rate of $0.6 \text{ mL}\cdot\text{min}^{-1}$ and at 35°C. A refractive index detector (model 2414; Waters Corp.) was used for quantification of the compounds (Publication I through Publication V). Amino acid concentrations were determined with an amino acid analyzer (Acquity UPLC®; Waters Corp.) with AccQ-Taq Ultra (Waters Corp.) column according to the manufacturer’s instructions (Publication III).

3.4 GENE EXPRESSION PROFILING

Agilent’s DNA microarrays were designed in eArray web portal in 8 X 15K format containing 3 and 7 probes per target on *E. coli* K-12 and *L. lactis* microarray, respectively (<https://earray.chem.agilent.com/earray/>). Target sequences were downloaded from KEGG. For both microorganisms, RNA degradation was halted and total RNA extracted with RNeasy Protect Bacteria Mini Kit (Qiagen, Valencia, CA). cDNA was synthesized with Superscript III (Invitrogen, Carlsbad, CA) and labeled indirectly with Cy3 (CyTM3 Mono Reactive Dye Pack, Amersham, Buckinghamshire, UK) or Cy5 (CyTM5 Mono Reactive Dye Pack, Amersham). Hybridization, slide washing and scanning was performed using standard Agilent’s reagents and hardware (www.chem.agilent.com), (see Publication II and Publication III). DNA microarray data is also available at NCBI Gene Expression Omnibus (GEO) (Reference series: GSE23920 (*E. coli*) and GSE26536 (*L. lactis*)).

3.5 SIMULATION OF A-STAT AND CHEMOSTAT DATA

The difference between *A-stat* and chemostat was simulated with an example involving acetate concentration in bioreactor. The following constants were used in calculations: biomass yield, $Y_{xs} = 0.4 \text{ g}_{\text{DCW}}\cdot\text{g}_{\text{glucose}}^{-1}$; culture volume, $V = 0.3 \text{ L}$ and concentration of glucose in medium, $S_o = 4.5 \text{ g}\cdot\text{L}^{-1}$. Initial dilution rate, D , was 0.3 h^{-1} and acetate production normalized to biomass (O_{acetate}) was $0.0 \text{ mmol}\cdot\text{g}_{\text{DCW}}^{-1}$. Starting from the 6th hour of simulation, the dilution rate was increased to 0.0001666 h^{-1} per minute that corresponds to an acceleration of dilution of 0.01 h^{-2} until a dilution rate of 0.5 h^{-1} after which the dilution rate was kept constant for five culture volumes (10 h). O_{acetate} was also increased linearly concurrently with the dilution rate increase, but with an increase of $0.0018 \text{ mmol}\cdot\text{g}_{\text{DCW}}^{-1}\cdot\text{min}^{-1}$ until a dilution rate of 0.5 h^{-1} . The increase of

O_{acetate} was chosen to reach a similar O_{acetate} value at $D = 0.5 \text{ h}^{-1}$ as in real chemostat experiments with *E. coli* K-12. Parameters were calculated using the following equations:

The consumption rate of glucose, I_{glucose} ($\text{g}_{\text{glucose}} \cdot \text{h}^{-1}$):

$$I_{\text{glucose}} = \frac{V \cdot D}{1000 \cdot S_o} \quad (3.1)$$

The biomass production rate, I_x ($\text{g}_{\text{DCW}} \cdot \text{h}^{-1}$):

$$I_x = Y_{xs} \cdot I_{\text{glucose}} \quad (3.2)$$

The rate of acetate input, I_{acetate} ($\text{mmol} \cdot \text{min}^{-1}$):

$$I_{\text{acetate}} = O_{\text{acetate}} \cdot \frac{I_x}{60} \quad (3.3)$$

The concentration of acetate in *A-stat* culture, C_{acetate} ($\text{mmol} \cdot \text{L}^{-1}$), was calculated with an interval of one minute as follows:

$$C_{\text{acetate}} = \frac{C_{\text{acetate}_o} + I_{\text{acetate}} - C_{\text{acetate}_o} \cdot \frac{D}{60}}{V}, \quad (3.4)$$

where C_{acetate_o} is the initial acetate concentration or the concentration one minute before C_{acetate} was calculated.

The acetate concentration in chemostat simulations was calculated as follows:

$$C_{\text{acetate}} = O_{\text{acetate}} \cdot Y_{xs} \cdot S_o \quad (3.5)$$

for the same dilution rates as in *A-stat* calculations. The difference between the chemostat and *A-stat* data was calculated by subtracting the acetate concentration in the chemostat from those in *A-stat*.

Protein concentration in the cells was calculated in a similar manor as the acetate concentration described above. Instead of O_{acetate} , O_{protein} ($O_{\text{protein}} = 1.7 \cdot 10^{16} \text{ molecules} \cdot \text{g}_{\text{DCW}}^{-1}$) was used and chosen to correspond to the concentration of the average protein in 1 L of culture ($\text{DCW} = 1.8 \text{ g}_{\text{DCW}} \cdot \text{L}^{-1}$). The concentration of an average protein was acquired from a study performed in our lab (unpublished data). Initial dilution rates were 0.1 h^{-1} , 0.3 h^{-1} or 0.5 h^{-1} . When an increase in dilution rate of 0.0001666 h^{-1} per min ($\alpha_d = 0.01 \text{ h}^{-2}$) was applied, O_{protein} decreased by either 2 times, 5 times or 10 times for all noted initial dilution rates. The concentration of protein in *A-stat* culture, C_{protein} ($\text{molecules} \cdot \text{L}^{-1}$), was calculated with an interval of one minute as follows:

$$C_{\text{protein}} = \frac{C_{\text{protein}_o} + I_{\text{protein}} - C_{\text{protein}_o} \cdot \frac{D + k_{\text{protein}}}{60}}{V}, \quad (3.6)$$

where C_{protein_0} is the initial protein concentration or the concentration one minute before C_{protein} was calculated, I_{protein} is the number of protein molecules synthesized per minute and k_{protein} stands for protein degradation rate ($k_{\text{protein}} = \frac{\ln(2)}{\text{average protein half-life in hours}}$).

Protein concentration in chemostat was calculated as follows:

$$C_{\text{protein}} = O_{\text{protein}} \cdot Y_{\text{xs}} \cdot S_0 \quad (3.7)$$

for the same dilution rates as in *A-stat* calculations. Relative absolute deviation was calculated from protein concentrations in *A-stat* and chemostat and the number of minutes it takes the value to decrease lower than 5% was determined. Using the number of minutes and an increase in dilution rate of 0.0001666 h^{-1} per min it was calculated that the corresponding dilution rate value in *A-stat* is similar to that obtained in chemostat (ΔD , h^{-1}).

3.6 MUTATION ANALYSIS (PUBLICATION IV)

3.6.1 Genomic DNA extraction

An aliquot of lyophilised stock culture (4.2×10^6 cells) and two whole-population samples (not single colonies) acquired at $D = 0.11 \text{ h}^{-1}$ (8.4×10^9 cells) and 0.48 h^{-1} (3.0×10^9 cells) from one *A-stat* experiment were chosen for DNA extraction and subsequent HT DNA sequencing analysis. Genomic DNA for re-sequencing and mutation validation was extracted using the RTP Bacteria DNA Mini Kit (Invitex) following the manufacturer's protocol.

3.6.2 Illumina whole genome re-sequencing

Whole genome re-sequencing was performed by GATC Biotech AG using an Illumina Genome Analyzer II instrument. A single-end library was prepared from each genomic DNA sample and sequenced using the manufacturer's standard protocols. FASTQ read files were generated by Sequence Control Software (version 2.6) with Real Time Analysis (version 1.6.32) and the GA pipeline (version 1.5.1). Raw read data has been deposited in the NCBI Sequence Read Archive (SRA) (SRP006176).

3.6.3 Genome sequence data analysis

Sequencing reads were compared with the *E. coli* K-12 MG1655 reference genome (GenBank accession no. U00096.2) using the breseq analysis pipeline (version 1.00rc7). The source code for breseq is freely available online (<http://barricklab.org/twiki/bin/view/Lab/ToolsBacterialGenomeResequencing>). The online documentation describes the methods used to predict consensus point mutations, small indels, large deletions and new sequence junctions. Predictions of base substitutions and single-base indels that were polymorphic in the population (present only in some individuals) were performed

as detailed in the breseq documentation. Specifically, breseq was run with strict requirements for polymorphism prediction: only reads with alignments to the reference genome that spanned their entire sequence were considered, aligned bases with Phred quality scores of < 30 were ignored, and only predictions supported by E values $\leq 10^{-4}$ were accepted. The empirical per-base error model employed by breseq was found to underestimate the rates of indel sequencing errors in homopolymer repeats. Therefore, we chose to exclude putative low-frequency sub-populations with indels in reference sequence homopolymer repeats of six or more bases after manual examination. IS5 insertions were predicted as polymorphic by counting how many reads matched the two new sequence junctions associated with insertion of a new copy of this sequence (one at each end) versus the sequence junction in the original genome.

3.6.4 Mutation validation with Sanger sequencing

Predicted mutations were validated by performing PCR followed by Sanger sequencing. Sanger sequencing was performed by the Estonian Biocentre using an Applied Biosystems 3730xl DNA analyser and the BigDye Terminator v3.1 Cycle Sequencing kit (Applied Biosystems). The PCR mixture contained 2.5 μl 10 \times PCR buffer [KCl, $(\text{NH}_4)_2\text{SO}_4$ and 20 mM MgCl_2], 2 μl of each deoxynucleotide triphosphate (2.5 mM), 0.1 μl DreamTaq DNA polymerase (5 U μl^{-1}) (all obtained from Fermentas), 2 μl of each primer (10 μM) (Microsynth) (Supplementary Table S2 of Publication V), template DNA (50 ng or single colony) and diethylpyrocarbonate (DEPC)-treated water up to a total volume of 25 μl . The PCR thermoprofile consisted of an initial denaturing temperature of 95°C for 2 minutes, followed by 30 amplification cycles: denaturation at 95°C for 30 s, primer annealing for 30 s at the temperature specified in Supplementary Table S2 of Publication V, extension at 72°C for 1 minute per kb of product, followed by a final extension period of 10 min at 72°C. Agarose gel electrophoresis [1% $\frac{\text{w}}{\text{v}}$ agarose] of the PCR product was carried out, and bands were visualized using ethidium bromide (0.2 $\mu\text{g}\cdot\text{ml}^{-1}$). A GeneJET PCR Purification kit (Fermentas) was used for purification of PCR products prior to Sanger sequencing. Subpopulations with base substitutions were confirmed by Sanger sequencing PCR products from mixed population samples. Mixed signal peaks in chromatograms at genome positions corresponding to *betA* (choline dehydrogenase), *cspH/cspG* (stress protein, member of the *CspA* family/cold-shock protein), *glyA* (serine hydroxymethyltransferase) and *dppD* (ATP-binding component of the dipeptide ABC transporter) mutations were found in population samples but not in negative control samples that did not contain the sub-population. Low-scoring putative single-nucleotide polymorphisms (SNPs) in *allD* (ureidoglycolate dehydrogenase) and *recB* (exonuclease V, beta subunit) were rejected using this approach. For *yahE* (predicted protein), this validation procedure was inconclusive. Therefore, PCR products generated from 23 single colonies were combined in groups of three or four for subsequent sequence determination and chromatogram analysis as stated above. IS-related mutations: *flhD/uspC* (subunit of flagella regulator (FlhD2C2)/universal stress protein) and *yadL* (gene of predicted chaperone-usher fimbrial operon), were validated by screening colonies isolated from the stock culture for PCR product length differences.

RESULTS AND DISCUSSION

THE PROCESSES THAT OCCUR in cellular systems together form a complicated dynamic system with a large number of interacting components. In addition, cells adjust their metabolism to environmental conditions. Because of these adjustments, it is often important to control the environmental conditions under which cells are grown, and if possible, perform the cell physiology studies in parallel experiments. The specific growth rate is an important parameter that is often controlled by controlling access to a substrate limiting media component or other required resource such as light in the case of photoautotrophs. Control of specific growth rate is often readily achieved in chemostat and *A-stat* cultivation. Chemostat cultivation has now been practiced for over 60 years [1, 2], and *A-stat* for over 17 years [3]. Despite this length of time, *A-stat* cultivation has not been validated extensively. This dissertation is a critical evaluation of the factors that determine the accuracy and quality of quantitative data acquired using *A-stat* cultivation.

4.1 EXPERIMENTS WITH *Escherichia coli* K-12

Reproducibility is self-evidently a critical characteristic of cultivation methods, and requires careful study. Reproducible values of μ_{\max} and μ_{critical} (see Figure 1) as well as Y_{xs} (biomass yield per consumed glucose) were investigated (see Table 1).

Table 1 – Reproducibility of the three glucose-limited accelerostat experiments with *E. coli* K-12 MG1655 (Publication I). RSD is the relative standard deviation. Starred values (*) were calculated as an average in the range of dilution rates $D = 0.3 - 0.5 \text{ h}^{-1}$ of three biological replicates.

	μ_{\max} h^{-1}	μ_{critical} h^{-1}	Y_{xs} $\text{g}_{\text{DCW}} \cdot \text{g}_{\text{glucose}}^{-1}$
Average	0.48	0.34	0.48*
RSD (%)	3.2	3.4	5.4*

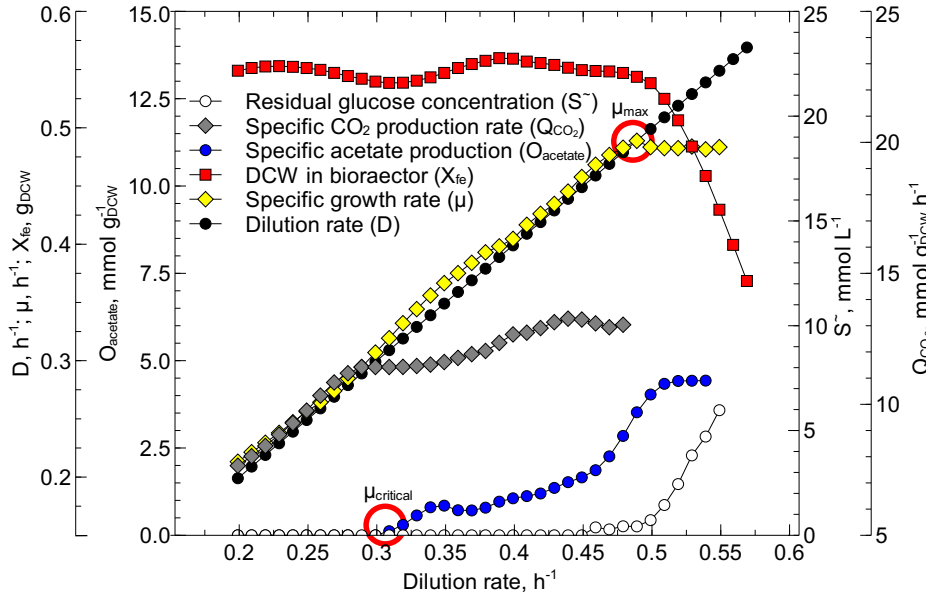


Figure 1 – Typical glucose-limited accelerostat experiment with *E. coli* K-12. Red circles indicate accelerostat specific characteristics. D is the dilution rate, h^{-1} ; μ is the specific growth rate, h^{-1} ; X_{fe} is the amount of biomass in bioreactor, g_{DCW} ; S^- is the residual glucose concentration, $\text{mmol}\cdot\text{L}^{-1}$; Q_{CO_2} is the specific CO_2 production rate, $\text{mmol}\cdot\text{g}_{\text{DCW}}^{-1}\cdot\text{h}^{-1}$.

In order to test if data obtained from *A-stat* experiments is reproducible, we analyzed another glucose-limited accelerostat data-set with *E. coli* K-12 MG1655. In contrast to the data summarized in [Publication I](#) (see [Table 1](#)) upgraded fermentation system allowed us analyze additional parameters, including specific productions of *cAMP*, acetate and CO_2 (O_{cAMP} , O_{acetate} , and O_{CO_2}). [Table 2](#) shows relative standard deviations from three *A-stat* experiments. It should be noted that the relatively high RSD for O_{acetate} was caused by differences in low acetate concentrations at the start of acetate overflow.

Table 2 – Reproducibility of the three glucose-limited accelerostat experiments with *E. coli* K-12 MG1655 ([Publication II](#)). Because every *A-stat* experiment starts as a chemostat, RSD of the chemostat experiments at a dilution rate or 0.11 h^{-1} are presented. The average of relative standard deviations of three replicates are shown in all cases. RSD is the relative standard deviation. ND*, acetate is not excreted at a dilution rate of 0.11 h^{-1}

μ h^{-1}	RSD of O_{CO_2} %	RSD of O_{cAMP} %	RSD of Y_{xs} %	RSD of O_{acetate} %
0.11 – 0.47	5.6	9.1	2.0	28
chemostat (0.11)	4.5	10.3	3.5	ND*

For instance, the RSD was 6.3% if only acetate concentrations over 2 mM are included. The fact that every *A-stat* starts as a chemostat allowed us also to obtain data on chemostat reproducibility. As seen from Table 2 the RSDs of the chemostat data were similar to those from the *A-stat* experiments. The latter indicated that the continuous increase of dilution rate in *A-stat* experiments did not change the reproducibility. Furthermore, *A-stat* is also reproducible at the proteome level (see Figure 2). Pearson correlation coefficients (R) between *A-stat* samples were between 0.95 – 0.97, and is comparable to the chemostat sample correlation of 0.99.

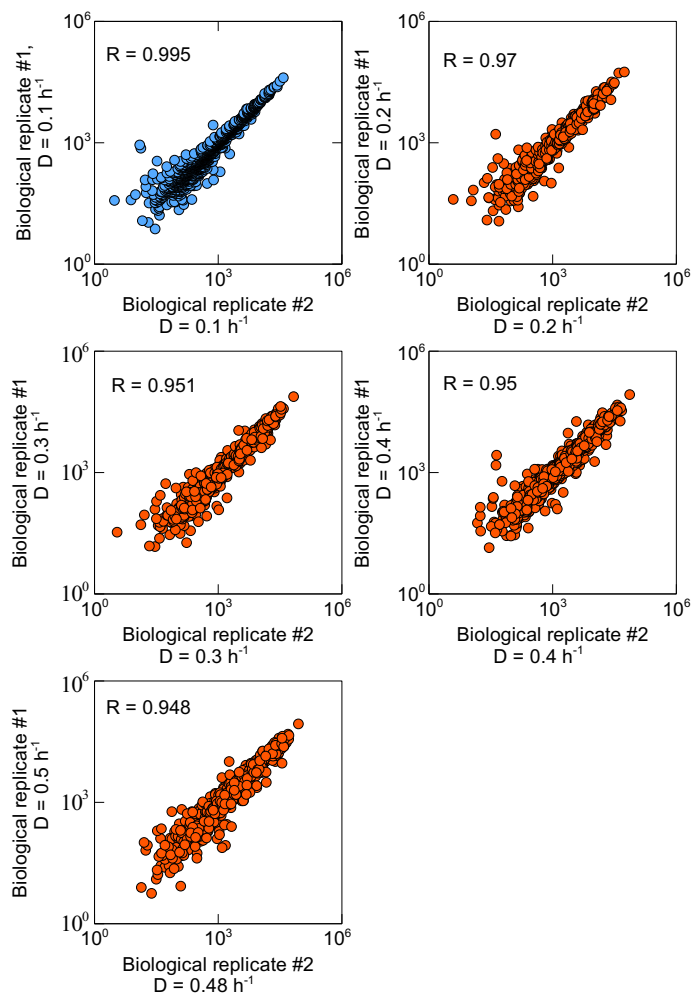


Figure 2 – Comparison of *E. coli* K-12 MG1655 absolute proteome data (copies per cell) of replicate *A-stat* and chemostat experiments (unpublished data). Blue dots represent chemostat and red ones *A-stat* data. Correlation of chemostat biological replicates is similar with *A-stat*. R is the Pearson correlation coefficient, D is the dilution rate, h^{-1} .

4.2 EXPERIMENTS WITH *L. lactis*

Table 3 summarizes the results of a study of how reproducible the following parameters are in accelerostat experiments of *L. lactis* IL1403: Y_{xs} , Y_{lg} (produced lactate per consumed glucose), I_{glucose} (specific consumption of glucose), I_{AA} (total amount of amino acids consumed per dry biomass) and O_{lactate} (specific production of lactate). The RSD values were, with one exception better, than 5%, and similar to *E. coli* K-12 MG1655 experiments, RSD of the main physiological parameters in chemostat are comparable with those determined in A-stat.

A high correlation of both proteome and transcriptome data was also found (Figure 3 and Figure 4). Importantly, these figures show that the correlation of proteome and transcriptome data in biological replicates is similar for A-stat and chemostat.

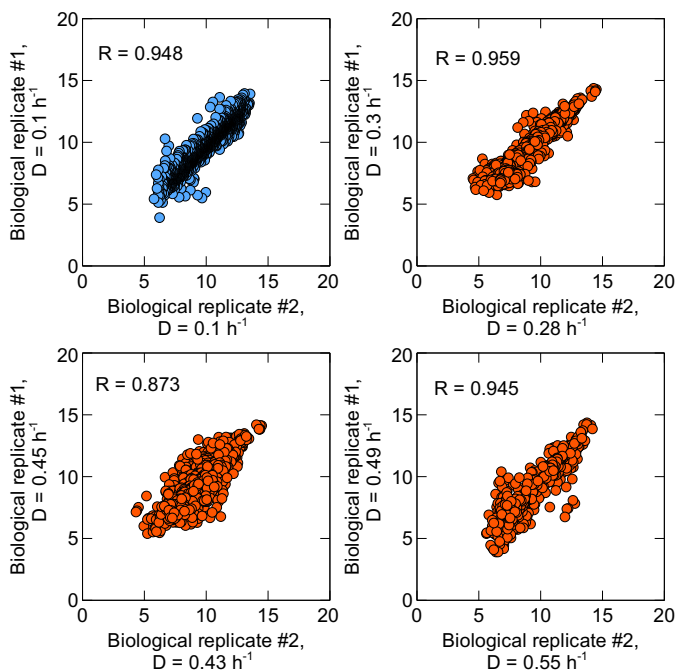


Figure 3 – Correlation of *L. lactis* IL1403 transcriptome data (\log_2) of DNA microarray spot intensities). Blue dots represent chemostat and red dots A-stat data. Correlation of chemostat biological replicates is similar with A-stat (Publication III). R is the Pearson correlation coefficient, D is the dilution rate, h^{-1}

Table 3 – Reproducibility of five glucose-limited accelerostat experiments with *L. lactis* IL1403. The values of RSD of the chemostats at a dilution rate 0.1 h^{-1} are also presented in Publication III. Average of relative standard deviations of five replicates are shown in all cases.

μ h^{-1}	RSD of Y_{xs} %	RSD of Y_{Lg} %	RSD of I_{glucose} %	RSD of I_{AA} %	RSD of O_{lactate} %
0.1 – 0.6	4.6	2.9	4.4	4.1	6.7
chemostat (0.1)	2.3	2.7	2.3	3.4	5.5

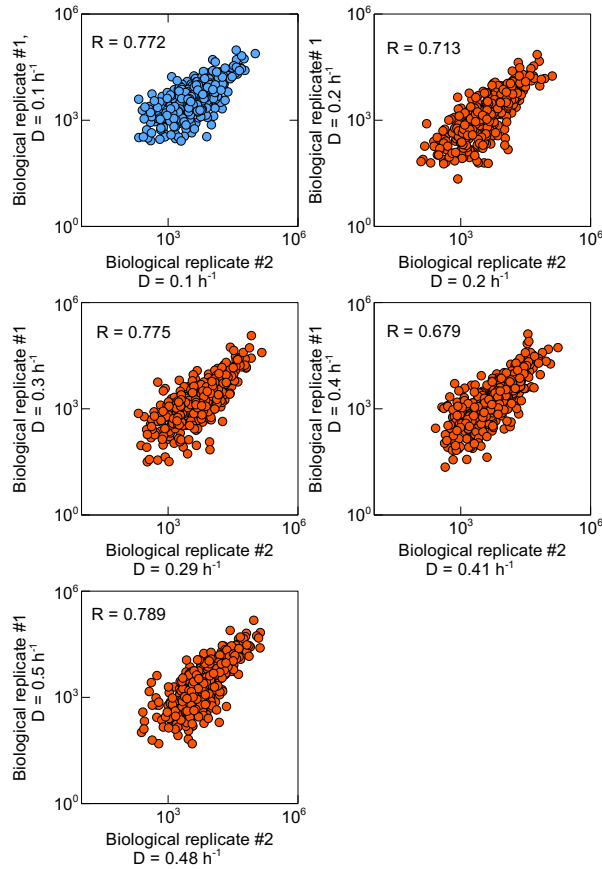


Figure 4 – Correlation of *L. lactis* IL1403 absolute proteome data (copies per cell) of biological replicates of A-stat and chemostat [47]. Blue dots represent chemostat and red dots A-stat data. Correlation of chemostat biological replicates is similar with A-stat. R is the Pearson correlation coefficient, D is the dilution rate, h^{-1} .

4.3 COMPARISON OF ACCELEROSTAT WITH CHEMOSTAT (PUBLICATION II AND PUBLICATION III)

4.3.1 Comparison using *E. coli* K-12

The choice of the acceleration of dilution is one of the main factors that may lead to differences in quantitative data between accelerostat and chemostat cultivation experiments. In chemostat, steady state is usually achieved by pumping through at least five working volumes, which ensures that most of the fermentation products from previous growth conditions not synthesized at the steady growth rate are diluted to trace levels. Because it is unusual to apply such long dilutions in *A-stat* it is clear that concentrations in *A-stat* experiments may differ from those performed in chemostat. The concordance between *A-stat* and chemostat was validated in glucose-limited *E. coli* K-12 MG1655 experiments. A relatively large difference between glucose-limited cultures of *E. coli* K-12 W3350 in *A-stat* and chemostat was shown earlier [3], however, no such deviation of quantitative data was observed in the current study (Figure 5). This figure shows that specific products in glucose-limited *A-stat* and chemostat experiments were similar.

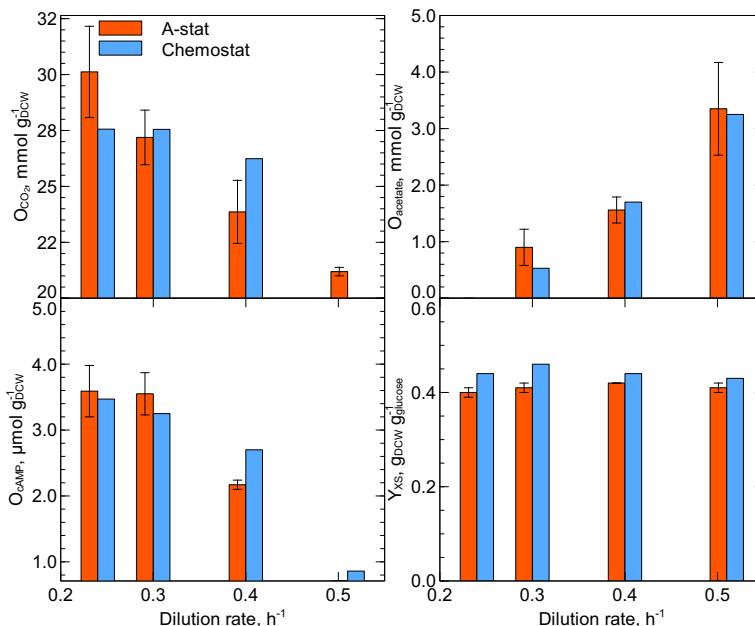


Figure 5 – Comparison of *A-stat* and chemostat glucose-limited cultivations of *E. coli* K-12 MG1655 at dilution rates: 0.24 h^{-1} , 0.30 h^{-1} , 0.40 h^{-1} , 0.51 h^{-1} . Red bars indicate data from *A-stat* experiments and blue bars from chemostat experiments. Error bars show standard deviations between three replicates. Note that CO_2 was not determined in chemostat at $D = 0.5 \text{ h}^{-1}$. Acetate was not detected at a dilution rate of 0.24 h^{-1} in *A-stat* and chemostat nor was cAMP found in *A-stat* at a dilution rate of 0.5 h^{-1} . O_{CO_2} is the specific production of CO_2 , $\text{mmol} \cdot \text{g}_{\text{DCW}}^{-1}$; O_{acetate} is the specific production of acetate, $\text{mmol} \cdot \text{g}_{\text{DCW}}^{-1}$; O_{cAMP} is the specific production of cAMP, $\mu\text{mol} \cdot \text{g}_{\text{DCW}}^{-1}$; Y_{xs} is the biomass yield, $\text{g}_{\text{DCW}} \cdot \text{g}_{\text{glucose}}^{-1}$

Although the specific production of acetate was similar in *A*-stat and chemostat experiments, acetate concentrations were smaller in *A*-stat (see Figure 6). This can be explained by the difference in the extent of dilution of the acetate in the cultures. To show the differences in metabolite concentrations between *A*-stat and chemostat, we simulated the concentration of acetate in the bioreactor. Figure 7 illustrates the situation for the case where acceleration of dilution is 0.01 h^{-2} and mimics acetate accumulation in the bioreactor while taking into consideration only dilution. The simulation starts at a dilution rate of 0.3 h^{-1} where acetate production is zero. When the dilution rate is increased, acetate production starts and rises linearly with rising dilution rate in both in *A*-stat and in chemostat until a dilution rate of 0.5 h^{-1} . The simulated acetate concentration in *A*-stat is around $0.4 - 0.5 \text{ mM}$ lower than in chemostat (see Figure 7).

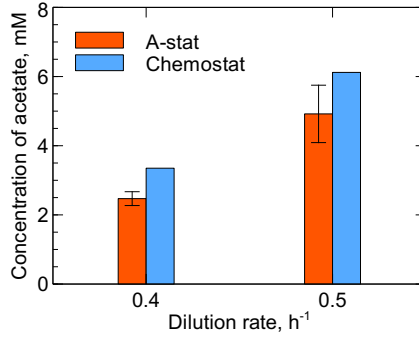


Figure 6 – Comparison of *A*-stat and chemostat in glucose-limited cultivation of *E. coli* K-12 MG1655 at dilution rates: 0.40 h^{-1} , 0.51 h^{-1} . Red bars indicate data from *A*-stat and blue bars from chemostat experiments. Error bars show standard deviations between three replicate *A*-stat experiments.

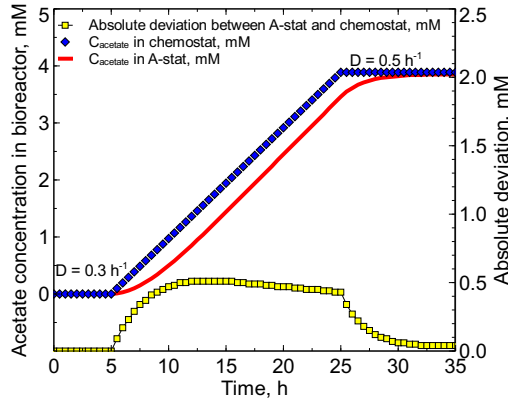


Figure 7 – Simulation of the difference in the amount of acetate in the bioreactor between *A*-stat and chemostat experiments. Y_{xs} is constant during the simulation, but O_{acetate} is increasing linearly with rising dilution rate. Acceleration of dilution in *A*-stat is 0.01 h^{-2} . Note that for chemostat concentrations, the time on the x-axis is not relevant; Every point on the figure stands for separate experiment. D is the dilution rate, h^{-1} . C_{acetate} is the concentration of acetate, mM

It is clear that concentration differences in *A-stat* and chemostat may reduce concordance between *A-stat* and chemostat data. Acetate is known to have a negative effect on bacterial growth [48] and therefore one could suspect that lower concentration in *A-stat* may result in less stressed cells. That could cause differences in *A-stat* and chemostat data. The influence of acetate to maximal specific growth rate has been studied before and it has been shown that notable decrease is caused by 8 mM of acetate [49]. That is significantly more than the acetate concentration difference calculated above (0.4-0.5 mM) and, therefore, it is likely that the effect of reduced acetate concentration on cells metabolism is negligible.

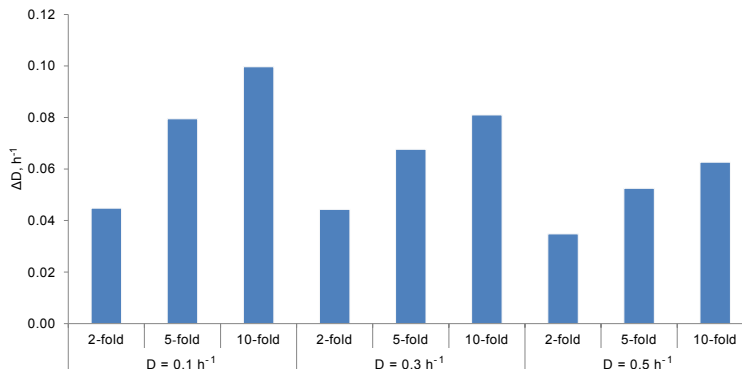


Figure 8 – Simulation of the difference in protein concentration in *A-stat* and chemostat when protein expression is suddenly decreased while dilution rate is increased. Change of dilution rate (ΔD) shows how much dilution rate could increase in *A-stat* until the protein concentration difference from chemostat is less than 5%. Fold changes represent decreases in protein expression and dilution rates corresponding to dilution rates where a decrease in protein expression was simulated. D is the dilution rate, h^{-1} .

Considering the discussion in Section 1.1.2 it appears that removal of proteins after down-regulation is relatively slow process that could cause differences between *A-stat* and chemostat. Therefore, we simulated of how long it takes for *A-stat* culture to reach similar protein concentrations as chemostat when protein expression is suddenly decreasing during an increase in dilution rate. Decrease of protein concentration in cells depends on a dilution effect that is caused by cell growth and protein degradation rate (average protein half-life = 3 h, (unpublished data)). Simulations were performed at different dilution rates to illustrate the more profound dilution effect at higher dilution rates (see Figure 8). Self-evidently, the greater the protein expression decrease the more time (larger ΔD) it takes in *A-stat* to reach chemostat protein concentrations, therefore, different extents of protein expression changes were analyzed (see Figure 8). It should be noted that *A-stat* protein concentration was considered similar to chemostat when the calculated concentration difference was less than 5%. Figure 8 illustrates the results and shows that in case of a 2 times protein expression decrease *A-stat* culture would have about 0.04 h^{-1} higher dilution rate when protein concentration reaches similar value to chemostat. That shows that when protein expression decreases by 2 times at $D = 0.1 \text{ h}^{-1}$, protein concentrations in *A-stat* are higher between dilution rates $0.1 - 0.14 \text{ h}^{-1}$

compared to chemostat. The difference is greater when the protein expression decrease is larger. It should be noted that at higher dilution rates the difference between *A-stat* and chemostat is smaller due to the greater dilution effect.

The calculated results should be interpreted as general guidelines rather than exact values because an average protein degradation rate is used in the simulations. Moreover, the calculations consider a sudden specific growth rate dependent protein expression decrease that occurs when the dilution rate is increased within only 0.00017 h^{-1} . This should be considered a worse case scenario because it is more likely that cells are not so sensitive to specific growth rate. The latter is supported by the fact that *E. coli* is able to increase its growth rate very rapidly when a glucose pulse is applied [21, 22]. When the protein expression change is not so sudden, then protein concentration in *A-stat* would be more similar to the change in chemostat.

4.3.1.1 Comparison at the transcriptome and proteome level

In addition to the previous analysis, the differences of *A-stat* and chemostat were also determined at the transcriptome level at a dilution rate 0.51 h^{-1} and 0.48 h^{-1} in chemostat and *A-stat*, respectively (Publication II). Figure 9 provides the results and shows that the Pearson's correlation coefficient for DNA microarray spot intensities is 0.95. The correlation value is similar to the one obtained for technical replicates of transcriptomic data. The latter indicated that the proportional distribution of mRNAs in *A-stat* and chemostat cultures can be considered similar. One could suspect that the difference between *A-stat* and chemostat at the proteome level is due to the relatively long half-lives of proteins. However, that seems to be not the case, because correlation between protein expressions determined from *A-stat* and chemostat at similar dilution rates was relatively high and exceeded even the R value of corresponding differences in chemostats (see Figure 10).

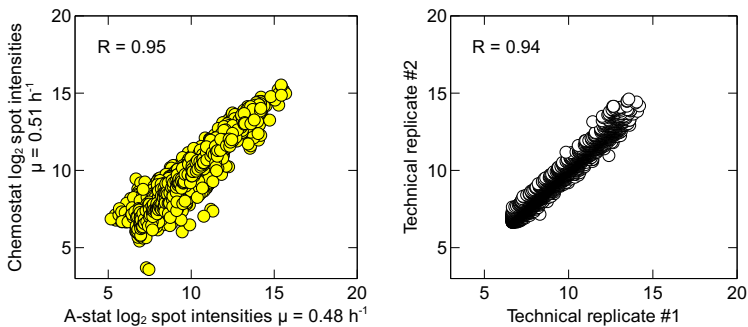


Figure 9 – Comparison of *A-stat* and chemostat at the transcriptome level. $\log(2)$ DNA microarray spot intensities of *A-stat* at $\mu = 0.48 \text{ h}^{-1}$ and chemostat at $\mu = 0.51 \text{ h}^{-1}$ experiments with *E. coli* K-12 MG1655 compared with the correlation of technical replicates (Publication II). Only values over 100 intensity units are reported.

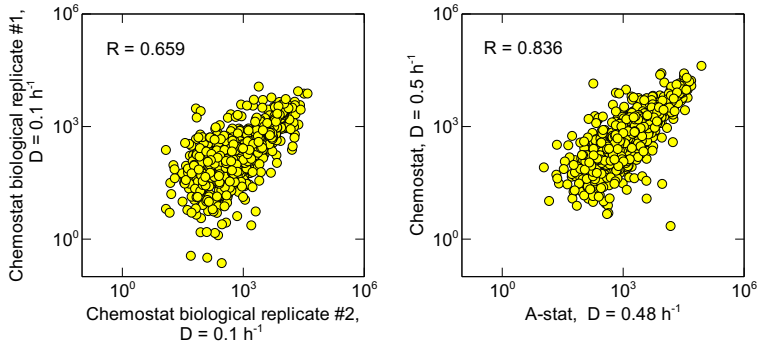


Figure 10 – Comparison of *A-stat* and chemostat at the proteome level. Absolute proteome numbers (copies per cell) of *A-stat* at $D = 0.48 \text{ h}^{-1}$ and chemostat at $D = 0.50 \text{ h}^{-1}$ experiments with *E. coli* K-12 MG1655 compared with the correlation of chemostat biological replicates (unpublished data).

4.3.2 Comparison using *L. lactis* IL1403

From the data published so far, it could be expected that the concordance between *A-stat* and chemostat may be species dependent. To test this we compared quantitative data from glucose-limited *A-stat* and chemostat ($D = 0.45 \text{ h}^{-1}$) of *L. lactis* IL1403. Note that in the case of *L. lactis*, a two times slower acceleration of dilution (0.005 h^{-2}) was used because of the experiments performed earlier [50]. Figure 11 summarizes the result of this *A-stat* and chemostat comparison which shows remarkable similarity.

Considering all comparison experiments, we can say that the reproducibility of *A-stat* experiments is comparable to that of chemostat experiments. In addition, it was shown that carrying out the *A-stat* results are representative of steady state data if appropriate acceleration of dilution values are used: $\alpha_d = 0.01 \text{ h}^{-2}$ in the case of *E. coli* K-12 and 0.005 h^{-2} in the case of *L. lactis* IL1403. That was shown at the level of measured growth parameters for both *L. lactis* IL1403 and *E. coli* K-12 and, importantly, the transcriptome and proteome level for *E. coli* K-12.

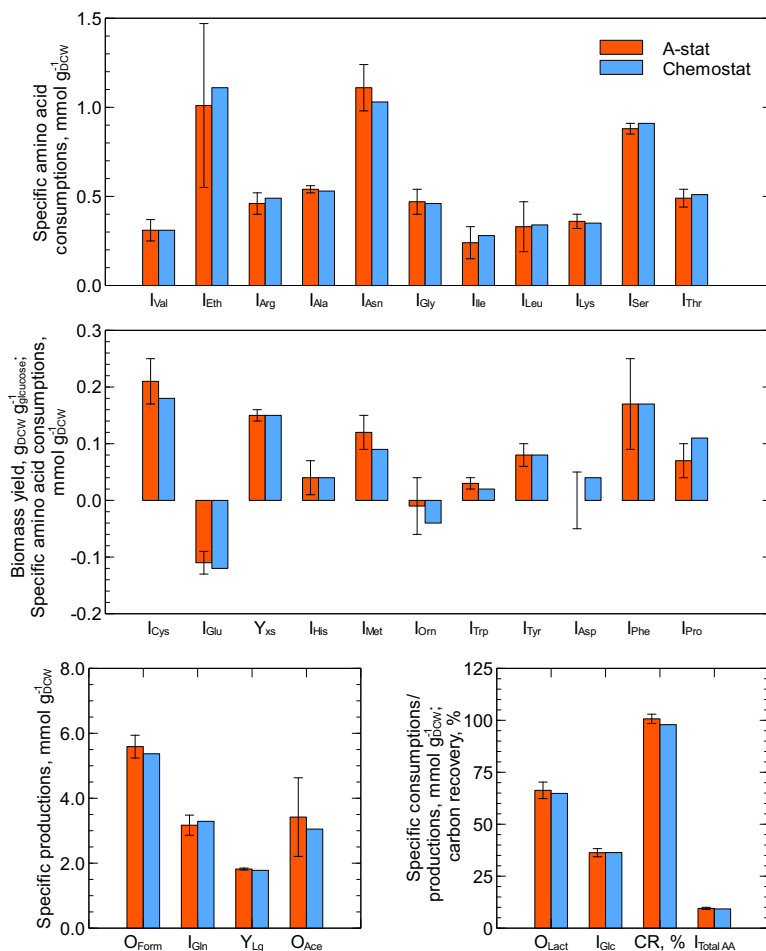


Figure 11 – Comparison of A-stat and chemostat in glucose-limited cultivation of *L. lactis* IL1403 at $D = 0.45 \text{ h}^{-1}$. Red bars indicate data from A-stat and blue bars from chemostat. Error bars show standard deviations between five replicates. The symbols I and O refer to specific consumption and production and have units of $\text{mmol} \cdot \text{g}_{\text{DCW}}^{-1}$ for the following: I_{Val} (L-Valine), I_{Glc} (glucose), I_{Arg} (L-Arginine), I_{Ala} (L-Alanine), I_{Asn} (L-Asparagine), I_{Gly} (L-Glycine), I_{Ile} (L-Isoleucine), I_{Leu} (L-Leucine), I_{Lys} (L-Lysine), I_{Ser} (L-Serine), I_{Thr} (L-Threonine), I_{Cys} (L-Cysteine), I_{Glu} (L-Glutamate), I_{His} (L-Histidine), I_{Met} (L-Methionine), I_{Orn} (L-Ornithine), I_{Trp} (L-Tryptophane), I_{Tyr} (L-Tyrosine), I_{Asp} (L-Aspartate), I_{Phe} (L-Phenylalanine), I_{Pro} (L-Proline), I_{Gln} (L-Glutamine), I_{Total AA} (total amount of amino acids consumed per biomass), O_{Form} (formate), O_{Ace} (acetate), O_{Lact} (lactate), and O_{Eth} (ethanol). Y_{Lg} is the production of lactate per consumed glucose ($\text{mol} \cdot \text{mol}^{-1}$). Y_{xs} is the biomass yield ($\text{g}_{\text{DCW}} \cdot \text{g}_{\text{glucose}}^{-1}$). CR is the carbon recovery (%). Note that negative consumption indicates production.

4.4 CULTURE ADAPTATION IN CHANGE-STAT CULTURES (PUBLICATION IV AND PUBLICATION V)

4.4.1 Culture hysteresis in *D*-stat (Publication IV)

Glucose-limited cultures of *L. lactis* IL1403 were studied in relatively long (around 60 generations) dilution rate (*D*-stat) experiments in Publication IV. pH or temperature was smoothly changed symmetrically from optimum to stress conditions and back during the experiments. It was expected that culture parameters, *e.g.* Y_{xs} and O_{lactate} will follow the parameter being changed (pH and/or temperature) and for the end of the experiment initial Y_{xs} and O_{lactate} values will be restored. Looking at Figure 12 this is clearly not the case. Both Y_{xs} and O_{lactate} acquired stable concentrations that are different from their initial concentrations during the final chemostat phase; Hysteresis occurred during the experiment. In case of *D*-stat with a pH change, hysteresis was also determined at the gene expression level. The expression levels of certain arginine and citrate metabolism genes changed during the first pH shift: *arcA* (arginine deiminase), *arcC1* (carbamate kinase), *arcC2* (carbamate kinase), *arcD1* (arginine-ornithine antiporter), *argE* (acetylornithine deacetylase), *argR* (arginine catabolic regulator), *citC* (acetate-SH-citrate lyase ligase), and *citD* (citrate lyase subunit gamma). However, instead of recovering their expression after moving back to initial environmental conditions, these genes remained expressed at the level attained during the first pH shift. This phenomena is likely caused by culture adaptation that occurred because of applied stress conditions during this long fermentation experiment. Interestingly, no difference in biomass yield and extracellular metabolome was observed in chemostats with the same dilution rate. This observation of hysteresis raises a question: How long can we run changestat experiments to avoid mutational adaptation?

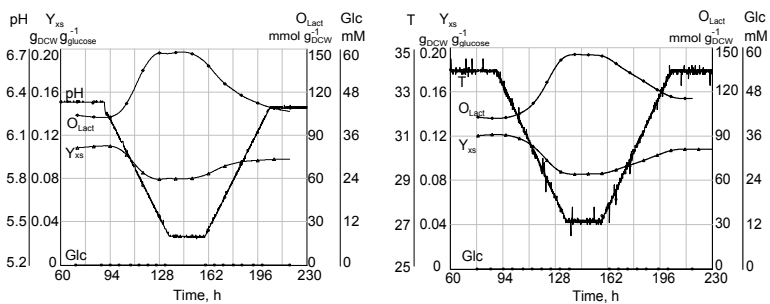


Figure 12 – *L. lactis* IL1403 *D*-stat experiments with the change of pH or temperature performed at $D = 0.2 \text{ h}^{-1}$. Glc is the glucose concentration in the bioreactor (mM); O_{Lact} is the lactate yield based on biomass production ($\text{mmol} \cdot \text{g}_{\text{DCW}}^{-1}$); T is the temperature ($^{\circ}\text{C}$); Y_{xs} is the biomass yield based on glucose consumption ($\text{g}_{\text{DCW}} \cdot \text{g}_{\text{glucose}}^{-1}$)

gltP (glutamate and aspartate dicarboxylate/amino acid:cation symporter) and *yjcO* (conserved protein) was found. Mutations that improve glucose uptake, for instance in the glucose phosphotransferase system *ptsG*, or the stress induced sigma factor *rpoS*, might be expected during continuous cultivation based on results in similar chemostat environments [37–40, 43, 51]. However, we did not detect the appearance of either of these mutations.

Table 4 – Consensus mutations in all HT DNA sequenced samples.

Related gene(s)	Genome position	Mutation	Annotation	Function(s) of related gene(s)
<i>ylbE</i>	547,694	A → G	pseudogene	Predicted protein
<i>ylbE</i>	547,835	+G	pseudogene	Predicted protein
<i>flhD,uspC</i>	Δ1,976,527 - 1,977,302	IS1 deletion	intergenic	Subunit of flagella regulator FlhD ₂ C ₂ universal stress protein
<i>rrlD</i>	3,422,257 - 3,422,259	ATC → CAT	noncoding	23S ribosomal RNA
<i>ppiC,yifO</i>	3,957,957	C → T	intergenic	Peptidyl-prolyl cis-trans isomerase C / conserved protein
<i>gltP,yjcO</i>	4,294,291	T → C	intergenic	Glutamate and aspartate DAACS transporter / conserved protein
<i>gltP,yjcO</i>	Δ4,294,305 - 4,294,415	Δ 111 bp	intergenic	Glutamate and aspartate DAACS transporter / conserved protein

Detection of mutations in all samples could point to errors in the reference genome sequence as well as problems of handling of cultures in stock centers. To address the latter possibility, we sequenced these regions in an *E. coli* K-12 MG1655 strain that was ordered from another stock center (SSI). The presence of identical mutations in MG1655 strains with different origin would suggest errors in the reference genome whereas variation of the mutations present in different stocks would indicate problems in strain handling. We found that six out of seven mutations detected in the MG1655 strain obtained from the DSMZ collection (see Table 4) were also present in the SSI strain. In addition, most of the consensus mutations found in the current study have been reported before in HT DNA sequencing studies of *E. coli* K-12 MG1655 strains acquired from other sources [52–54]. Together, these observations suggest that most of the differences observed (see Table 4) were actually sequencing errors in the reference genome. On the other hand, our results also demonstrate that the two *E. coli* K-12 MG1655 strains investigated were not exactly the same in different stock centers (only the SSI strain had the IS1 insertion in the *flhD* regulon). This observation highlights a problem that may arise during strain handling. The population bottleneck caused by picking a single colony before sub-culturing is particularly prone to fixing a new mutation in the resultant sample.

4.4.4 Evolution did not take place during *A-stat* cultivation

Next, we turned our attention to the dynamics of polymorphic mutations in the population, *i. e.* to the mutations present only in a subset of individuals. Using HT DNA sequencing data with 111 times average genome coverage mutations present only in sub-populations we predicted (see Table 5). Only a few of these appeared to be in more than 5% of the whole population by the end of the experiment. All predicted sub-populations were smaller than 20% of the whole population (see Supplemental Table S1). A problem in analysing sub-populations with low frequency using HT DNA sequencing data is that one has to distinguish true sub-populations from false positives caused by sequencing errors with nontrivial biases. Hence, additional validation with Sanger sequencing was performed for high-scoring predictions (see Supplemental Table S1). Three high-scoring sub-populations (*betA*, *cspH/cspG*, *glyA*) with a rising trend during the experiment were validated from the sample taken at $D = 0.48 \text{ h}^{-1}$. Two of the three mutations (*betA*, *cspH/cspG*) were also detected in the stock culture (see Figure 14). The one sub-population that was not detected with HT DNA sequencing in the stock culture, therefore, might have arose during the experiment, was a SNP in *glyA*. However, the presence of a *glyA* population in the stock culture was verified by colony screening (see below) proving that all of these sub-populations were also present in the stock culture at detectable frequencies.

Table 5 – Mutations present in sub-populations in the HT DNA sequenced samples. This table shows experimentally validated sub-populations. See Supplemental Table S1 for complete information about all high-scoring sub-populations predicted from the HT DNA sequencing data. Positions of IS5 insertions give the target site nucleotides that were duplicated upon insertion of the new IS copy. Both new IS5 copies inserted in the forward (+) orientation in the genome.

Related gene(s)	Genome position	Mutation	Annotation	Function(s) of related gene(s)
<i>yadL</i>	152,081 - 152,084	IS5 insertion	coding region	Gene of predicted chaperone-usher fimbrial operon
<i>betA</i>	326,446	C → T	G9D (GGT → GAT)	Choline dehydrogenase
<i>yahE</i>	335,361	T → C	F71F (TTT → TTC)	Predicted protein
<i>cspH,cspG</i>	1,050,465	T → A	intergenic	<i>CspA</i> -family member, cold shock protein
<i>flhD,uspC</i>	1,977,510 - 1,977,513	IS5 insertion	intergenic	Subunit of flagella regulator FlhD ₂ C ₂ universal stress protein
<i>glyA</i>	2,683,035	G → A	H165H (CAC → CAT)	Serine hydroxymethyl-transferase
<i>dppD</i>	3,701,283	G → A	L197L (CTG → TTG)	Dipeptide ABC transporter ATP-binding component.

To further confirm that the detected heterogeneity did not arise during the cultivation experiment or result from differences between stock culture aliquots, the occurrence of sub-populations in two additional *A-stat* experiments (started from separate aliquots of the same stock culture) was investigated. If the sub-population distribution at the end of the *A-stat* experiments was reproducible, one could conclude that the discovered mutations were the consequence of selection acting on existing variation, *i. e.* the set of mutations already present in the stock culture at detectable levels. Indeed, it was found that all sub-populations with SNPs that had a rising trend (*betA*, *cspH/cspG*, *glyA*) were present in all three replicate *A-stat* experiments at similar frequencies. This observation further supported the hypothesis that the previously mentioned sub-populations were already present in the stock culture. Therefore, we conclude that the current 20-generation continuous cultivation duration of *E. coli* K-12 MG1655 in *A-stat* was short enough to avoid the emergence of new sub-populations, making it suitable for studying cell physiology and collecting quantitative data for metabolic modeling without interference from new spontaneous mutations.

4.4.5 Heterogeneity of stock culture

After confirming that the stock culture was a mixed culture, we further investigated the predicted sub-populations. The following sub-populations were predicted (frequencies ranging between 6.5-17.0% in stock culture) and validated: *dppD*, *allD*, *recB*, *yahE* (see Supplemental Table S1). It was found that the putative mutations in *allD* and *recB* with low scores were false positives (data not shown) whereas high-scoring predictions in *dppD* and *yahE* were genuine (data not shown). In addition, two IS-related mutations, namely, IS5 insertions in the *flhD* regulon (*flhD/uspC*) and in *yadL* were detected in the HT DNA sequencing data and were verified to have frequencies below 10% (data not shown).

We next investigated whether any of these mutations existed in combination in the same cells. Four mutations had increasing allele frequencies during the experiment: *betA*, *cspH/cspG*, *glyA* and *flhD/uspC*. IS elements in the regulatory region of *flhD* that lead to increased motility were common in *E. coli* [34]. Therefore, we screened colonies acquired from the stock culture used in the *A-stat* experiments for increased motility as described by Baker and co-workers [34]. Out of the 42 investigated clones, four turned out to be motile and contained the IS5 insertion described above (data not shown). All the motile colonies were screened for *betA*, *cspH/cspG* or *glyA* mutations. Two clones had the *betA* and *cspH/cspG* SNPs, and the other two contained the *glyA* mutation (data not shown). Next, we hypothesised that mutations in *yahE* and *yadL* might also exist in the same sub-population because the frequency of both alleles remained constant during the course of the experiment (see Supplemental Table S1). Screening of stock culture clones revealed that all but one clone isolated with the mutation in *yahE* also contained the IS5 insertion in *yadL*.

The fact that the mutation in *yahE* was synonymous made it seem likely that the single *yahE* mutant clone without *yadL* harboured additional mutations. Therefore, we tested it for the presence of a *yhdJ/yhdU* (predicted methyltransferase / predicted membrane protein) mutation because it was the only predicted mutation with considerable reliability

(high overall score, see [Supplemental Table S1](#) legend for description) with a change in allele frequency was similar to *yahE* in the *A-stat* experiment (see [Supplemental Table S1](#)). It turned out that the *yhdJ/yhdU* mutation was not present in the *yahE* clone (data not shown). However, given its low frequency in the population, we cannot exclude the possibility that an undetected mutation may be present in this genetic background. After resolving the genetic linkage between the most common mutations in the population, we conclude that roughly 31% of our stock culture contained at least one mutation relative to the majority genotype.

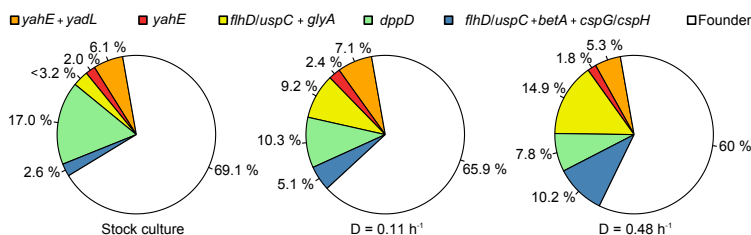


Figure 14 – Change of the population heterogeneity in an *E. coli* K-12 MG1655 *A-stat* experiment. All the sub-populations shown here were verified with Sanger sequencing. In stock culture, mutation in *glyA* was not detected with HT DNA sequencing, therefore, the frequency for this sample was estimated from genome coverage at a position where *glyA* mutation was detected in other samples. See [Supplemental Table S1](#) for abbreviations and details about mutations.

Our results showed that the current HT DNA sequencing technology was suitable and even necessary for accurate sub-population analysis. We also demonstrated specifically that *E. coli* K-12 MG1655 has sufficient genome stability to be used in glucose-limited *A-stat* experiments with duration of at least 20 generations of continuous cultivation for studying cell physiology, while avoiding mutations from adaptive evolution that occur during longer experiments. One has to be careful when receiving a strain from a culture collection because the culture may contain a considerable amount of mutational heterogeneity. Colony purification followed by genome sequence determination is necessary to be sure of a strain's genotype.

SUMMARY

CONCLUSIONS

FIVE CONCLUSIONS RESULT FROM THIS DOCTORAL WORK.

- I It was shown that the data obtained in *A-stat* experiments, including biomass yields, extracellular metabolomes as well as transcriptomes and proteomes in [Publication I](#), [Publication II](#), and [Publication III](#) are reproducible. In addition to highly reproducible quantitative data it was also possible to detect metabolic switch points, for example the start of acetate overflow, with relatively small deviations between replicate experiments.
- II *A-stat* data is steady state representative if appropriate acceleration of dilution values are used. It was confirmed in [Publication I](#) and [Publication II](#) that the recommended acceleration of dilution for *Escherichia coli* K-12 MG1655 is 0.01 h^{-2} , and in [Publication III](#) we found that for *Lactococcus lactis* IL1403 an appropriate acceleration of dilution is 0.005 h^{-2} . It was shown for the first time that the transcriptome and proteome data obtained in *A-stat* and chemostat experiments quantitatively coincide.
- III It was shown in [Publication V](#) that no new sub-populations emerged during *A-stat* experiments with *Escherichia coli* K-12 MG1655.
- IV It was shown in [Publication V](#) that the genetic heterogeneity observed in a cultivated population of cells originated from stab agar culture received from a stock collection (DSMZ).
- V Current *HT DNA* sequencing methods are suitable to validate the genomic stability of strains (or consortia), and this technique is recommended to be applied in quantitative cell physiology studies.

BIBLIOGRAPHY

BIBLIOGRAPHY

- [1] J Monod. La technique de culture continue, théorie et applications. *Annales de l'Institut Pasteur*, 79:390–410, 1950.
- [2] A Novick and L Szilard. Description of the chemostat. *Science*, 112(2920):715–716, December 1950.
- [3] Toomas Paalme, Anne Kahru, Raul Elken, Kalju Vanatalu, Kalle Tiisma, and Vilu Raivo. The computer-controlled continuous culture of *Escherichia coli* with smooth change of dilution rate (A-stat). *Journal of Microbiological Methods*, 24(2):145–153, December 1995.
- [4] Thomas Ferenci. Bacterial physiology, regulation and mutational adaptation in a chemostat environment. *Advances in microbial physiology*, 53:169–229, 2008.
- [5] R B Helling, C N Vargas, and J Adams. Evolution of *Escherichia coli* during growth in a constant environment. *Genetics*, 116(3):349–358, July 1987.
- [6] A Novick and L Szilard. Experiments with the chemostat on spontaneous mutations of bacteria. *Proceedings of the National Academy of Sciences of the United States of America*, 36(12):708–719, December 1950.
- [7] Andrea Veit, Tino Polen, and Volker F Wendisch. Global gene expression analysis of glucose overflow metabolism in *Escherichia coli* and reduction of aerobic acetate formation. *Applied microbiology and biotechnology*, 74(2):406–421, February 2007.
- [8] Alessandro G Franchini and Thomas Egli. Global gene expression in *Escherichia coli* K-12 during short-term and long-term adaptation to glucose-limited continuous culture conditions. *Microbiology*, 152(Pt 7):2111–2127, July 2006.
- [9] T C Dang, M Fujii, A L Rose, M Bligh, and T D Waite. Characteristics of the freshwater cyanobacterium *microcystis aeruginosa* grown in iron-limited continuous culture. *Applied and environmental microbiology*, 78(5):1574–1583, March 2012.
- [10] V Bryson and W Szybalski. Microbial selection. *Science (New York, N.Y.)*, 116(3003):45–51, July 1952.
- [11] R W Lovitt and J W Wimpenny. The gradostat: A bidirectional compound chemostat and its application in microbiological research. *Journal of general microbiology*, 127(2):261–268, December 1981.
- [12] Katrin Tomson, Jill Barber, and Kalju Vanatalu. Adaptastat—a new method for optimising of bacterial growth conditions in continuous culture: Interactive substrate limitation based on dissolved oxygen measurement. *Journal of microbiological methods*, 64(3):380–390, March 2006.

Bibliography

- [13] Kaja Kasemets, Monika Drews, Ildar Nisamedtinov, Kaarel Adamberg, and Toomas Paalme. Modification of A-stat for the characterization of microorganisms. *Journal of microbiological methods*, 55(1):187–200, October 2003.
- [14] Andreas O Helbig, Pascale Daran-Lapujade, Antonius J A van Maris, Erik A F de Hulster, Dick de Ridder, Jack T Pronk, Albert J R Heck, and Monique Slijper. The diversity of protein turnover and abundance under nitrogen-limited steady-state conditions in *Saccharomyces cerevisiae*. *Molecular bioSystems*, 7(12):3316–3326, December 2011.
- [15] K W Boehlke and J D Friesen. Cellular content of ribonucleic acid and protein in *Saccharomyces cerevisiae* as a function of exponential growth rate: calculation of the apparent peptide chain elongation rate. *Journal of bacteriology*, 121(2):429–433, February 1975.
- [16] Jonathan A. Bernstein, Pei-Hsun Lin, Stanley N. Cohen, and Sue Lin-Chao. Global analysis of *Escherichia coli* RNA degradosome function using DNA microarrays. *Proceedings of the National Academy of Sciences of the United States of America*, 101(9):2758–2763, March 2004.
- [17] H Bremer and P Dennis. Modulation of chemical composition and other parameters of the cell by growth rate. In FC Neidhardt, editor, *Escherichia coli and Salmonella: cellular and molecular biology*, volume 2, pages 1553–1569. ASM Press, Washington, D.C, 2 edition, 2002.
- [18] Ibrahim Mehmeti, Ellen M Faergestad, Martijn Bekker, Lars Snipen, Ingolf F Nes, and Helge Holo. Growth rate-dependent control in *Enterococcus faecalis*: Effects on the transcriptome and proteome, and strong regulation of lactate dehydrogenase. *Applied and environmental microbiology*, 78(1):170–176, January 2012.
- [19] Clémentine Dressaire, Emma Redon, Helene Milhem, Philippe Besse, Pascal Loubière, and Muriel Coccagn-Bousquet. Growth rate regulated genes and their wide involvement in the *Lactococcus lactis* stress responses. *BMC genomics*, 9:343, 2008.
- [20] Nobuyoshi Ishii, Kenji Nakahigashi, Tomoya Baba, Martin Robert, Tomoyoshi Soga, Akio Kanai, Takashi Hirasawa, Miki Naba, Kenta Hirai, Aminul Hoque, Pei Yee Ho, Yuji Kakazu, Kaori Sugawara, Saori Igarashi, Satoshi Harada, Takeshi Masuda, Naoyuki Sugiyama, Takashi Togashi, Miki Hasegawa, Yuki Takai, Katsuyuki Yugi, Kazuharu Arakawa, Nayuta Iwata, Yoshihiro Toya, Yoichi Nakayama, Takaaki Nishioka, Kazuyuki Shimizu, Hirotada Mori, and Masaru Tomita. Multiple high-throughput analyses monitor the response of *E. coli* to perturbations. *Science*, 316(5824):593–597, April 2007.
- [21] Sirichai Sunya, Frank Delvigne, Jean-Louis Uribelarrea, Carole Molina-Jouve, and Nathalie Gorret. Comparison of the transient responses of *Escherichia coli* to a glucose pulse of various intensities. *Applied microbiology and biotechnology*, 95(4):1021–1034, August 2012.

- [22] Hilal Taymaz-Nikerel, Walter M van Gulik, and Joseph J Heijnen. *Escherichia coli* responds with a rapid and large change in growth rate upon a shift from glucose-limited to glucose-excess conditions. *Metabolic engineering*, 13(3):307–318, May 2011.
- [23] Jochen Schaub and Matthias Reuss. In vivo dynamics of glycolysis in *Escherichia coli* shows need for growth-rate dependent metabolome analysis. *Biotechnology progress*, 24(6):1402–1407, December 2008.
- [24] C van der Sluis, B H Westerink, M M Dijkstal, S J Castelein, A J van Boxtel, M L Giuseppin, J Tramper, and R H Wijffels. Estimation of steady-state culture characteristics during acceleration-stats with yeasts. *Biotechnology and bioengineering*, 75(3):267–275, November 2001.
- [25] van Dijken JP, Bauer, Brambilla, Duboc, Francois, Gancedo, Giuseppin, Heijnen, Hoare, Lange, Madden, Niederberger, Nielsen, Parrou, Petit, Porro, Reuss, van Riel N, Rizzi, Steensma, Verrips, Vindeløv, and Pronk. An interlaboratory comparison of physiological and genetic properties of four *Saccharomyces cerevisiae* strains. *Enzyme and microbial technology*, 26(9-10):706–714, June 2000.
- [26] Helena Albergaria, Ana R Torrão, Timothy Hogg, and Francisco M Gírio. Physiological behaviour of *Hanseniaspora guilliermondii* in aerobic glucose-limited continuous cultures. *FEMS Yeast Research*, 3(2):211–216, April 2003.
- [27] Maria J. Barbosa, Jeroen Hoogakker, and René H. Wijffels. Optimisation of cultivation parameters in photobioreactors for microalgae cultivation using the A-stat technique. *Biomolecular Engineering*, 20(4–6):115–123, July 2003.
- [28] Maria J Barbosa, Jan Willem Zijffers, Adrian Nisworo, Woulter Vaes, Jan van Schoonhoven, and René H Wijffels. Optimization of biomass, vitamins, and carotenoid yield on light energy in a flat-panel reactor using the A-stat technique. *Biotechnology and bioengineering*, 89(2):233–242, January 2005.
- [29] L Girbal, J L Rols, and N D Lindley. Growth rate influences reductive biodegradation of the organophosphorus pesticide demeton by *Corynebacterium glutamicum*. *Biodegradation*, 11(6):371–376, 2000.
- [30] M Jishage and A Ishihama. Variation in RNA polymerase sigma subunit composition within different stocks of *Escherichia coli* w3110. *Journal of bacteriology*, 179(3):959–963, February 1997.
- [31] T Naas, M Blot, W M Fitch, and W Arber. Insertion sequence-related genetic variation in resting *Escherichia coli* K-12. *Genetics*, 136(3):721–730, March 1994.
- [32] T Naas, M Blot, W M Fitch, and W Arber. Dynamics of IS-related genetic rearrangements in resting *Escherichia coli* K-12. *Molecular biology and evolution*, 12(2):198–207, March 1995.

Bibliography

- [33] Eric Soupene, Wally C van Heeswijk, Jacqueline Plumbridge, Valley Stewart, Daniel Bertenthal, Haidy Lee, Gyaneshwar Prasad, Oleg Paliy, Parinya Charernnoppakul, and Sydney Kustu. Physiological studies of *Escherichia coli* strain MG1655: Growth defects and apparent cross-regulation of gene expression. *Journal of bacteriology*, 185(18):5611–5626, September 2003.
- [34] Clive S Barker, Birgit M Prüss, and Philip Matsumura. Increased motility of *Escherichia coli* by insertion sequence element integration into the regulatory region of the *flhD* operon. *Journal of bacteriology*, 186(22):7529–7537, November 2004.
- [35] Julian Adams. Microbial evolution in laboratory environments. *Research in microbiology*, 155(5):311–318, June 2004.
- [36] K Manch, L Notley-McRobb, and T Ferenci. Mutational adaptation of *Escherichia coli* to glucose limitation involves distinct evolutionary pathways in aerobic and oxygen-limited environments. *Genetics*, 153(1):5–12, September 1999.
- [37] L M Wick, M Quadroni, and T Egli. Short- and long-term changes in proteome composition and kinetic properties in a culture of *Escherichia coli* during transition from glucose-excess to glucose-limited growth conditions in continuous culture and vice versa. *Environmental microbiology*, 3(9):588–599, September 2001.
- [38] Lukas M Wick, Hansueli Weilenmann, and Thomas Egli. The apparent clock-like evolution of *Escherichia coli* in glucose-limited chemostats is reproducible at large but not at small population sizes and can be explained with monod kinetics. *Microbiology (Reading, England)*, 148(Pt 9):2889–2902, September 2002.
- [39] L Notley-McRobb and T Ferenci. Adaptive *mgl*-regulatory mutations and genetic diversity evolving in glucose-limited *Escherichia coli* populations. *Environmental microbiology*, 1(1):33–43, February 1999.
- [40] L Notley-McRobb and T Ferenci. The generation of multiple co-existing mal-regulatory mutations through polygenic evolution in glucose-limited populations of *Escherichia coli*. *Environmental microbiology*, 1(1):45–52, February 1999.
- [41] R F Rosenzweig, R R Sharp, D S Treves, and J Adams. Microbial evolution in a simple unstructured environment: Genetic differentiation in *Escherichia coli*. *Genetics*, 137(4):903–917, August 1994.
- [42] Ram P Maharjan, Thomas Ferenci, Peter R Reeves, Yang Li, Bin Liu, and Lei Wang. The multiplicity of divergence mechanisms in a single evolving population. *Genome biology*, 13(6):R41, 2012.
- [43] Lucinda Notley-McRobb, Shona Seeto, and Thomas Ferenci. The influence of cellular physiology on the initiation of mutational pathways in *Escherichia coli* populations. *Proceedings of the Royal Society B: Biological Sciences*, 270(1517):843–848, April 2003.

- [44] Thea King, Akira Ishihama, Ayako Kori, and Thomas Ferenci. A regulatory trade-off as a source of strain variation in the species *Escherichia coli*. *Journal of bacteriology*, 186(17):5614–5620, September 2004.
- [45] Elaine R Mardis. Next-generation DNA sequencing methods. *Annual review of genomics and human genetics*, 9:387–402, 2008.
- [46] J E Barrick and R E Lenski. Genome-wide mutational diversity in an evolving population of *Escherichia coli*. *Cold Spring Harbor symposia on quantitative biology*, 74:119–129, 2009.
- [47] Kaarel Adamberg, A. Seiman, and Raivo Vilu. Increased biomass yield of *Lactococcus lactis* by reduced overconsumption of amino acids and increased catalytic activities of enzymes. *PLoS One*, In press, 2012.
- [48] F Diez-Gonzalez and J B Russell. Effects of carbonylcyanide-m-chlorophenylhydrazone (CCCP) and acetate on *Escherichia coli* O157:H7 and K-12: uncoupling versus anion accumulation. *FEMS microbiology letters*, 151(1):71–76, June 1997.
- [49] K Nakano, M Rischke, S Sato, and H Märkl. Influence of acetic acid on the growth of *Escherichia coli* K12 during high-cell-density cultivation in a dialysis reactor. *Applied microbiology and biotechnology*, 48(5):597–601, November 1997.
- [50] Kaarel Adamberg, Petri-Jaan Lahtvee, Kaspar Valgepea, Kristo Abner, and Raivo Vilu. Quasi steady state growth of *Lactococcus lactis* in glucose-limited acceleration stat (A-stat) cultures. *Antonie van Leeuwenhoek*, 95(3):219–226, 2009.
- [51] Margie A Kinnersley, William E Holben, and Frank Rosenzweig. E Unibus Plurum: Genomic analysis of an experimentally evolved polymorphism in *Escherichia coli*. *PLoS genetics*, 5(11):e1000713, November 2009.
- [52] Tom M Conrad, Andrew R Joyce, M Kenyon Applebee, Christian L Barrett, Bin Xie, Yuan Gao, and Bernhard Ø Palsson. Whole-genome resequencing of *Escherichia coli* K-12 MG1655 undergoing short-term laboratory evolution in lactate minimal media reveals flexible selection of adaptive mutations. *Genome biology*, 10(10):R118, 2009.
- [53] Dennis R Harris, Steve V Pollock, Elizabeth A Wood, Reece J Goiffon, Audrey J Klingele, Eric L Cabot, Wendy Schackwitz, Joel Martin, Julie Eggington, Timothy J Durfee, Christina M Middle, Jason E Norton, Michael C Popelars, Hao Li, Sarit A Klugman, Lindsay L Hamilton, Lukas B Bane, Len A Pennacchio, Thomas J Albert, Nicole T Perna, Michael M Cox, and John R Battista. Directed evolution of ionizing radiation resistance in *Escherichia coli*. *Journal of bacteriology*, 191(16):5240–5252, August 2009.
- [54] Dae-Hee Lee and Bernhard Ø Palsson. Adaptive evolution of *Escherichia coli* K-12 MG1655 during growth on a nonnative carbon source, 1,1,2-propanediol. *Applied and environmental microbiology*, 76(13):4158–4168, July 2010.

CURRICULUM VITAE

CURRICULUM VITAE



Europass curriculum vitae

Personal information

Surname(s) / First name(s)	Nahku Ranno
Address(es)	Sõpruse pst 230-49, 13412, Tallinn
E-mail(s)	ranno@tftak.org
Nationality(-ies)	Estonian
Date of birth	06.12.1982
Gender	male

Desired employment / Occupational field	Researcher
--	-------------------

Work experience

Dates	01.07.05 – present time
Occupation or position held	researcher
Main activities and responsibilities	Continuous cultivation, gene expression analysis, growth media and mutants design for acetate overflow analysis. Investigation of culture adaptation
Name and address of employer	Competence Centre of Food and Fermentation Technologies, 15A, Akadeemia tee, 12618, Tallinn
Type of business or sector	biotechnology

Education and training

Dates	19.-22.11.2006
Principal subjects/Occupational skills covered	Introduction to microarray analysis
Name and type of organisation providing organisation and training	KTH microarray center, Stockholm
Dates	27.08.2007-20.12.2007
Principal subjects/Occupational skills covered	DNA microarray analysis of <i>C. glutamicum</i>
Name and type of organisation providing organisation and training	<i>Institut für Molekulare Mikrobiologie und Biotechnologie, Westfälische Wilhelms-Universität Münster, Münster</i>
Dates	25.-29.01.2010
Principal subjects/Occupational skills covered	Introduction to statistics for biologists 2010
Name and type of organisation providing organisation and training	Swiss Institute of Bioinformatics, Geneva
Dates	2005-2008
Title of qualification awarded	Master of Nature Science (Biotechnology)
Principal subjects/Occupational skills covered	Biotechnology, neurobiology, fermentation technology, immunology, oncobiology, bacterial genetics
Name and type of organisation providing organisation and training	Tallinn University of Technology, Tallinn
Dates	2001-2005
Title of qualification awarded	Bachelor of Nature Science (Gene Technology)
Principal subjects/Occupational skills covered	Gene technology, microbiology, molecular and cell biology, biochemistry, analytical chemistry, organic chemistry
Name and type of organisation providing organisation and training	Tallinn University of Technology, Tallinn

Personal skills and competences

Mother tongue(s)

Estonian

Other language(s)

Self-assessment

European level ^()*

English

Russian

German

<i>Understanding</i>		<i>Speaking</i>		<i>Writing</i>
<i>Listening</i>	<i>Reading</i>	<i>Spoken interaction</i>	<i>Spoken production</i>	
C1	C1	B2	B2	C2
A2	A2	A2	A2	A2
A1	A1	A1	A1	A1

^(*) Common European Framework of Reference (CEF) level

Technical skills and competences

Applikon BioBundle Fermentation Systems, HPLC, PCR, rt-PCR, DNA microarray analysis, mutation analysis with HT DNA sequencing, metabolic flux analysis

Computer skills and competences

MS Windows, MS Office, Bioexpert 2 and 3.8, Genepix 6, Roche Lightcycler 2 software, intermediate skills in R for DNA microarray data analysis and graphics. Intermediate knowledge of Gimp 2, Inscape and Veusz

Additional information

Bachelor's thesis - Comparison of *E. coli*'s central metabolic fluxes and transcriptome patterns at different growth conditions
 Master's thesis - Comparison of *Escherichia coli* K12 MG1655 transcriptome patterns at different specific growth rates

APPENDICES

?	Position	Mut	Overall score	Stock (0 gen)				Dilution rate (D) = 0.11 h ⁻¹ (18 gen)				Dilution rate (D) = 0.48 h ⁻¹ (34 gen)				Gene	Description	
				Mut %	Score	Q30 Mut	Q30 Ref	Mut %	Score	Q30 Mut	Q30 Ref	Mut %	Score	Q30 Mut	Q30 Ref			
																		Score
✓	335,361	T→C	79.6	12.5	3/3	44/24	98/55	9/7	45.3	9.5%	9/7	98/55	21.8	7.0%	6/3	91/28	<i>yehE</i>	predicted protein
✓	1,050,465	T→A	65.8	3.9	2/1	61/39	129/68	9/0	24.8	4.4%	9/0	129/68	37.1	10.7%	6/6	64/36	<i>ospH/cspG</i>	stress protein / DNA-binding transcriptional regulator
✓	3,701,283	G→A	40.8	19.4	6/2	27/12	44/17	4/3	15.4	10.3%	4/3	44/17	6.0	7.8%	1/3	29/18	<i>dppD</i>	dipeptide transporter
✓	2,683,035	G→A	30.2	-	0/0	19/12	34/35	4/3	15.2	9.2%	4/3	34/35	15.0	14.9%	4/3	19/21	<i>glvA</i>	serine hydroxymethyltransferase
✓	326,446	C→T	28.8	2.3%	0/1	13/29	33/108	1/7	16.5	5.7%	1/7	33/108	12.3	9.7%	4/2	14/42	<i>betA</i>	choline dehydrogenase
NT	3,410,579	T→A	26.5	6.6	2/2	62/25	110/86	2/1	3.1	1.5%	2/1	110/86	16.8	4.2%	2/5	86/74	<i>yhdJ/yhdU</i>	predicted methyltransferase / predicted membrane protein
NT	3,237,537	T→G	23.1	1.0	1/1	21/45	79/86	6/1	21.0	4.1%	6/1	79/86	1.1	1.7%	2/0	52/85	<i>atx</i>	predicted inner membrane protein
X	2,952,301	T→G	5.9	5.9	2/1	9/26	39/52	0/0	-	-	0/0	39/52	-	1.5%	0/1	24/33	<i>recB</i>	exonuclease V, beta subunit
NT	3,590,376	C→T	5.6	1.3%	0/2	76/71	84/127	2/3	5.6	2.3%	2/3	84/127	-	1.1%	1/1	89/99	<i>ugpB/uvrF</i>	glycerol-3-phosphate transporter subunit / branched chain AA transporter subunit
NT	432,228	Δ1bp	5.5	-	0/0	33/38	43/18	0/1	-	0.9%	0/1	63/48	5.5	4.1%	1/2	25/45	<i>ndrR</i>	conserved protein
NT	3,701,921	G→A	4.8	4.8	1/3	43/18	65/30	0/0	-	-	0/0	65/30	-	-	0/0	38/22	<i>dppC</i>	dipeptide transporter
X	545,057	A→G	4.4	2.5	1/2	22/21	16/23	0/3	1.9	7.1%	0/3	16/23	-	3.6%	0/1	10/17	<i>ailD</i>	ureidoglycolate dehydrogenase
NT	1,962,621	C→A	4.2	-	0/0	16/26	38/45	1/3	4.2	4.6%	1/3	38/45	-	-	0/0	19/29	<i>flhA</i>	predicted flagellar export pore protein

Top breseq predictions of base substitution and single-base indel polymorphisms in the sequenced populations are listed. Positions where a polymorphism with a significant score that passed bias tests was detected in any of the three samples are shown with statistics for all three samples. The methods behind these predictions are described in the breseq (1.00rc7) documentation (<http://barricklab.org/breseq>). Predictions are shaded based on whether they passed two specific test criteria: (1) $-\log_{10}$ E value score ≥ 4.0 for the likelihood-ratio test of a mixed base model (that there was a true sub-population with the variant base) versus a single base model (that discrepancies from the reference were sequencing errors) and (2) p value < 0.05 for Fisher's exact test for bias in the strands of reads supporting the variant sub-population versus the reference sequence. Green passed both tests, blue failed just the polymorphism test, red failed just the strand bias test, and no variant bases were observed for gray. **Overall scores** were calculated as sums of the scores for predictions across all samples.

Columns: ?, results of experimentally testing specific predictions: validated as detailed in the main text and supplement (✓), not detected by Sanger sequencing of the mixed population sample and, therefore, likely spurious (X), or not experimentally tested because of low Mut % and Overall score (NT); **Position**, in the reference genome sequence; **Mut**, change in sequence from reference genome; **Overall score**, as explained above; **Mut %**, maximum likelihood predicted frequency of sub-population with mutation; **Score**, $-\log_{10}$ E value for polymorphism test; **Q30 Mut**, number of bases with Phred quality scores ≥ 30 supporting the new sub-population in reads on the top/bottom genome strand; **Q30 Ref**, number of bases with Phred quality scores ≥ 30 supporting the reference base in reads on the top/bottom genome strand; **Annotation**, amino acid and codon changes for base substitution mutations in genes, location of mutations in reading frame for indels, or distance to the two neighboring genes for intergenic predictions with -/+ for orientation upstream or downstream of those genes, respectively; **Gene**, gene containing mutation or two neighboring genes separated by a slash; **Description**, description of gene containing mutation or two neighboring genes separated by a slash.

PUBLICATION I

Nahku R, Valgepea K, Lahtvee PJ, Erm S, Abner K, Adamberg K, Vilu R

Specific growth rate dependent transcriptome profiling of *Escherichia coli* K12 MG1655 in accelerostat cultures

Journal of Biotechnology, 145(1):60-65, (2010)



Specific growth rate dependent transcriptome profiling of *Escherichia coli* K12 MG1655 in accelerostat cultures

Ranno Nahku^{a,b}, Kaspar Valgepea^{a,b}, Petri-Jaan Lahtvee^{a,b}, Sten Erm^{a,b},
Kristo Abner^{a,b}, Kaarel Adamberg^{b,c}, Raivo Vilu^{a,b,*}

^a Tallinn University of Technology, Department of Chemistry, Ehitajate tee 5, 19086 Tallinn, Estonia

^b Competence Centre of Food and Fermentation Technologies, Akadeemia tee 15b, 12618 Tallinn, Estonia

^c Tallinn University of Technology, Department of Food Processing, Ehitajate tee 5, 19086 Tallinn, Estonia

ARTICLE INFO

Article history:

Received 31 July 2009

Received in revised form 2 October 2009

Accepted 15 October 2009

Keywords:

A-stat

Accelerostat

Continuous culture

Escherichia coli

Overflow metabolism

Microarray

ABSTRACT

Specific growth rate dependent gene expression changes of *Escherichia coli* K12 MG1655 were studied by microarray and real-time PCR analyses. The bacteria were cultivated on glucose limited minimal medium using the accelerostat method (A-stat) where starting from steady state conditions (chemostat culture) dilution rate is constantly increased. At specific growth rate (μ) 0.47 h^{-1} , *E. coli* had focused its metabolism to glucose utilization by down-regulation of alternative substrate transporters expression compared to $\mu = 0.3 \text{ h}^{-1}$. It was found that acetic acid accumulation began at $\mu = 0.34 \pm 0.01 \text{ h}^{-1}$ and two acetate synthesis pathways – phosphotransacetylase-acetate kinase (*pta-ackA*) and pyruvate oxidase (*poxB*) – contributed to the synthesis at the beginning of overflow metabolism, i.e. onset of acetate excretion. On the other hand, *poxB*, *pta* and *ackA* expression patterns suggest that pyruvate oxidase may be the only enzyme synthesizing acetate at $\mu = 0.47 \text{ h}^{-1}$. Loss of glucose and acetate co-utilization represented by down-regulation of *acs-yjch-actP* operon between specific growth rates $0.3\text{--}0.42 \text{ h}^{-1}$ and acetic acid accumulation from $\mu = 0.34 \pm 0.01 \text{ h}^{-1}$ allows one to surmise that the acetate utilization operon expression might play an important role in overflow metabolism.

© 2009 Elsevier B.V. All rights reserved.

1. Introduction

A continuous culture method chemostat was introduced in 1950 by Novick and Szilard (Novick and Szilard, 1950) and since then it has been widely used for studying microorganisms in defined (steady state) conditions at constant dilution rate which is equal to specific growth rate (μ) of cells. The presence of steady state is its main and most important advantage over batch cultivation where dependence of growth characteristics on specific growth rate is hard to determine. Conducting experiments in batch cultures result in complex data patterns reflecting uncontrolled changes of growth conditions, which are often difficult or even impossible to interpret (Hoskisson and Hobbs, 2005). It has been proposed that steady state can be obtained in batch cultures in exponential phase while substrate consumption by cells is maximal, however, within that time, metabolite concentrations and pH are constantly changing and latter is known to affect gene expression (Richard and Foster, 2004, 2007; Rosenthal et al., 2008). For these reasons, chemostat is a bet-

ter choice for studying bacterial physiology. On the other hand, to obtain steady state in chemostat, five culture volumes of medium are usually needed to be pumped through the reactor in fixed conditions, making cultivation experiments time consuming and thus limiting the number of specific growth rates to be studied. Moreover, chemostat culture is open to random mutations and therefore, it is important to reduce the duration of experiment (Ferenci, 2008).

Accelerostat (A-stat) method was introduced to overcome the problems associated with chemostat (Paalme and Vilu, 1993). A-stat begins as chemostat: batch phase is followed by stabilization of the culture at fixed specific growth rate to obtain steady state. Subsequently, the dilution rate which equals specific growth rate is changed with constant speed until the culture cannot keep up with the rising dilution rate, resulting in wash-out. It has been shown before that transition from acceleration phase to chemostat does not result in a significant change in culture parameters if the chosen changing rate of dilution rate is not too fast (Adamberg et al., 2009). In the latter case, culture is in quasi-steady state which is a physiological state of a microorganism where every point represents the corresponding steady state value. Great advantages of A-stat are the possibilities to monitor bacterial growth in real time to study physiology in a large variety of specific growth rates while reducing the duration of experiment at the same time.

* Corresponding author at: Mailing address: Tallinn University of Technology, Department of Chemistry, Akadeemia tee 15, 12618, Tallinn, Estonia.

Tel.: +372 6204831; fax: +372 6202828.

E-mail address: raivo@kbfi.ee (R. Vilu).

Producing recombinant proteins and other biotechnologically important substances has significantly increased in recent years. *Escherichia coli* is often used as a production system due to its ability to grow aerobically on glucose and reach high biomass concentrations. In addition to its relatively low cultivation cost, *E. coli* is a Gram-negative bacterium which makes purification of products relatively cheap. Generally, production yields are better at higher specific growth rates, however, this is where the main problem in aerobic *E. coli* cultivation on glucose arises – excretion of acetic acid as the result of overflow. It is believed that acetate production, i.e. overflow metabolism is caused by an imbalance between glucose uptake and TCA cycle capacity resulting in pyruvate and acetyl-CoA accumulation (Akeson et al., 1999; Farmer and Liao, 1997; Wolfe, 2005). Acetate is known to reduce maximum growth rate and inhibit protein production, moreover, it diverts carbon from biomass formation (Nakano et al., 1997; Contiero et al., 2000; March et al., 2002). For those reasons, many strategies have been developed to abolish acetate production (De Mey et al., 2007; Eiteman and Altman, 2006; Wolfe, 2005).

Two main pathways are known synthesizing acetate. Acetyl-CoA is converted into acetyl-P by phosphotransacetylase (*pta*) through phosphotransacetylase-acetate kinase (*pta-ackA*) pathway and acetate kinase (*ackA*) catalyzes the reaction from acetyl-P to acetate. Alternatively, acetate can be synthesized directly from pyruvate in the presence of pyruvate oxidase (*poxB*) (Phue and Shiloach, 2004; Phue et al., 2005). Deletion of *pta-ackA* pathway results in a significant reduction of acetate excretion, specific growth rate and elevation in formate and lactate production (Chang and Cronan, 1999; Contiero et al., 2000; Dittrich et al., 2005). *poxB* disruption results in reduced biomass yield (Abdel-Hamid et al., 2001). Despite the considerable amount of studies with genetically engineered *E. coli* strains, there is still no clear understanding about the regulation of acetic acid synthesis pathways, making the matter intriguing. As overflow metabolism is known to be specific growth rate dependent, continuous monitoring of specific growth rate effect on bacterial physiology should be made for gaining more detailed insights into overflow metabolism regulation. The method enabling the latter is A-stat.

The aim of this study was to characterize *E. coli* K12 MG1655 metabolism at various specific growth rates at transcriptional level using A-stat cultivation method which has not been done before. Additionally, accelerostat experiments gave an excellent opportunity to precisely monitor the course of metabolism and directly connect growth phenotype to gene expression data. Special attention was drawn for characterising acetate metabolism.

2. Materials and methods

2.1. Bacterial strain and culture medium

The *E. coli* K12 MG1655 strain used in the current study was obtained from Statens Serum Institute, Denmark. Growth and physiological characteristics were determined using a defined medium with the composition as follows (g l^{-1}): $\text{FeSO}_4 \cdot 7\text{H}_2\text{O}$ 0.005, $\text{MgSO}_4 \cdot 7\text{H}_2\text{O}$ 0.5, $\text{MnSO}_4 \cdot 5\text{H}_2\text{O}$ 0.002, $\text{CaCl}_2 \cdot 2\text{H}_2\text{O}$ 0.005, $\text{ZnSO}_4 \cdot 7\text{H}_2\text{O}$ 0.002, $\text{CoSO}_4 \cdot 7\text{H}_2\text{O}$ 0.0006, $\text{CuSO}_4 \cdot 5\text{H}_2\text{O}$ 0.0005, $(\text{NH}_4)_6\text{Mo}_7\text{O}_{24} \cdot 4\text{H}_2\text{O}$ 0.0026 were dissolved in 50 ml 5 M HCl; C-source – α -D-glucose 10, N-source – NH_4Cl 3.5 and buffer – K_2HPO_4 were autoclaved separately and mixed together afterwards.

2.2. Accelerostat cultivation

The A-stat cultivation system consisted of 1.251 Biobundle bioreactor (Applikon Biotechnology B.V., Schiedam, the

Netherlands) controlled by an ADI 1030 biocontroller (Applikon Biotechnology B.V.) and a cultivation control program “BioXpert NT” (Applikon Biotechnology B.V.). The system was equipped with pH, $p\text{O}_2$ and temperature sensors. Two variable speed pumps (feeding and out-flow) were controlled using “BioXpert NT” control software. The bioreactor was set on a balance whose output was used as the control variable to ensure constant culture volume (300 ± 1 ml). Similarly, the inflow was controlled through measuring the mass of the fresh culture medium.

Four cultivation experiments with accelerations – 0.01 h^{-2} or 0.005 h^{-2} – were carried out at 37°C under aerobic conditions with an agitation speed of 500 rpm. pH of the culture was controlled using 5 M NaOH and temperature with a heating blanket. The growth characteristics of the bacteria in A-stat experiments were calculated on the basis of OD, total volume of medium pumped out from bioreactor (L) and organic acid concentrations in culture medium (mM). Formulas and cultivation system used were as described in previous studies (Kasemets et al., 2003; Adamberg et al., 2009).

2.3. Analytical methods

The concentrations of organic acids (lactate, acetate and formate), ethanol and glucose in the culture medium were analyzed by high pressure liquid chromatography (Alliance; Waters Corp., Milford, MA), using a BioRad HPX-87H column (Hercules, CA), and isocratic elution at a flow rate of 0.6 ml min^{-1} with $0.005 \text{ M H}_2\text{SO}_4$ at temperature 35°C . Refractive index detector (model 2414; Waters Corp.) was used for detection and quantification of the substances. The samples of culture medium (1.5 ml) were centrifuged ($14,000 \times g$, 4 min), supernatant was collected and analyzed directly or stored at -20°C before HPLC analyses. Data processing was performed using Empower software (Waters Corp.).

Biomass concentration was measured gravimetrically: centrifuging 10 ml of culture, washing twice with physiological solution, resuspending in dH_2O , drying on aluminum plates at 100°C for 24 h and cooling down in a desiccator prior to weighing.

2.4. Gene expression profiling

The microarrays used in the study were obtained from KTH Microarray Center (Stockholm, Sweden). *E. coli* Genome Oligo Set Version 1.0 (Operon Biotechnologies Inc., Huntsville, AL) containing 4289 *E. coli* K12 open reading frames was used in the spotting process. For microarray analyses, steady state chemostat culture of *E. coli* K12 MG1655 was used as a reference ($\mu = 0.3 \text{ h}^{-1}$). Quasi-steady state point at specific growth rate $0.47 \pm 0.02 \text{ h}^{-1}$ was compared to the reference sample in triplicate biological parallels. Compared samples were obtained from experiments carried out with 10 g l^{-1} of glucose in medium.

RNA degradation was halted, total RNA extracted, cDNA synthesized and labeled as described previously (Lahtvee et al., 2009), with minor modifications: less concentrated lysozyme solution, no proteinase K and 25 μg of total RNA was used for cDNA synthesis. Microarrays were incubated for 30 min at 42°C in prehybridization solution containing (per slide): 0.5 μg BSA, 12.5 ml $20 \times \text{SSC}$, 0.5 ml 10% SDS. Slides were rinsed 10 times in MilliQ water, twice in 2-propanol and dried with centrifugation. After purification of the labeled cDNA, the hybridization solution ($20 \times \text{SSC}$ 16.3 μl , 100% formamide 32.5 μl , 10% SDS 0.65 μl , *E. coli* tRNA 1 μl (5 μg)) was added, followed by hybridization for 35 h at 42°C .

2.5. Microarray data analysis

Microarray slides were scanned using an Affymetrix 428 Array Scanner (Santa Clara, CA). Spot intensities and corresponding

background signals were quantified with Genepix Pro (version 6; Axon Instruments [http://www.moleculardevices.com/pages/software/gn_genepix_pro.html]). Spots which had signal-to-noise ratio less than three were filtered. Further analysis was carried out in R environment (version 2.6.1 [<http://www.r-project.org/>]) using KTH package (KTH Microarray Center [<http://www.biotech.kth.se/molbio/microarray/dataanalysis/index.html>]). Flagged spots and background were extracted before “printTipLoess” normalization. Data from the independent experiments were combined and further analyzed with web based tool Marray (G-language Project [<http://www.g-language.org/data/marray/software/map2swf.cgi>]) that enables gene expression data visualization on KEGG pathways. Input data and instructions for Marray and Supplementary Table S1 for gene expression measurement results can be found at our homepage (<http://tftak.eu/?id=68>). DNA microarray data is also available at NCBI Gene Expression Omnibus (Reference series: GSE18183).

2.6. Real-time PCR assay

RNA was extracted and cDNA synthesized as described by Lahtvee et al. (2009), except regular nucleotides were used for cDNA synthesis. Real-time PCR reactions were carried out using Roche LightCycler 2.0 (Basel, Switzerland) and Platinum SYBR Green qPCR SuperMix-UDG (Invitrogen). Per one reaction 5.25 μL 2 \times platinum SYBR Green qPCR SuperMix-UDG, 3 μL primer mix (1.67 μM), 0.5 μL BSA and 2 μL cDNA (concentration ca 20 ng μL^{-1}) were used. PCR conditions were set according to the Platinum SYBR Green qPCR SuperMix-UDG manual. Gene expression changes for *acs*, *pta*, *ackA*, *poxB*, *sucC* were derived comparing samples from dilution rates of 0.36 h^{-1} ; 0.42 h^{-1} ; 0.45 h^{-1} ; 0.47 h^{-1} to the reference sample at dilution rate 0.3 h^{-1} . All samples were normalized according to biomass and ribosomal RNA content. The changes in ribosomal RNA content were estimated using gel electrophoresis. Equal volumes of total RNA were loaded to 1% agarose gel and rRNA band intensities were compared. As equal amounts of total RNA (25 μg) were used as a starting material for cDNA synthesis, it was assumed that higher rRNA amount lead to proportional reduction of mRNA pool.

3. Results

3.1. A-stat growth characteristics and reproducibility

Three parallel experiments were carried out (with 10 g L^{-1} glucose) where the culture was stabilized in chemostat at 0.3 h^{-1} and after achieving steady state, dilution rate was smoothly changed (increased) with acceleration of 0.01 h^{-2} (Fig. 1). A-stat enabled precise determination of *E. coli* K12 MG1655 growth parameters – acetate overflow began at $\mu = 0.34 \pm 0.01 \text{ h}^{-1}$ and cells had problems keeping up with rising dilution rate at specific growth rate $0.48 \pm 0.02 \text{ h}^{-1}$ (Fig. 1). Glucose started to accumulate in the culture medium simultaneously with the latter point. Three characteristic cultivation points were chosen to validate reproducibility: specific growth rate when acetate starts to accumulate ($\mu = 0.34 \pm 0.01 \text{ h}^{-1}$), specific growth rate when μ started lagging D ($\mu = 0.48 \pm 0.02 \text{ h}^{-1}$) and specific growth rate when glucose started to accumulate ($\mu = 0.48 \pm 0.02 \text{ h}^{-1}$). The average relative standard deviation of each of these three points in quasi-steady state cultures was 3.3%. For further characterization of the good reproducibility of A-stat experiments it was shown that the average relative standard deviation of biomass yields (Y_{xs} [g g^{-1}]) was 5.4% in quasi-steady state conditions (data not shown).

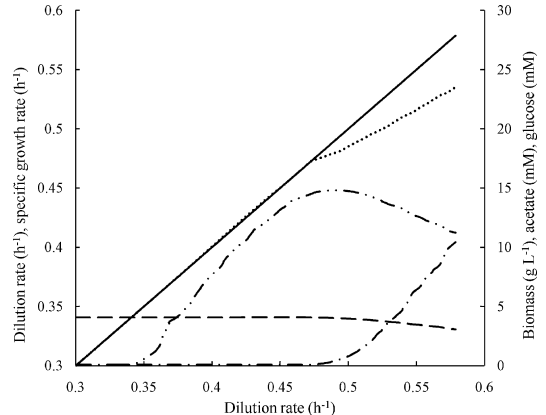


Fig. 1. A-stat cultivation of *E. coli* K12 MG1655 with 10 g L^{-1} of glucose as the limiting substrate. Measurement rate for all parameters was dilution rate 0.01 h^{-1} . Solid line represents dilution rate (h^{-1}), dotted line – specific growth rate (h^{-1}), dashed line – biomass concentration (g L^{-1}), dashed dot line – glucose concentration (mM), dashed dot dot line – acetate concentration (mM).

3.2. Glucose repression in *E. coli* K12 MG1655

In microarray analysis quasi-steady state points at specific growth rate $0.47 \pm 0.02 \text{ h}^{-1}$ and the reference steady state points at 0.30 h^{-1} were compared. According to the data, alternative substrate utilization and transport transcript expression analysis revealed 3–20-fold reduction of genes associated with the metabolism of maltose (*malBEFKM*), β -methylgalactoside (*MglABC*), D-ribose (*rbsABC*), L-arabinose (*araF*), galactitol (*gatABC*), N-acetyl glucosamine (*nagE*), acetate (*actP*, *yjcH*) and C_4 -dicarboxylates (*dctA*). Glucose repression was also seen by strong down-regulation of *tnaA*, *cstA*, *aspA*, *dadX* and *ilvBN* (see Supplementary Table S1), observed as well by Oh and colleagues (Oh et al., 2002).

3.3. Struggle against acetate stress

The major sugar transport system in *E. coli* is the phosphotransferase system (PTS) enabling fast glucose transport. Latter causes accumulation of pyruvate that may lead to acetate production (Vemuri et al., 2006). Microarray data showed a times decrease in the expression of glucose specific PTS gene *ptsG* at higher growth rate while glucose consumption per biomass produced was constant. Reduced glucose uptake rate through PTS is likely compensated by increase in alternative non-PTS transport. We found 3- and 5-fold increase in galactose permease (*galP*) and predicted transporter *tsgA* respectively, but a 2.5 times decrease in glucokinase (*glk*) expression. Alternatively, pyruvate pool could have been reduced by converting phosphoenolpyruvate to oxaloacetate by minor up-regulation (1.6 times) of phosphoenolpyruvate carboxylase (*ppc*), 9-fold down-regulation of phosphoenolpyruvate carboxylase (*pck*) and down-regulation of pyruvate synthesis from malate by NADP-dependent malic enzyme (*maeB*) (Fig. 2).

Acetic acid effect on metabolism was also observed by three fold up-regulation of acid stress genes *hdeAB* at $\mu = 0.47 \text{ h}^{-1}$ where extracellular acetate concentration was approximately 15 mM. Similarly, around 2-fold elevation in *gadW* expression, known activator of acid response genes, occurred (Tramonti et al., 2008).

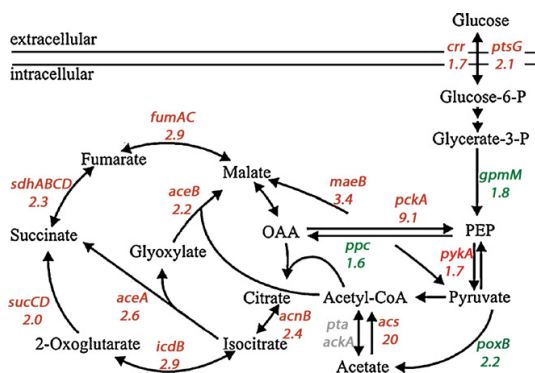


Fig. 2. Central carbon metabolism gene expression changes at $\mu = 0.30 \text{ h}^{-1}$ vs. 0.47 h^{-1} in *E. coli* K12 MG1655 A-stat cultivation. Down-regulated genes are indicated in red, up-regulated in green and no significant changes are indicated in grey. Number below gene name shows the expression fold-change (average fold change is shown in case of several genes). Arrowhead indicates the expected reaction direction. The figure is based on Nanchen et al. (2008). (For interpretation of the references to color in this figure legend, the reader is referred to the web version of the article.)

3.4. Energy metabolism

Most of the energy for anabolic reactions during aerobic growth of *E. coli* K12 on glucose is derived from NADH, FADH_2 generated in Krebs cycle and ATP which is synthesized via oxidative phosphorylation. Microarray data showed that Krebs cycle operon genes *sdhCDAB*, *sucABCD* and *fumAC* were averagely 2-fold down-regulated at specific growth rate 0.47 h^{-1} compared to 0.3 h^{-1} (Fig. 2). Expression of *sucC* (succinyl-CoA synthetase, β subunit) was quantified as described above using real-time PCR assay which confirmed the decrease of *sucC* at mRNA level (Fig. 3). In oxidative phosphorylation, no significant changes in ATP synthase, cytochrome *c* oxidase, cytochrome *bd* complex and NADH dehydrogenase I subunits encoding mRNA levels were monitored. At the same time, a significant increase of *ndh* (NADH dehydrogenase II, 3-fold), *mgo* (malate dehydrogenase, 9-fold), *pyrD* (dihydroorotate oxidase, 2-fold) and *poxB* (pyruvate oxidase, 2-fold) expression

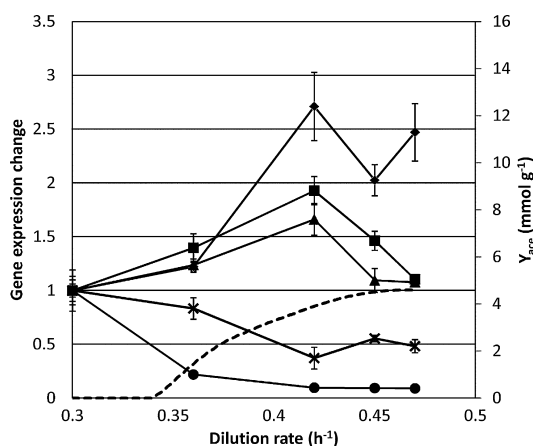


Fig. 3. Gene expression changes in *E. coli* K12 MG1655 A-stat cultivation. *ackA* (■), *pta* (▲), *poxB* (◆), *acs* (●) and *sucC* (×) – relative gene expression of acetate kinase, phosphotransacetylase, pyruvate oxidase and acetyl-CoA synthase, respectively. Dashed line represents specific acetate production per biomass (Y_{acet} ; mmol g^{-1}). Error bars represent standard deviations of three to five technical replicates.

levels was observed at rising dilution rates (Supplementary Table S1 and Fig. 2).

3.5. Acetate production

Two main pathways are known to synthesize acetate – phosphotransacetylase-acetate kinase (*pta-ackA*) and pyruvate oxidase (*poxB*). Microarray data revealed that *pta* and *ackA* had no significant changes in mRNA expression levels between compared specific growth rates, however the expression of *poxB* increased around two times at higher specific growth rate (0.47 h^{-1}). Concurrently, acetate utilization and transport operon genes acetyl-CoA synthetase (*acs*), *yjcH* and *actP* were strongly repressed (>20 times) (Fig. 2). To confirm and further characterize the course of acetate metabolism, *pta*, *ackA*, *poxB* and *acs* genes were validated with real-time PCR (Fig. 3). The analysis confirmed microarray data, moreover, it was revealed that *pta-ackA* pathway was slightly induced in parallel with acetate accumulation and down-regulated back to the pre-overflow metabolism level ($\mu = 0.3 \text{ h}^{-1}$) after acetate production had reached its near-maximum value ($\mu = 0.42 \text{ h}^{-1}$). In contrast, *poxB* expression increased and stayed 2-fold higher compared to chemostat at 0.3 h^{-1} (Fig. 3).

4. Discussion

Modeling cell metabolism and creating strains of microorganisms for production of various biotechnologically important substances is a challenge for the 21st century. These goals can be achieved exclusively if data about microorganism's physiology is acquired from controlled steady state conditions. Besides well-known chemostat, accelerostat offers good quality data with high reproducibility and complements chemostat in two aspects – it enables to study dynamic response of cells, monitor metabolic switch points corresponding to specific growth rate and empowers the possibility to acquire (quasi-steady state) samples from vast number of specific growth rate values during one continuous experiment.

Whereas the glucose yield (Y_{glc} , mmol g^{-1}) was constant throughout the experiments, changes in glucose uptake genes expression were observed. A decrease in *ptsG* expression at higher glucose consumption rates was seen. *ptsG* encodes the glucose specific phosphotransferase system (PTS) transporter, which is a major glucose transporter in *E. coli* K12 (Becker et al., 2006). *ptsG* expression has been studied previously in glucose limited chemostat cultures at different specific growth rates by Seeto et al. (2004). This study is in consonance with our data, showing lower *ptsG* expression at higher specific growth rates. Glucose transport via PTS generates pyruvate directly, since one mole of pyruvate is produced per one mole of glucose taken up. That may lead to accumulation of pyruvate and trigger the beginning of acetate accumulation resulting in stress (Vemuri et al., 2006). Acid stress response was confirmed on transcriptional level (up-regulation of *hdeAB*, *gadW*). Therefore, it is beneficial for the bacteria to reduce glucose transport through PTS, because it provides *E. coli* with an opportunity to bypass some of the carbon “around” pyruvate. It is known that over-expression of phosphoenolpyruvate carboxylase (*ppc*), knockout of phosphoenolpyruvate carboxykinase (*pck*) reduces acetate formation (Farmer and Liao, 1997; Yang et al., 2003). As phosphoenolpyruvate is needed for the uptake of glucose via PTS, conversion of PEP to oxaloacetate by *ppc* reduces the available pool of PEP, resulting in a decrease of pyruvate accumulation. Indeed, we observed up-regulation in *ppc* and a remarkable decrease in *pck* mRNA levels at higher dilution rates. When PTS transport is reduced, it is likely that *E. coli* K12 MG1655 consumes some of glucose through an alternative non-PTS type transporter(s).

One such glucose transport system is encoded by *galP* (galactose permease). It has been shown that over-expression of *galP* and glucokinase (*glk*) in PTS disruption mutant reduced acetate formation and increased recombinant protein production (DeAnda et al., 2006; Wong et al., 2008). Gene expression analysis revealed a more than 3-fold up-regulation of *galP* expression with rising dilution rate. Another candidate for non-PTS glucose uptake could be the putative transporter *tsgA* which expression increased more than five times under catabolite repression conditions. However, expression of glucokinase (*glk*) catalyzing glucose phosphorylation was down-regulated at higher specific growth rates (Supplementary Table S1). Thus, alternative enzymes which are able to catalyze glucose uptake and therewith reduce acetate production should be present.

Considering microarray data about acetate metabolism in the literature, it should be concluded that there is no clear explanation about the synthesis routes from pyruvate to acetate, making the data about acetate metabolism controversial (Ishii et al., 2007; Vemuri et al., 2006). The main pathway for acetate synthesis at higher specific growth rates can be through *pta-ackA* (Ishii et al., 2007) or co-expression of *ackA* and *poxB* (Vemuri et al., 2006). Phue and Shiloach found that in *E. coli* K12 batch culture pyruvate oxidase (*poxB*) is a major route for acetate synthesis (Phue and Shiloach, 2004). Our study showed that at the beginning of overflow metabolism ($D = 0.34 \pm 0.01 \text{ h}^{-1}$), *pta-ackA* pathway is induced, but shifted down to $D = 0.3 \text{ h}^{-1}$ level before wash-out of the culture ($D = 0.48 \text{ h}^{-1}$). Concurrently, *poxB* expression increased approximately 2-fold (Fig. 3). *poxB*, *pta* and *ackA* expression patterns at higher specific growth rates suggest that pyruvate oxidase may be the only enzyme synthesizing acetate which is in concordance with Phue and colleagues (Phue and Shiloach, 2004; Phue et al., 2005). It is possible that *poxB* is favorable to balance NADH/NAD⁺ ratio as the maximal NADH throughput in respiratory chain is exhausted, inhibiting additional NADH production via pyruvate dehydrogenase.

It has been shown by Vemuri and colleagues that excess NADH production will eventually down-regulate TCA cycle. Similarly, expression of respiratory chain components (NADH dehydrogenase I subunits, ATP synthase) encoding genes will be shifted down as well (Vemuri et al., 2006). From our data, NADH accumulation seems to be diminished by up-regulation of *ndh* that encodes alternative NADH dehydrogenase (complex II) (Bott and Niebisch, 2003) and by reduction of TCA flux. The latter causes reduction of electron donation to quinone pool, but *E. coli* seems to compensate it by enhancing the gene expressions of the enzymes mediating other routes for electron transfer (*mgo*, *pyrD* and *poxB*).

Many genes that encode proteins responsible for utilization and transport of substrates other than glucose were strongly repressed at higher specific growth rates. This effect is known as carbon catabolite repression (CCR), which is a metabolic response of the bacteria to utilize the substrate that is most abundant and guarantees the fastest growth (comprehensive review by Görke and Stülke, 2008). According to our results and data from the literature, it can be concluded that at relatively low specific growth rates, *E. coli* K12 MG1655 cells are ready for co-utilization of different substrates without the need of gene expression changes (Franchini and Egli, 2006; Ihssen and Egli, 2005; Lendenmann et al., 1996). Ability to rapidly utilize more than one substrate at a time gives *E. coli* an advantage in its natural environment. Since the competition in gastrointestinal tract for substrates is high, the bacteria that consume nutrients the fastest might have a significant advantage.

When looking at co-utilization of growth substrates from a different perspective, it is intriguing that according to real-time PCR data, down-regulation of *acs* occurs between dilution rates 0.3 h^{-1} and 0.42 h^{-1} (Fig. 3). Therefore, it can be expected that the ability to co-utilize glucose and acetate is lost between the mentioned dilu-

tion rates. Latter may have a significant influence to the beginning and course of overflow metabolism since acetic acid accumulation starts at dilution rate $0.34 \pm 0.01 \text{ h}^{-1}$ according to our data. However, the relationship between glucose repression and acetate-glucose co-utilization is poorly studied. Therefore, we are currently investigating the latter phenomenon using A-stat and dilution rate stat (D-stat) (Lahtvee et al., 2009) with adding acetic acid smoothly to the bioreactor while keeping the limiting substrate concentration constant.

A-stat is a cultivation method that enables real-time monitoring of culture parameters, e.g. culture optical density, oxygen consumption and by-product formation during continuous change of specific growth rate. Latter is especially important to characterize metabolic phenomena, e.g. overflow metabolism. *E. coli* K12 MG1655 has been studied before at different specific growth rates using chemostat and microarrays (Vemuri et al., 2006). Comparing gene expression changes at similar specific growth rates in the latter chemostat experiments and A-stat revealed that most of the strategies that *E. coli* K12 MG1655 execute when coping with rising dilution rate are essentially the same in both cases. Therefore, when studying bacterial metabolism at various specific growth rates A-stat could be considered as an effective and reproducible method for precise determination of switch points in metabolism regulation, e.g. beginning of overflow metabolism, induction and repression of specific genes, etc.

Acknowledgements

The financial support for this research was provided by the Enterprise Estonia project EU22704, and Ministry of Education, Estonia, through the grant SF0140090s08.

Appendix A. Supplementary data

Supplementary data associated with this article can be found, in the online version, at doi:10.1016/j.jbiotec.2009.10.007.

References

- Abdel-Hamid, A.M., Attwood, M.M., Guest, J.R., 2001. Pyruvate oxidase contributes to the aerobic growth efficiency of *Escherichia coli*. *Microbiology* 147, 1483–1498.
- Adamberg, K., Lahtvee, P., Valgepea, K., Abner, K., Vilu, R., 2009. Quasi steady state growth of *Lactococcus lactis* in glucose-limited acceleration stat (A-stat) cultures. *Antonie van Leeuwenhoek* 95 (3), 219–226.
- Akesson, M., Karlsson, E.N., Hagander, P., Axelsson, J.P., Tocaj, A., 1999. On-line detection of acetate formation in *Escherichia coli* cultures using dissolved oxygen responses to feed transients. *Biotechnol. Bioeng.* 64 (5), 590–598.
- Becker, A., Zeppenfeld, T., Staab, A., Seitz, S., Boos, W., Morita, T., et al., 2006. Yeel, a novel protein involved in modulation of the activity of the glucose-phosphotransferase system in *Escherichia coli* K-12. *J. Bacteriol.* 188, 5439–5449.
- Bott, M., Niebisch, A., 2003. The respiratory chain of *Corynebacterium glutamicum*. *J. Biotechnol.* 104 (1–3), 129–153.
- Chang, Y.Y., Cronan, J.E., 1999. Membrane cyclopropane fatty acid content is a major factor in acid resistance of *Escherichia coli*. *Mol. Microbiol.* 33, 249–259.
- Contiero, J., Beatty, C.M., Kumari, S., DeSanti, C., Strohl, W., Wolfe, A.J., et al., 2000. Effects of mutations in acetate metabolism in high-cell-density growth of *Escherichia coli*. *J. Ind. Microbiol. Biotechnol.* 24, 421–430.
- De Mey, M., Lequeux, G.J., Beauprez, J.J., Van Horen, E., Soetaert, W.K., Vanrolleghem, P.A., et al., 2007. Comparison of different strategies to reduce acetate formation in *Escherichia coli*. *Biotechnol. Prog.* 23, 1053–1063.
- DeAnda, R., Lara, A.R., HermC Ndez, V., HermC Ndez-Montalvo, V., Gosset, G., BolCvar, F., et al., 2006. Replacement of the glucose phosphotransferase transport system by galactose permease reduces acetate accumulation and improves process performance of *Escherichia coli* for recombinant protein production without impairment of growth rate. *Metab. Eng.* 8, 281–290.
- Dittrich, C.R., Bennett, G.N., San, K., 2005. Characterization of the acetate-producing pathways in *Escherichia coli*. *Biotechnol. Prog.* 21 (4), 1062–1067.
- Eiteman, M.A., Altman, E., 2006. Overcoming acetate in *Escherichia coli* recombinant protein fermentations. *Trends Biotechnol.* 24, 530–536.
- Farmer, W.R., Liao, J.C., 1997. Reduction of aerobic acetate production by *Escherichia coli*. *Appl. Environ. Microbiol.* 63, 3205–3210.
- Ferenci, T., 2008. Bacterial physiology, regulation and mutational adaptation in a chemostat environment. *Adv. Microbial Physiol.* 53, 169–229.

- Franchini, A.G., Egli, T., 2006. Global gene expression in *Escherichia coli* K-12 during short-term and long-term adaptation to glucose-limited continuous culture conditions. *Microbiology* 152 (Pt 7), 2111–2127.
- Görke, B., Stülke, J.R., 2008. Carbon catabolite repression in bacteria: many ways to make the most out of nutrients. *Nat. Rev. Microbiol.* 6 (8), 613–624.
- Hoskisson, P.A., Hobbs, G., 2005. Continuous culture—making a comeback. *Microbiology* 151 (Pt 10), 3153–3159.
- Ihssen, J., Egli, T., 2005. Global physiological analysis of carbon- and energy-limited growing *Escherichia coli* confirms a high degree of catabolic flexibility and preparedness for mixed substrate utilization. *Environ. Microbiol.* 7 (10), 1568–1581.
- Ishii, N., Nakahigashi, K., Baba, T., Robert, M., Soga, T., Kanai, A., et al., 2007. Multiple high-throughput analyses monitor the response of *E. coli* to perturbations. *Science* 316, 593–597.
- Kasemets, K., Drews, M., Nisamedtinov, I., Adamberg, K., Paalme, T., 2003. Modification of A-stat for the characterization of microorganisms. *J. Microbiol. Methods* 55 (1), 187–200.
- Lahtvee, P., Valgepea, K., Nahku, R., Abner, K., Adamberg, K., Vilu, R., et al., 2009. Steady state growth space study of *Lactococcus lactis* in D-stat cultures. *Antonie van Leeuwenhoek*.
- Lendenmann, U., Nozzi, M., Egli, T., 1996. Kinetics of the simultaneous utilization of sugar mixtures by *Escherichia coli* in continuous culture. *Appl. Environ. Microbiol.* 62, 1493–1499.
- March, J.C., Eiteman, M.A., Altman, E., 2002. Expression of an anaplerotic enzyme, pyruvate carboxylase, improves recombinant protein production in *Escherichia coli*. *Appl. Environ. Microbiol.* 68 (11), 5620–5624.
- Nakano, K., Rischke, M., Sato, S., Märkl, H., 1997. Influence of acetic acid on the growth of *Escherichia coli* K12 during high-cell-density cultivation in a dialysis reactor. *Appl. Microbiol. Biotechnol.* 48 (5), 597–601.
- Nanchen, A., Schicker, A., Revelles, O., Sauer, U., 2008. Cyclic AMP-dependent catabolite repression is the dominant control mechanism of metabolic fluxes under glucose limitation in *Escherichia coli*. *J. Bacteriol.* 190 (7), 2323–2330.
- Novick, A., Szilard, L., 1950. Description of the chemostat. *Science* 112 (2920), 715–716.
- Oh, M., Rohlin, L., Kao, K.C., Liao, J.C., 2002. Global expression profiling of acetate-grown *Escherichia coli*. *J. Biol. Chem.* 277 (15), 13175–13183.
- Paalme, T., Vilu, R., 1993. A new method of continuous cultivation with computer-controlled change of dilution rate. *Control Eng. Prac.* 1 (4), 299–302.
- Phue, J., Shiloach, J., 2004. Transcription levels of key metabolic genes are the cause for different glucose utilization pathways in *E. coli* B (BL21) and *E. coli* K (JM109). *J. Biotechnol.* 109 (1–2), 21–30.
- Phue, J., Noronha, S.B., Hattacharyya, R., Wolfe, A.J., Shiloach, J., 2005. Glucose metabolism at high density growth of *E. coli* B and *E. coli* K: differences in metabolic pathways are responsible for efficient glucose utilization in *E. coli* B as determined by microarrays and Northern blot analyses. *Biotechnol. Bioeng.* 90 (7), 805–820.
- Richard, H., Foster, J.W., 2004. *Escherichia coli* glutamate- and arginine-dependent acid resistance systems increase internal pH and reverse transmembrane potential. *J. Bacteriol.* 186, 6032–6041.
- Richard, H., Foster, J.W., 2007. Sodium regulates *Escherichia coli* acid resistance, and influences GadX- and GadW-dependent activation of *gadE*. *Microbiology* 153 (9), 3154–3161.
- Rosenthal, A.Z., Kim, Y., Gralla, J.D., 2008. Regulation of transcription by acetate in *Escherichia coli*: in vivo and in vitro comparisons. *Mol. Microbiol.* 68, 907–917.
- Seeto, S., Notley-McRobb, L., Ferenci, T., 2004. The multifactorial influences of RpoS, Mlc and cAMP on ptsG expression under glucose-limited and anaerobic conditions. *Res. Microbiol.* 155, 211–215.
- Tramonti, A., Canio, M.D., Biase, D.D., 2008. GadX/GadW-dependent regulation of the *Escherichia coli* acid fitness island: transcriptional control at the *gady-gadW* divergent promoters and identification of four novel 42 bp GadX/GadW-specific binding sites. *Mol. Microbiol.* 70, 965–982.
- Vemuri, G.N., Altman, E., Sangurdekar, D.P., Khodursky, A.B., Eiteman, M.A., 2006. Overflow metabolism in *Escherichia coli* during steady-state growth: transcriptional regulation and effect of the redox ratio. *Appl. Environ. Microbiol.* 72, 3653–3661.
- Wolfe, A.J., 2005. The acetate switch. *Microbiol. Mol. Biol. Rev.* 69, 12–50.
- Wong, M.S., Wu, S., Causey, T.B., Bennett, G.N., San, K., 2008. Reduction of acetate accumulation in *Escherichia coli* cultures for increased recombinant protein production. *Metab. Eng.* 10, 97–108.
- Yang, C., Hua, Q., Baba, T., Mori, H., Shimizu, K., 2003. Analysis of *Escherichia coli* anaplerotic metabolism and its regulation mechanisms from the metabolic responses to altered dilution rates and phosphoenolpyruvate carboxykinase knockout. *Biotechnol. Bioeng.* 84 (2), 129–144.

PUBLICATION II

Valgepea K, Adamberg K, Nahku R, Lahtvee PJ, Arike L, Vilu, R

Systems biology approach reveals that overflow metabolism of acetate in *Escherichia coli* is triggered by carbon catabolite repression of acetyl-CoA synthetase.

BMC Systems Biology, 4:166, (2010)

RESEARCH ARTICLE

Open Access

Systems biology approach reveals that overflow metabolism of acetate in *Escherichia coli* is triggered by carbon catabolite repression of acetyl-CoA synthetase

Kaspar Valgepea^{1,2}, Kaarel Adamberg^{2,3}, Ranno Nahku^{1,2}, Petri-Jaan Lahtvee^{1,2}, Liisa Arike^{2,3}, Raivo Vilu^{1,2*}

Abstract

Background: The biotechnology industry has extensively exploited *Escherichia coli* for producing recombinant proteins, biofuels etc. However, high growth rate aerobic *E. coli* cultivations are accompanied by acetate excretion *i.e.* overflow metabolism which is harmful as it inhibits growth, diverts valuable carbon from biomass formation and is detrimental for target product synthesis. Although overflow metabolism has been studied for decades, its regulation mechanisms still remain unclear.

Results: In the current work, growth rate dependent acetate overflow metabolism of *E. coli* was continuously monitored using advanced continuous cultivation methods (A-stat and D-stat). The first step in acetate overflow switch (at $\mu = 0.27 \pm 0.02 \text{ h}^{-1}$) is the repression of acetyl-CoA synthetase (Acs) activity triggered by carbon catabolite repression resulting in decreased assimilation of acetate produced by phosphotransacetylase (Pta), and disruption of the PTA-ACS node. This was indicated by acetate synthesis pathways PTA-ACKA and POXB component expression down-regulation before the overflow switch at $\mu = 0.27 \pm 0.02 \text{ h}^{-1}$ with concurrent 5-fold stronger repression of acetate-consuming Acs. This in turn suggests insufficient Acs activity for consuming all the acetate produced by Pta, leading to disruption of the acetate cycling process in PTA-ACS node where constant acetyl phosphate or acetate regeneration is essential for *E. coli* chemotaxis, proteolysis, pathogenesis etc. regulation. In addition, two-substrate A-stat and D-stat experiments showed that acetate consumption capability of *E. coli* decreased drastically, just as Acs expression, before the start of overflow metabolism. The second step in overflow switch is the sharp decline in cAMP production at $\mu = 0.45 \text{ h}^{-1}$ leading to total Acs inhibition and fast accumulation of acetate.

Conclusion: This study is an example of how a systems biology approach allowed to propose a new regulation mechanism for overflow metabolism in *E. coli* shown by proteomic, transcriptomic and metabolomic levels coupled to two-phase acetate accumulation: acetate overflow metabolism in *E. coli* is triggered by Acs down-regulation resulting in decreased assimilation of acetic acid produced by Pta, and disruption of the PTA-ACS node.

Background

Escherichia coli has not only been the prime organism for developing new molecular biology methods but also for producing recombinant proteins, low molecular weight compounds etc. in industrial biotechnology for decades due to its low cost manufacturing and end-

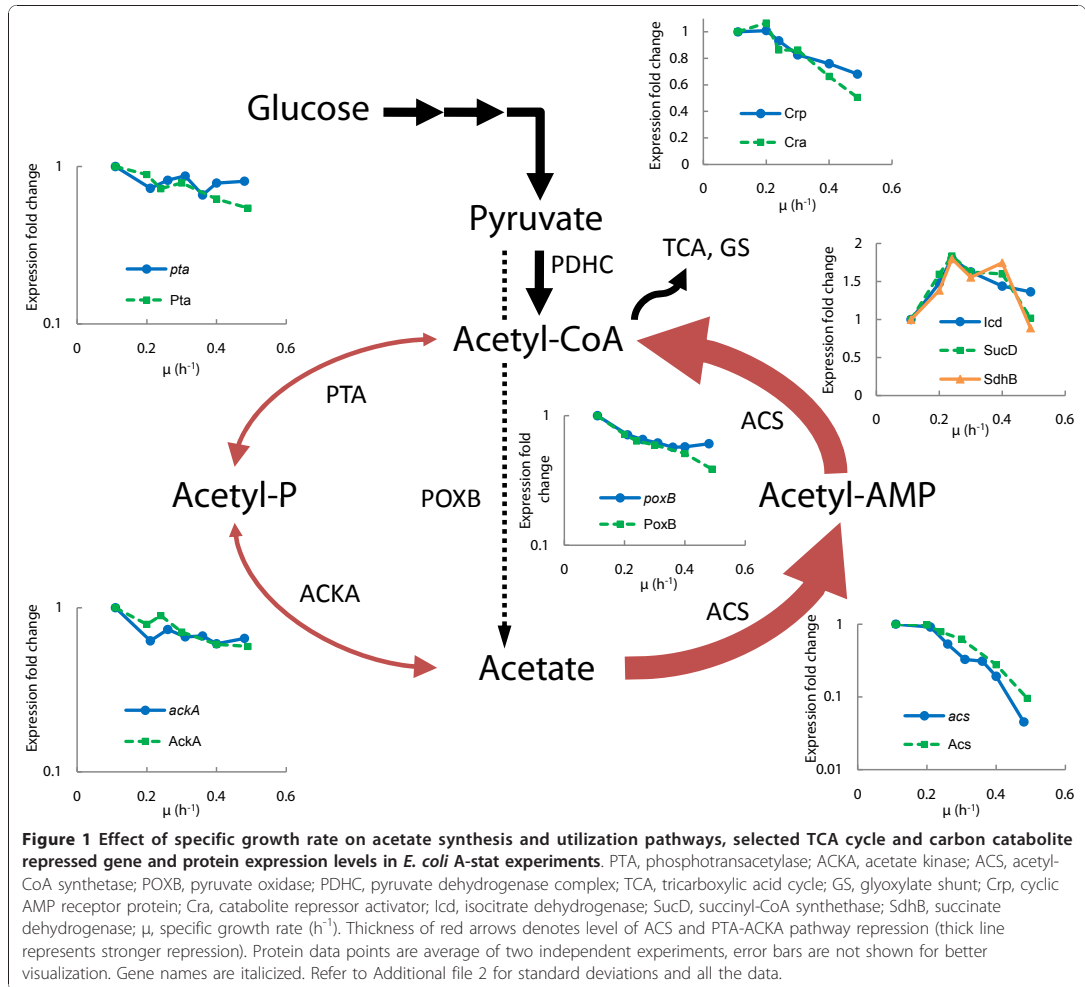
product purification and its ability to reach high cell densities grown aerobically [1,2]. However, a major problem exists with aerobic *E. coli* cultivation on glucose at high growth rates-formation and accumulation of considerable amounts of acetic acid *i.e.* overflow metabolism. In addition to being detrimental for target product synthesis, accumulated acetate inhibits growth and diverts valuable carbon from biomass formation [3,4].

The acetate synthesis and utilization pathways [5] can be seen in Figure 1: acetate can be synthesized by

* Correspondence: raivo@kbf.ee

¹Tallinn University of Technology, Department of Chemistry, Akadeemia tee 15, 12618 Tallinn, Estonia

Full list of author information is available at the end of the article



phosphotransacetylase (PTA)/acetate kinase (ACKA) and by pyruvate oxidase (POXB). Acetic acid can be metabolized to acetyl-CoA either by the PTA-ACKA pathway or by acetyl-CoA synthetase (ACS) through an intermediate acetyl-AMP. The high affinity (K_m of 200 μM for acetic acid) ACS scavenges acetate at low concentrations whereas the low affinity PTA-ACKA pathway (K_m of 7-10 mM) is activated in the presence of high acetate concentrations [6].

The phenomenon of overflow metabolism has been studied widely over the years and it is commonly believed to be caused by an imbalance between the fluxes of glucose uptake and those for energy production and biosynthesis [7,8]. Several explanations such as the saturation of catalytic activities in the tricarboxylic

acid (TCA) cycle [9,10] and respiratory chain [7,11,12], energy generation [5,13] or the necessity for coenzyme A replenishment [14] have been proposed. In addition to bioprocess level approaches [1,15], various genetic modifications of the acetate synthesis pathways extensively reviewed in De Mey *et al.* [15] have been made to minimize acetic acid production. For instance, it has been shown that deleting the main acetate synthesis route PTA-ACKA results in a strong reduction (up to 80%) of acetate excretion, maximum growth rate (*ca* 20%) and elevated levels of formate and lactate (*ca* 30-fold) [4,16-18], whereas *poxB* disruption causes reduction in biomass yield (*ca* 25%) and loss of aerobic growth efficiency of *E. coli* [19]. The latter indicates that acetate excretion cannot be simply excluded by

disrupting its synthesis routes without encountering other unwanted effects. Unfortunately, no clear conclusions could be drawn from batch experiments with an *acs* knock-out strain [4]. It should be noted that studies with *E. coli* genetically modified strains engineered to diminish acetate production in batch cultures have not fully succeeded in avoiding acetate accumulation together with increasing target product production yields and rates [15]. Additionally, these studies have not allowed elucidating the mechanism of overflow metabolism unequivocally [4,20,21].

Acetate overflow is a growth rate dependent phenomenon, but no study has specifically focused on growth rate dependency of protein and gene expression regulation, intra- and extracellular metabolite levels using also metabolic modeling. Describing the physiology of an organism on several 'omic levels is the basis of systems biology that facilitates better understanding of metabolic regulation [22]. In this study, *E. coli* metabolism at proteomic, transcriptomic and metabolomic levels was investigated using continuous cultivation methods prior to and after overflow metabolism was switched on. Usually, chemostat cultures are used for steady state metabolism analysis, however, we applied two changestat cultivation techniques: accelerostat (A-stat) and dilution rate stat (D-stat), see Methods section for details [23,24]. These cultivation methods were used as they provide three advantages over chemostat. Firstly, these changestat cultivation techniques precisely detect metabolically relevant switch points (e.g. start of overflow metabolism, maximum specific growth rate) and enable to monitor the dynamic patterns of several metabolic physiological responses simultaneously which could be left unnoticed using chemostat. Secondly, it is possible to collect vast amount of steady state comparable samples and by doing so, save time. Thirdly, both A-stat and D-stat enable to quantitatively study specific growth rate dependent co-utilization of growth substrates. Latter advantage was applied for investigating acetic acid consumption capability of *E. coli* at various dilution rates in this study. Combining changestat cultivation methods enables to study metabolism responses of the same genotype at different physiological states in detail without encountering the possible metabolic artifacts accompanied when using genetically modified strains.

Results obtained by studying specific growth rate dependent changes in *E. coli* proteome, transcriptome and metabolome in continuous cultures together with metabolic modeling allowed us to propose a new theory for acetate overflow: acetate excretion in *E. coli* is triggered by carbon catabolite repression mediated down-regulation of *Acs* resulting in decreased assimilation of acetate produced by *Pta*, and disruption of the PTA-ACS node.

Results

E. coli metabolic switch points characterization

In all accelerostat (A-stat) cultivation experiments, after the culture had been stabilized in chemostat at 0.10 h^{-1} to achieve steady state conditions, continuous increase in dilution rate with acceleration rate (a) 0.01 h^{-2} (0.01 h^{-1} per hour) was started. Continuous change of specific growth rate resulted in detecting several important changes in *E. coli* metabolism as demonstrated in Figure 2. Firstly, in A-stat cultivations where glucose was the only carbon source in the medium, acetic acid started to accumulate (i.e. overflow metabolism switch) at $\mu = 0.27 \pm 0.02 \text{ h}^{-1}$ (average \pm standard deviation) and a two-phase acetate accumulation pattern was observed (discussed below; Figure 2). Cells reached maximum CO_2 production and O_2 consumption at $\mu = 0.46 \pm 0.02 \text{ h}^{-1}$ and metabolic fluctuations were observed at $\mu = 0.49 \pm 0.03 \text{ h}^{-1}$ followed by washout of culture at $\mu = 0.54 \pm 0.03 \text{ h}^{-1}$ (corresponding to maximum specific growth rate at given conditions). The nature of these fluctuations will be studied further and not covered in the current publication. All A-stat results were reproduced with relative standard deviation less than 10% with the exception of acetate production per biomass (Y_{OAc}) (Table 1 and Figure S1 in Additional file 1).

Metabolomic responses to rising specific growth rate

A-stat cultivation enabled to study acetic acid accumulation profile in detail with increasing specific growth rate. Interestingly, a two-phase acetate accumulation pattern was observed (Figure 2). Slow accumulation of acetic

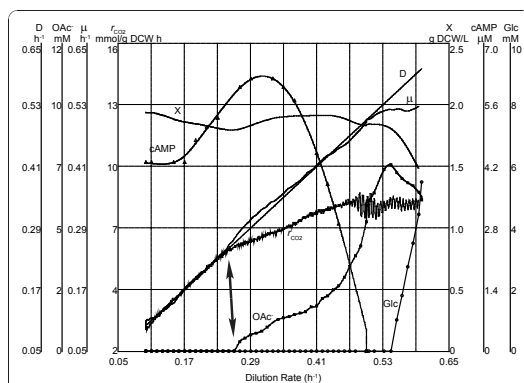


Figure 2 Increasing dilution rate dependent *E. coli* metabolism characterization in one A-stat cultivation ($a = 0.01 \text{ h}^{-2}$). D, dilution rate (h^{-1}); X, biomass concentration (g dry cellular weight (DCW)/L); μ , specific growth rate (h^{-1}); r_{CO_2} , specific CO_2 production rate (mmol/g DCW h); OAc, acetate concentration (mM); Glc, glucose concentration (mM); cAMP, cyclic AMP concentration (μM). Arrow indicates the start of overflow metabolism. Start of vertical axes was chosen for better visualization.

Table 1 A-stat and chemostat growth characteristics comparison and A-stat reproducibility over the studied specific growth rate range for three independent experiments

	$\mu = 0.24 \text{ h}^{-1}$		$\mu = 0.30 \text{ h}^{-1}$		$\mu = 0.40 \text{ h}^{-1}$		$\mu = 0.51 \text{ h}^{-1}$		$\mu = 0.10\text{-}0.47 \text{ h}^{-1}$ A-stat RSD, %
	Chemostat	A-stat	Chemostat	A-stat	Chemostat	A-stat	Chemostat	A-stat	
Y_{XS}^a	0.44	0.40 ± 0.01	0.46	0.41 ± 0.01	0.44	0.42 ± 0.00	0.43	0.41 ± 0.01	2.0
Y_{OAc}^b	NDE	NDE	0.53	0.90 ± 0.32	1.70	1.56 ± 0.23	3.25	3.35 ± 0.82	ND
Y_{cAMP}^c	3.47	3.59 ± 0.39	3.25	3.55 ± 0.32	2.70	2.17 ± 0.07	0.86	0.71 ^e	9.1
$Y_{CO_2}^d$	27.56	30.12 ± 2.04	27.55	27.19 ± 1.22	26.24	23.86 ± 1.41	ND	21.19 ± 0.19	5.6

A-stat values represent the average from three independent experiments and standard deviation follows the ± sign. Chemostat values from one experiment. NDE, not detected. ND, not determined. RSD, relative standard deviation.

^aBiomass yield is given in g dry cell weight (DCW)/g glucose consumed (g DCW/g glucose).

^bAcetic acid production per biomass is given in mmol acetic acid/g DCW.

^ccAMP production per biomass is given in μmol cAMP/g DCW.

^dCarbon dioxide (CO₂) production per biomass is given in mmol CO₂/g DCW.

^eData from one A-stat experiment.

acid started at $\mu = 0.27 \pm 0.02 \text{ h}^{-1}$ with concomitant change in specific CO₂ production rate (Figure 2). Faster accumulation of acetate was witnessed after cells had reached maximum CO₂ production at $\mu = 0.46 \pm 0.02 \text{ h}^{-1}$. Quite surprisingly, production of the important carbon catabolite repression (CCR) signal molecule cAMP (Y_{cAMP}) rose from steady state chemostat level $2.45 \pm 0.26 \mu\text{mol/g}$ dry cellular weight (DCW) ($\mu = 0.10 \text{ h}^{-1}$) to $3.55 \pm 0.32 \mu\text{mol/g}$ DCW ($\mu = 0.30 \text{ h}^{-1}$) after which it sharply decreased to $1.30 \pm 0.44 \mu\text{mol/g}$ DCW at $\mu = 0.45 \text{ h}^{-1}$ (Figure S1 in Additional file 1). This abrupt decline took place simultaneously with the faster acetate accumulation profile described above (Figure 2 and Figure S1 in Additional file 1). In addition, similar two-phase acetate accumulation phenomenon was observed in a two-substrate (glucose + acetic acid) A-stat during the decrease of cAMP around specific growth rate 0.39 h^{-1} (Figure S2 in Additional file 1).

Significant fall in two of the measured pentose phosphate pathway intermediates ribose-5-phosphate (R5P) and erythrose-4-phosphate (E4P) was detected with increasing specific growth rate which could point to possible limitation in RNA biosynthesis during growth (Figure 3A). PTA-ACS node related compound nonesterified acetyl-CoA (HS-CoA) level declined two-fold simultaneously with cAMP after acetate started to accumulate (Figure 3B). This indicates the possible increase of other CoA containing compounds e.g. succinyl-CoA. Accumulation of TCA cycle intermediates α -ketoglutarate and isocitrate (Figure 3B) with increasing dilution rate could be associated with pyrimidine deficiency and decrease of ATP expenditure in the PTA-ACS cycle. Concurrently, intracellular concentrations of fructose-1,6-bisphosphate (FBP) and glyceraldehyde-3-phosphate (GAP) from the upper part of energy generating glycolysis increased 6- and 3-fold, respectively (Figure 3C).

Functional-genomic responses to rising specific growth rate

The two main known pathways for acetate synthesis phosphotransacetylase-acetate kinase (PTA-ACKA) and pyruvate oxidase (POXB) were down-regulated, both on gene and protein expression levels, from $\mu = 0.20 \text{ h}^{-1}$ i.e. before acetate overflow was switched on. At the same time, there was a concurrent 10-fold repression of the acetic acid utilization enzyme acetyl-CoA synthetase (Acs). This substantial difference (5-fold) between the acetate synthesis and assimilation pathways expression suggests that the synthesized acetic acid cannot be fully assimilated with increasing growth rates (Figure 1).

We observed the beginning of carbon catabolite repression (CCR) induction prior to acetate accumulation in parallel with Acs down-regulation. This was indicated by down-regulation (3-fold on average) of CCR-mediated components: alternative (to glucose) substrate transport and utilization systems like galactose (MglAB), maltose (MalBEFKM), galactitol (GatABC), L-arabinose (AraF), D-ribose (RbsAB), C₄-dicarboxylates (DctA) and acetate (ActP, YjcH) (Figure 4C and Additional file 2). Moreover, expression of transcription activator Crp (cyclic AMP receptor protein which regulates the expression of Acs transcribing *acs-yjcH-actP* operon) and Cra (catabolite repressor activator; a global transcriptional protein essential for acetic acid uptake [25]) were reduced 1.5 and 2 times, respectively, in like manner to carbon catabolite repressed proteins mentioned above (Figure 1). Simultaneously, components of the gluconeogenesis pathway (Pck, MaeB, Pps) and glyoxylate shunt enzymes AceA, AceB (vital for acetate consumption) were repressed with growth rate increase (Figure 4B and Additional file 2). It should be emphasized that most of the TCA cycle gene and protein levels were maintained or even increased up to $\mu = 0.40 \text{ h}^{-1}$

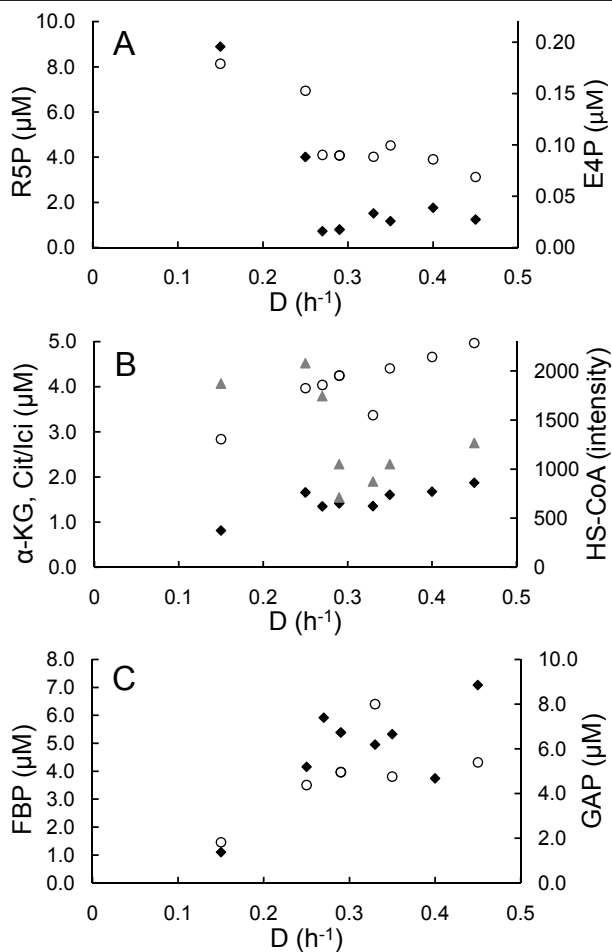


Figure 3 Dilution rate dependent intracellular metabolite patterns in one *E. coli* A-stat experiment. D, dilution rate (h^{-1}). (A) Pentose phosphate pathway metabolites. R5P, ribose-5-phosphate concentration (black diamond); E4P, erythrose-4-phosphate concentration (open circle). (B) TCA cycle metabolites and co-factor free CoA. α -KG, α -ketoglutarate concentration (black diamond); Cit/Ici, citrate/isocitrate pool concentration (open circle); HS-CoA, co-factor free CoA level (grey triangle). (C) Glycolysis (upper part) metabolites. FBP, fructose-1,6-bisphosphate concentration (black diamond); GAP, glyceraldehyde-3-phosphate concentration (open circle).

followed by sudden repression simultaneous to achieving maximum specific CO_2 production rate ($\mu = 0.46 \pm 0.02 \text{ h}^{-1}$, see above; Figure 1 Figure 2 and Figure 4A). This may allude to no limitation at the TCA cycle level around the specific growth rate where overflow metabolism was switched on.

Acetic acid consumption capability studied by dilution rate stat (D-stat) and two-substrate A-stat cultivations

The beginning of a strong decrease in acetate assimilation enzyme Acs expression before overflow switch point implies to a possible connection between acetate

assimilation capability and overflow metabolism of acetate (Figure 1). Therefore, specific growth rate dependent acetic acid consumption capabilities were investigated using D-stat and two-substrate A-stat methods. It was shown by D-stat experiments at various dilution rates that more than a 12-fold reduction in acetate consumption capability took place around overflow switch point, and its total loss was detected between dilution rates 0.45 and $0.505 \pm 0.005 \text{ h}^{-1}$ (Figure 5). Acetic acid consumption and production was also studied in a single experiment using two substrate (glucose + acetic acid) A-stat cultivation (Figure S2 in Additional file 1) which

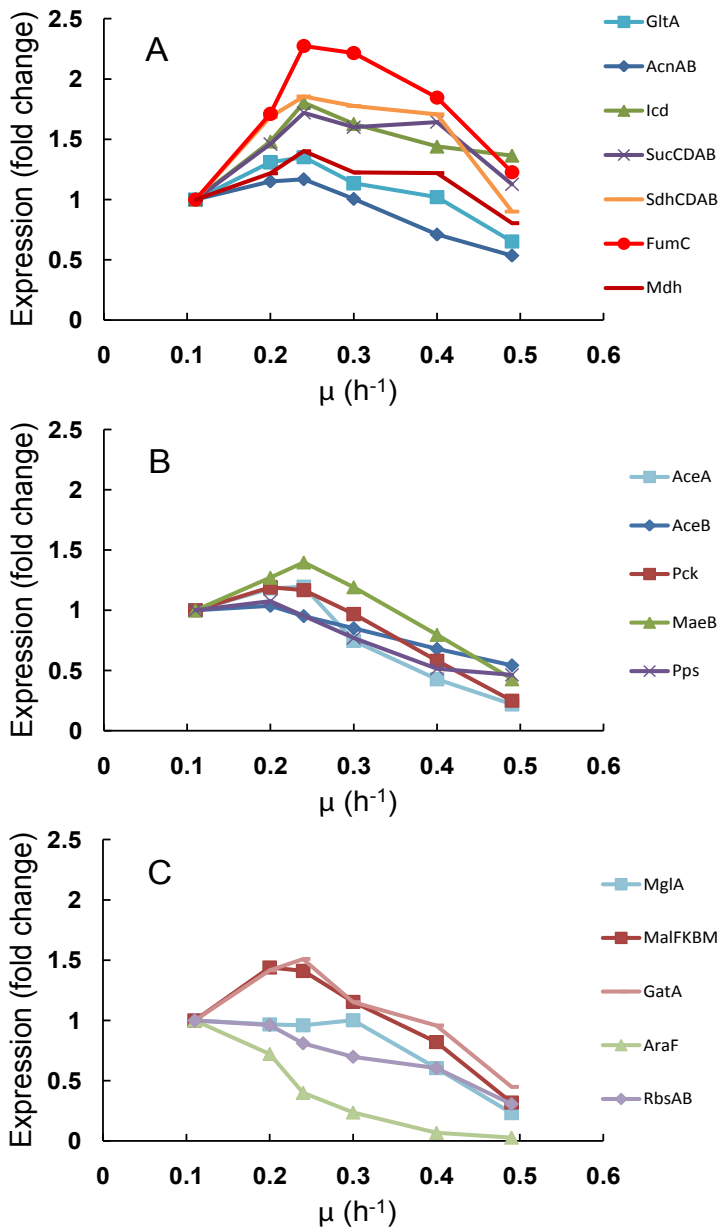
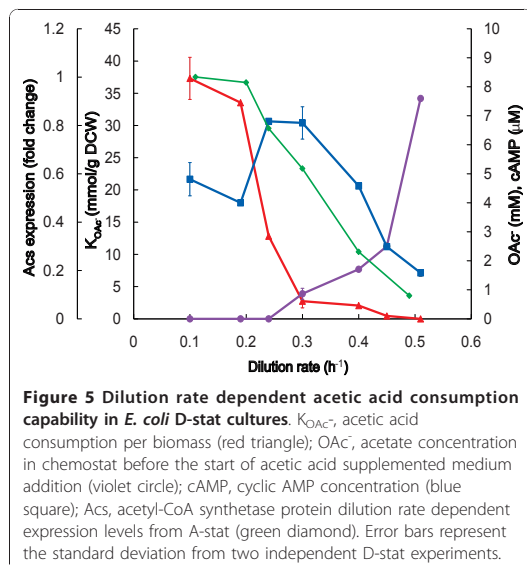


Figure 4 Specific growth rate dependent TCA cycle, glyoxylate shunt, glyconeogenesis and carbon catabolite repressed protein expression changes in *E. coli* A-stat cultures. μ , specific growth rate (h^{-1}). (A) TCA cycle (average of proteins from the same operon are depicted as one point e.g. AcnAB). (B) Glyoxylate shunt (AceA, AceB) and glyconeogenesis. (C) Carbon catabolite repressed proteins. Protein data points are average of two independent experiments, error bars are not shown for better visualization (refer to Additional file 2 for standard deviations).



demonstrated that acetic acid consumption started to decrease at $\mu = 0.25 \text{ h}^{-1}$ and was completely abolished at $\mu = 0.48 \text{ h}^{-1}$ which fits into the range of dilution rates observed in D-stat.

A-stat comparison with chemostat

As could be seen from Table 1 major growth characteristics such as biomass yield (Y_{XS}), acetate (Y_{OAc}), cyclic AMP (Y_{cAMP}) and carbon dioxide (Y_{CO_2}) production per biomass from A-stat and chemostat are all fully quantitatively comparable. The latter results enable to use A-stat data for quantitative modeling calculations. In addition, the two continuous cultivation methods were examined at transcriptome level using DNA microarrays. Transcript spot intensities from quasi steady state A-stat sample at $\mu = 0.48 \text{ h}^{-1}$ and chemostat sample at $\mu = 0.51 \text{ h}^{-1}$ showed an excellent Pearson product-moment correlation coefficient $R = 0.964$ (Figure S3 in Additional file 1; Additional file 3). This indicates good biological correlation between *E. coli* transcript profiles at similar specific growth rates in chemostat and A-stat. These results showed that our quasi steady state data from A-stat and D-stat cultures are steady state representative.

Proteome and transcriptome comparison

E. coli protein expression ratios for around 1600 proteins were generated by comparing two biological replicates at specific growth rates 0.20 ± 0.01 ; 0.26 ; 0.30 ± 0.01 ; 0.40 ± 0.00 ; $0.49 \pm 0.01 \text{ h}^{-1}$ with sample at $\mu = 0.10 \pm 0.01 \text{ h}^{-1}$ (chemostat point prior to the start of

acceleration in A-stat) which produced Pearson correlation coefficients for two biological replicates in the indicated pairs of comparison in the range of $R = 0.788-0.917$ (Figure S4 in Additional file 1).

DNA microarray analysis of 4,321 transcripts was conducted with the Agilent platform using the samples from one A-stat cultivation. Gene expression ratios between specific growth rates 0.21 ; 0.26 ; 0.31 ; 0.36 ; 0.40 ; 0.48 h^{-1} and $\mu = 0.11 \text{ h}^{-1}$ (chemostat point prior to the start of acceleration in A-stat) were calculated. Comparison of gene and protein expression changes (between respective specific growth rates) revealed that components of the PTA-ACS node were regulated at transcriptional level as the absolute majority of the studied transcripts and proteins indicated by the good correlation between transcriptome and proteome expression profiles (Figure 1 and Figure S5 in Additional file 1).

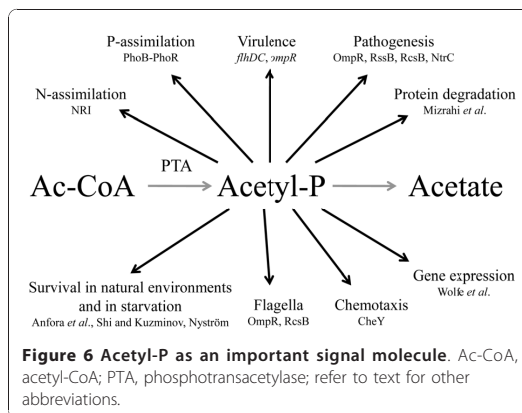
Most recent studies have either failed to find a significant correlation between protein and mRNA abundances or have observed only a weak correlation (reviewed in [22]). It has been suggested that the main reasons for uncoupling of mRNA and protein abundances are protein regulation by post-translational modification, post-transcriptional regulation of protein synthesis, differences in the half-lives of mRNA and proteins, or possible functional requirement for protein binding [22]. As the cells in these studies were mostly cultured in non steady state condition, our steady state data with very good correlation between transcriptome and proteome implies that the physiological state of the culture (steady state vs. non steady state) could be an important factor in terms of mRNA and protein correlation determination. Transcriptome and proteome data are presented in Additional file 2 and at NCBI Gene Expression Omnibus and PRIDE database (see Methods for details), respectively.

Discussion

To gain better insights into the regulation of acetate overflow metabolism in *E. coli*, we studied specific growth rate dependent proteomic, transcriptomic and metabolomic patterns combined with metabolic modeling using advanced continuous cultivation methods, which has not been carried out before. Continuous monitoring of the specific growth rate effect on *E. coli* metabolism enabled us to precisely detect important metabolic shift points, the most important being the start of acetate overflow at $\mu = 0.27 \pm 0.02 \text{ h}^{-1}$ (Figure 2), and changing patterns of a number of important metabolites e.g. acetate, cAMP. Quite surprising was the down-regulation of the known acetate synthesis pathways, PTA-ACKA and POXB expression before overflow switch with increasing growth rate (Figure 1). A similar pattern has been seen before in chemostat cultures

but without emphasizing the possible physiological consequences [26-28]. A 10-fold repression of the acetic acid utilization enzyme acetyl-CoA synthetase (Acs) expression was observed concurrently with the down-regulation of the PTA-ACKA pathway indicating that acetic acid synthesis might exceed its assimilation (Figure 1). Our two substrate A-stat and D-stat experiments directly proved that acetate consumption capability of *E. coli* is specific growth rate dependent as acetate consumption started to decrease at $\mu = 0.25 \text{ h}^{-1}$ (Figure S2 in Additional file 1) and acetate consumption capability decreased 12-fold around overflow switch growth rate $\mu = 0.27 \pm 0.02 \text{ h}^{-1}$, respectively (Figure 5). In addition, it was shown that activation of carbon catabolite repression (CCR) and repression of Acs take place simultaneously prior to the start of overflow metabolism (Figure 1 Figure 4 and Figure 5). As a result, it is proposed that acetate overflow metabolism in *E. coli* is triggered by Acs down-regulation resulting in decreased assimilation of acetic acid produced by Pta, and disruption of the PTA-ACS node.

We showed that Acs was concurrently down-regulated five times more compared to the acetate synthesis pathways (Figure 1). In addition, the TCA cycle flux decrease as shown by change in CO_2 production at overflow switch growth rate indicates that carbon is not metabolized by the TCA cycle after the start of acetate accumulation with pre overflow switch rates (Figure 2 and Additional file 4). The latter is caused because the amount of acetyl-CoA entering the TCA cycle decreases after carbon is lost into excreted acetate. Stronger repression of the acetate consuming Acs in comparison with acetate synthesizing PTA-ACKA together with a decline in TCA cycle flux suggest disruption of acetic acid cycling at the PTA-ACS node (Figure 1). While this node may seem as a futile cycle, the fact is that numerous metabolic tasks involving the intermediate molecules of this cycle-acetyl phosphate (acetyl-P) and acetyl-AMP-are essential for proper *E. coli* growth (Figure 6). For instance, these molecules play a crucial role in bacterial chemotaxis regulation in which flagellar rotation is controlled by the activation level of the response regulator CheY [29] through either phospho-transfer from CheA [30,31] or acetyl-P [31,32], acetylation by acetyl-AMP [33,34] or co-regulation of both mechanisms [29]. It has been also demonstrated that acetyl-P synthesis is vital for EnvZ-independent regulation of outer membrane porins [35], pathogenesis [36] and regulation of several virulence factors [5]. Furthermore, it has been presented that acetyl-P interacts with phosphate concentration regulators PhoB-PhoR [37] and NRI protein which is part of a complex nitrogen sensing system [38]. Acetyl-P is critical for efficient degradation of unfolded or damaged proteins by ATP-dependent



proteases [39]. Altogether, acetyl-P can influence the regulation of almost 100 other genes [40]. Finally, *pta* and/or *ackA* mutations were shown to affect repair-deficient *E. coli* mutants [41] and a *pta* mutant has been reported to be impaired in its ability to survive during glucose starvation, while the *ackA* mutant survived as well as the parent strain [42]. It is important to note that the only known pathway in *E. coli* for acetyl-P synthesis is the PTA-ACKA [5,31]. Taking all the previous into account, we conclude that acetyl-P as well as acetyl-AMP are essential for cellular growth of *E. coli*, and as acetic acid formation is the result of their dephosphorylation, acetic acid should be synthesized and consumed simultaneously during growth to maintain proper balance between metabolites of the PTA-ACS node. This is in agreement with Shin *et al.* [28] who proposed that wild-type *E. coli* constitutively synthesizes acetate even when growing on non-acetogenic carbon source succinate or at low growth rates in carbon limited cultures. It also has to be mentioned that acetic acid is a by-product in the synthesis of cysteine, methionine and arginine, covering around 0.4 mmol/g DCW (Additional file 4). Based on our experimental and literature data, production and re-assimilation of acetate might be over 1 mmol/g DCW at $\mu = 0.2 \text{ h}^{-1}$ (Text S2 in Additional file 1) which further supports the hypothesis of the necessity for constant acetic acid synthesis.

A similar regulation for overflow metabolism of acetate was posed for *Saccharomyces cerevisiae* by Postma and co-workers: they postulated that acetate accumulation is the result of insufficient acetyl-CoA synthetase activity for the complete functioning of the pyruvate dehydrogenase bypass because of glucose repression of ACS at high growth rates [43]. The hypothesis proposed here is also consistent with the observation that an *acs* mutant of *E. coli* accumulated acetate in chemostat cultures at dilution rate (D) 0.22 h^{-1} whereas acetate

overflow was started in wild-type at a higher $D = 0.35 \text{ h}^{-1}$ [28]. Furthermore, it has been shown that over-expression of *acs* [44] and constitutively expressed *acs* together with glyoxylate shunt repressors *iclR* and *fadR* mutant resulted in a significant reduction in acetate accumulation in glucose batch fermentations [28]. Adams and co-workers showed that as a result of micro-evolution, *E. coli* increased acetate consumption capability by over-expressing *Acs* (not *AckA*) [45,46], further supporting the connection between *Acs* activity and acetate accumulation.

As *Acs* down-regulation is responsible for triggering overflow metabolism and the resulting accumulation of acetate is detrimental to cellular growth, it bears questioning why *E. coli* has not evolved towards maintaining sufficient *Acs* levels for acetate assimilation in all growth conditions. Growth conditions in *E. coli* native environments are rough as concentrations of utilizable carbon sources including acetate are in the low mg L^{-1} range and access to nutrients is troublesome [47]. These harsh conditions force *E. coli* to make its metabolism ready for scavenging all possible carbon sources including acetate. However, in nutrient rich laboratory conditions, *E. coli* focuses on anthropic growth [48] and biomass production rate, primarily realized by enhancing readily oxidizable substrate (glucose) uptake kinetics which in turn results in *Acs* repression through CCR and thus, acetate accumulation [46]. This indicates that an active *Acs* is not essential for rapid growth for *E. coli*. It seems that maintaining high expression levels of acetate assimilation components (and also other alternative substrates ones) is energetically not favorable at higher growth rates. Moreover, as the space on cell membrane is limited and as *E. coli* achieves more rapid growth probably by increasing the number of glucose transport machinery components on the membrane, using area for alternative substrate transport proteins is not beneficial for faster growth. Interestingly, even in one of its natural environments-urinary tract-where a continuous dilution of acetate occurs, it has been shown that metabolizing acetate to acetyl-CoA by *Acs* is not essential for normal *E. coli* colonization as PTA-*AckA* pathway and maintenance of a proper intracellular acetyl-P concentration are necessary for colonizing murine urinary tract [32].

Based on all the points discussed above, PTA-*ACS* might function as a futile cycle to provide rapid regulation of acetyl-P concentration in the cell for an active chemotaxis that is vital in natural nutrient-depleted environments, fighting against other organisms (acetate production), pathogenesis, biofilm formation etc. This hypothesis is consistent with the fact that the flagellar assembly and regulation operon (*tar-tap-cheRBYZ*) was more intensively expressed at lower growth rates (Additional file 2) where residual glucose concentration is smaller.

Concerning *Acs* down-regulation, it is possible that CCR is responsible for its repression as proposed by Treves *et al.* [46] showing the link between *ACS* expression level and acetate accumulation. In our experiments, it was shown that activation of CCR and repression of *Acs* take place simultaneously prior to the start of overflow metabolism (Figure 1 and Figure 4). As it is well known that CCR is initiated by the presence of glucose in the medium [49,50], we propose that increasing residual glucose concentration accompanying smooth rise of dilution rate in A-stat triggers *Acs* down-regulation by CCR. The cAMP-Crp complex is one of the major players in CCR of *E. coli* as cAMP binding to Crp drastically increases its affinity towards activating the promoters of catabolic enzymes, including *Acs* [6,49,50]. We measured a 1.5-fold decrease in Crp expression with increasing growth rate (Figure 1) that is in agreement with the data in the literature [51]. In addition, when *E. coli* mutant defective in the gene *crp* was cultivated in glucose-limited chemostat at a low $D = 0.10 \text{ h}^{-1}$, it accumulated acetate whereas the wild-type did not [52]. Furthermore, it exhibited a 34% higher biomass yield relative to the wild-type-this increase might be explained by reduced ATP wasting in the acetate futile cycle, which can be directed to biomass synthesis. Moreover, Khankal *et al.* [53] noted that *E. coli* CRP* mutants that do not require Crp binding to cAMP to activate the expression of catabolic genes showed lowered glucose effect on xylose consumption, 3.6 times higher *acs* expression levels and secreted substantially less acetate in xylitol producing batch fermentations. The connection between cAMP concentration and acetic acid consumption capability, together with the two-phase acetate accumulation profile observed in A-stat and D-stat cultures (Figure 2 and Figure 5) suggests a correlation between increasing residual glucose concentration mediated cAMP-Crp repression and acetate accumulation. Thus, cAMP-Crp dependent regulation of *Acs* transcribing *acs-yjch-actP* operon might be a reason for acetate excretion, as also proposed by Veit *et al.* [10]. Our hypothesis of the CCR mediated acetate overflow metabolism is as well in agreement with the fact that rising glucose lowers the intracellular Crp level through the autoregulatory loop of the *crp* gene [54]. However, other mechanisms can also be involved in *Acs* down-regulation, for example by *Cra* (Figure 1). Indeed, Sarkar and colleagues have shown that glucose uptake and acetate production rates increased with a decrease of acetate consumption in an *E. coli* *cra* mutant [55].

What could be the biological relevance of the disruption of the PTA-*ACS* node? Firstly, decline of the ATP-spending PTA-*ACS* cycle throughput with increasing growth rate points to possible lower ATP spilling (our model calculations). Secondly, disruption of the PTA-

ACS node decreases the energy needed for expression of this cycle's components. As the disruption of PTA-ACS cycle is CCR-mediated, repression of other alternative substrate transport and utilization enzymes by CCR enables to save additional energy. This could all lead to the decrease of ATP production as was indicated by the diminishing TCA cycle fluxes (Figure 2). Hence, it is plausible that cells repress (by CCR) the expression levels of alternative substrate utilization components (including Acs) for making space on the cell membrane for more preferred substrate (glucose) utilization and ATP producing components to achieve faster growth (see above).

Finally, it was demonstrated that highly reproducible A-stat data are well comparable to chemostat at the level of major growth characteristics and transcriptome, hence quasi steady state data from A-stat can be considered steady state representative (Table 1; Figure S1 and Figure S3 in Additional file 1). Furthermore, as shown also by Postma *et al.* for *S. cerevisiae* [43], chemostat is not fully suitable for characterization of dilution rate dependent metabolic transitions, whereas A-stat should be considered an appropriate tool for this. A-stat is especially well suited for the studies of the details of transient metabolism processes. Dynamic behavior of acetate, cAMP etc. with increasing specific growth rate (Figure 2 Figure 3 and Figure S1 in Additional file 1) and change in acetic acid consumption capability in the two-substrate A-stat (Figure S2 in Additional file 1) could be cited as good examples of the latter.

Conclusion

This study is an excellent example of how a systems biology approach using highly reproducible advanced cultivation methods coupled with multiple 'omics analysis and metabolic modeling allowed to propose a new possible regulation mechanism for overflow metabolism in *E. coli*: acetate overflow is triggered by carbon catabolite repression mediated Acs down-regulation resulting in decreased assimilation of acetate produced by Pta, and disruption of the PTA-ACS node. The practical implications derived from this could lead to better engineering of *E. coli* in overcoming several metabolic obstacles, increasing production yields etc.

Methods

Bacterial strain, medium and continuous cultivation conditions

The *E. coli* K12 MG1655 (λ^- F⁻ *rph-1Fnr*⁺; Deutsche Sammlung von Mikroorganismen und Zellkulturen, Germany) strain was used in all experiments. Growth and physiological characteristics in accelerostat (A-stat) cultivations were determined using a defined minimal medium as described before by Nahku *et al.* [51], except

4.5 g/L α -(D)-glucose and 100 μ l L⁻¹ Antifoam C (Sigma Aldrich, St. Louis, LO) was used. The latter was also used in dilution rate stat (D-stat) experiments as the main cultivation medium. In addition, a second medium was used in D-stat where the main medium was supplemented by acetic acid and prepared as follows: 300 ml medium was withdrawn from the main cultivation medium and supplemented with 3 ml of glacial acetic acid (99.9%). One A-stat experiment (referred to as two-substrate A-stat) was carried out with the same medium as other A-stats, but in addition supplemented with acetic acid (final concentration 5 mM).

The continuous (both A-stat and D-stat) cultivation system consisted of 1.25 L Biobundle bioreactor (Applikon Biotechnology B.V., Schiedam, the Netherlands) controlled by an ADI 1030 biocontroller (Applikon Biotechnology B.V.) and a cultivation control program "BioXpert NT" (Applikon Biotechnology B.V.). The system was equipped with OD, pH, pO₂, CO₂ and temperature sensors. The bioreactor was set on a balance whose output was used as the control variable to ensure constant culture volume (300 \pm 1 mL). Similarly, the inflow was controlled through measuring the mass of the fresh culture medium.

A-stat cultivation system and control algorithms used are described in more detail in our previous works [24,51,56]. Dilution rate stat (D-stat) is a continuous cultivation method where dilution rate is constant as in a chemostat while an environmental parameter is smoothly changed [24]. The D-stat experiments in this study were carried out with a slight modification: instead of changing an environmental parameter, two different media were used to keep dilution rate constant. After achieving steady state conditions in chemostat using minimal medium supplemented with glucose, addition of the second medium complemented with glucose and acetic acid was started. The feeding rate of the initial medium was decreased at the same time, resulting in constant glucose concentration in the feed. The acetic acid concentration in the bioreactor as a result of inflow has to be determined to enable precise acetic acid consumption/production rate calculation for the bacteria. Hence, increase of acetic acid concentration in bioreactor was calculated and validated in duplicate non-inoculated D-stat test experiments producing an average standard deviation of 1.24 mM between calculated and measured acetic acid concentrations.

All continuous cultivation experiments were carried out at 37°C, pH 7 and under aerobic conditions (air flow rate 150 ml min⁻¹) with an agitation speed of 800 rpm. Four A-stat cultivations were performed with acceleration rate (a) 0.01 h⁻². Duplicate D-stat experiments were performed at dilution rates 0.10; 0.30; 0.505 \pm 0.005 h⁻¹ and single experiments at 0.19; 0.24;

0.40; 0.45 h⁻¹. The acetic acid addition profile was set to achieve 32 ± 6 mM and 58 ± 5 mM in 7 hours inside the bioreactor for experiments at dilution rates 0.10-0.24 h⁻¹ and 0.30-0.51 h⁻¹, respectively. The growth characteristics of the bacteria were calculated on the basis of total volume of medium pumped out from bioreactor (L), biomass (g DCW), organic acid concentrations in culture medium (mM) and CO₂ concentration in the outflow gas (mM). Formulas were as described in a previous study [24]. It should be noted that the absolute CO₂ concentrations could be error-prone due to measurement difficulties. However, this does not influence the dynamic pattern of specific CO₂ production rate (r_{CO_2}) during specific growth rate increase.

Analytical methods

The concentrations of organic acids (lactate, acetate and formate), ethanol and glucose in the culture medium were determined by HPLC and cellular dry weight (expressed as DCW) as described by Nahku *et al.* [51].

Protein expression analysis

Refer to Text S1 in Additional file 1 for detailed description. Shortly, protein expression ratios for around 1600 proteins (identified for each growth rate at a > 95% confidence interval in average from 89,303 distinct 2 or more high-confidence peptides) were generated from mass spectrometric spectra by firstly calculating the ratios between continuous cultivation samples at specific growth rates 0.10 ± 0.01 h⁻¹ (chemostat point prior to the start of acceleration in A-stat); 0.20 ± 0.01; 0.26; 0.30 ± 0.01; 0.40 ± 0.00; 0.49 ± 0.01 h⁻¹ and batch sample grown on medium containing ¹⁵NH₄Cl as the only source of ammonia. Secondly, the ratios between the mentioned specific growth rates with chemostat point ($\mu = 0.10 \pm 0.01$ h⁻¹) for two biological replicates were calculated to yield protein expression levels for respective specific growth rates. Protein (and gene) expression measurement results are shown in Additional file 2. Proteomic analysis data is also available at the PRIDE database [57] <http://www.ebi.ac.uk/pride> under accession numbers 12189-12199 (username: review74613, password: Ge9T48e8). The data was converted using PRIDE Converter <http://code.google.com/p/pride-converter> [58].

Gene expression profiling

DNA microarray analysis of 4,321 transcripts was conducted with the Agilent platform using the data from one A-stat cultivation ($a = 0.01$ h⁻²), and gene expression ratios between specific growth rates 0.21; 0.26; 0.31; 0.36; 0.40; 0.48 h⁻¹ and $\mu = 0.11$ h⁻¹ were calculated. Transcript spot intensities of chemostat sample (sample from D-stat prior to acetic acid addition) from $\mu = 0.51$

h⁻¹ and A-stat $\mu = 0.48$ h⁻¹ were used for the two method's comparison at transcriptome level. Gene (and protein) expression measurement results are shown in Additional file 2. DNA microarray data is also available at NCBI Gene Expression Omnibus (Reference series: GSE23920). The details of the procedure are provided in Text S1 in Additional file 1.

Metabolome analysis

Sampling was carried out by the rapid centrifugation method. Acquity UPLC (Waters, Milford, MA) together with end-capped HSS C18 T3 1.8 μ m, 2.1 × 100 mm column for compound separation coupled to TOF-MS with an electrospray ionization (ESI) source was used for detection (LCT Premiere, Waters). The details of the procedure are provided in Text S1 in Additional file 1.

Additional material

Additional file 1: Detailed Methods (Text S1); calculation of acetate reconsumption (Text S2); Supplementary Figures S1-S5.

Additional file 2: Growth rate dependent gene (one A-stat) and average protein expression changes of two A-stat experiments with *Escherichia coli* K12 MG1655. Transcriptome and proteome analysis results, also with standard deviations.

Additional file 3: Gene spot intensities of A-stat at $\mu = 0.48$ h⁻¹ and chemostat at $\mu = 0.51$ h⁻¹ experiments with *Escherichia coli* K12 MG1655. Data for A-stat and chemostat transcriptome comparison.

Additional file 4: Simplified metabolic flux analysis. Detailed description of model calculations with simplified metabolic flux analysis.

Acknowledgements

The financial support for this research was provided by the Enterprise Estonia project EU29994, and Ministry of Education, Estonia, through the grant SF0140090s08. The authors would like to thank Lauri Peil and Elina Pelonen for help in carrying out 'omics analysis.

Author details

¹Tallinn University of Technology, Department of Chemistry, Akadeemia tee 15, 12618 Tallinn, Estonia. ²Competence Centre of Food and Fermentation Technologies, Akadeemia tee 15b, 12618 Tallinn, Estonia. ³Tallinn University of Technology, Department of Food Processing, Ehitajate tee 5, 19086 Tallinn, Estonia.

Authors' contributions

KV, KA, and RV drafted the manuscript. RN, PL, and LA helped in preparing the manuscript. KV, RN, and PL designed and performed the experiments. KV analysed the experimental data. RN, PL, and LA carried out the 'omics analysis. KV, KA, and RV guided and coordinated the project. All authors read and approved the manuscript.

Received: 16 June 2010 Accepted: 1 December 2010

Published: 1 December 2010

References

1. Eiteman MA, Altman E: Overcoming acetate in *Escherichia coli* recombinant protein fermentations. *Trend Biotechnol* 2006, **24**:530-536.
2. Clomburg JM, Gonzalez R: Biofuel production in *Escherichia coli*: the role of metabolic engineering and synthetic biology. *Appl Microbiol Biotechnol* 2010, **86**:419-434.

3. Nakano K, Rischke M, Sato S, Märkl H: Influence of acetic acid on the growth of *Escherichia coli* K12 during high-cell-density cultivation in a dialysis reactor. *Appl Microbiol Biotechnol* 1997, **48**:597-601.
4. Contiero J, Beatty CM, Kumari S, DeSanti CL, Strohl WR, Wolfe AJ: Effects of mutations in acetate metabolism in high-cell-density growth of *Escherichia coli*. *J Ind Microbiol Biotechnol* 2000, **24**:421-430.
5. Wolfe AJ: The acetate switch. *Microbiol Mol Biol Rev* 2005, **69**:12-50.
6. Kumari S, Beatty CM, Browning DF, Busby SJ, Simel EJ, Hovel-Miner G, Wolfe AJ: Regulation of acetyl coenzyme A synthetase in *Escherichia coli*. *J Bacteriol* 2000, **182**:4173-4179.
7. Han K, Lim HC, Hong J: Acetic acid formation in *Escherichia coli* fermentation. *Biotechnol Bioeng* 1992, **39**:663-671.
8. Farmer WR, Liao JC: Reduction of aerobic acetate production by *Escherichia coli*. *Appl Environ Microbiol* 1997, **63**:3205-3210.
9. Majewski RA, Domach MM: Simple constrained-optimization view of acetate overflow in *E. coli*. *Biotechnol Bioeng* 1990, **35**:732-738.
10. Veit A, Polen T, Wendisch V: Global gene expression analysis of glucose overflow metabolism in *Escherichia coli* and reduction of aerobic acetate formation. *Appl Microbiol Biotechnol* 2007, **74**:406-421.
11. Varma A, Palsson BO: Stoichiometric flux balance models quantitatively predict growth and metabolic by-product secretion in wild-type *Escherichia coli* W3110. *Appl Environ Microbiol* 1994, **60**:3724-3731.
12. Paalme T, Elken R, Kahru A, Vanatalu K, Vilu R: The growth rate control in *Escherichia coli* at near to maximum growth rates: the A-stat approach. *Antonie van Leeuwenhoek* 1997, **71**:217-230.
13. Kayser A, Weber J, Hecht V, Rinas U: Metabolic flux analysis of *Escherichia coli* in glucose-limited continuous culture. I. Growth-rate-dependent metabolic efficiency at steady state. *Microbiology* 2005, **151**:693-706.
14. El-Mansi M: Flux to acetate and lactate excretions in industrial fermentations: Physiological and biochemical implications. *J Ind Microbiol Biotechnol* 2004, **31**:295-300.
15. De Mey M, De Maeseneire S, Soetaert W, Vandamme E: Minimizing acetate formation in *E. coli* fermentations. *J Ind Microbiol Biotechnol* 2007, **34**:689-700.
16. El-Mansi EM, Holms WH: Control of carbon flux to acetate excretion during growth of *Escherichia coli* in batch and continuous cultures. *J Gen Microbiol* 1989, **135**:2875-2883.
17. Yang Y-T, Bennett GN, San K-Y: Effect of inactivation of *nuc* and *ackA-pta* on redistribution of metabolic fluxes in *Escherichia coli*. *Biotechnol Bioeng* 1999, **65**:291-297.
18. Dittrich CR, Vadali RV, Bennett GN, San K-Y: Redistribution of metabolic fluxes in the central aerobic metabolic pathway of *E. coli* mutant strains with deletion of the *ackA-pta* and *poxB* pathways for the synthesis of isoamyl acetate. *Biotechnol Prog* 2005, **21**:627-631.
19. Abdel-Hamid AM, Attwood MM, Guest JR: Pyruvate oxidase contributes to the aerobic growth efficiency of *Escherichia coli*. *Microbiology* 2001, **147**:1483-1498.
20. Phue J, Noronha SB, Hattacharyya R, Wolfe AJ, Shiloach J: Glucose metabolism at high density growth of *E. coli* B and *E. coli* K: differences in metabolic pathways are responsible for efficient glucose utilization in *E. coli* B as determined by microarrays and Northern blot analyses. *Biotechnol Bioeng* 2005, **90**:805-820.
21. Castaño-Cerezo S, Pastor JM, Renilla S, Bernal V, Iborra JL, Cánovas M: An insight into the role of phosphotransacetylase (*pta*) and the acetate/acetyl-CoA node in *Escherichia coli*. *Microb Cell Fact* 2009, **8**:54.
22. Zhang W, Li F, Nie L: Integrating multiple 'omics' analysis for microbial biology: application and methodologies. *Microbiology* 2010, **156**:287-301.
23. Paalme T, Kahru A, Elken R, Vanatalu K, Tiisma K, Vilu R: The computer-controlled continuous culture of *Escherichia coli* with smooth change of dilution rate. *J Microbiol Methods* 1995, **24**:145-153.
24. Kasemets K, Dreves M, Nisamedtinov I, Adamberg K, Paalme T: Modification of A-stat for the characterization of microorganisms. *J Microbiol Methods* 2003, **55**:187-200.
25. Saier MH, Ramseier TO: The Catabolite Repressor/Activator (Cra) Protein of Enteric Bacteria. *J Bacteriol* 1996, **178**:3411-3417.
26. Vemuri GN, Altman E, Sangurdekar DP, Khodursky AB, Eiteman MA: Overflow metabolism in *Escherichia coli* during steady-state growth: transcriptional regulation and effect of the redox ratio. *Appl Environ Microbiol* 2006, **72**:3653-3661.
27. Ishii N, Nakahigashi K, Baba T, Robert M, Soga T, Kanai A, Hirasawa T, Naba M, Hirai K, Hoque A, Ho PY, Kakazu Y, Sugawara K, Igarashi S, Harada S, Masuda T, Sugiyama N, Togashi T, Hasegawa M, Takai Y, Yugi K, Arakawa K, Iwata N, Toya Y, Nakayama Y, Nishioka T, Shimizu K, Mori H, Tomita M: Multiple high-throughput analyses monitor the response of *E. coli* to perturbations. *Science* 2007, **316**:593-597.
28. Shin S, Chang D, Pan JG: Acetate Consumption Activity Directly Determines the Level of Acetate Accumulation During *Escherichia coli* W3110 Growth. *J Microbiol Biotechnol* 2009, **19**:1127-1134.
29. Barak R, Abouhamad WN, Eisenbach M: Both acetate kinase and acetyl coenzyme A synthetase are involved in acetate-stimulated change in the direction of flagellar rotation in *Escherichia coli*. *J Bacteriol* 1998, **180**:985-988.
30. Da Re SS, Deville-Bonne D, Tolstyk T, Vron M, Stock JB: Kinetics of CheY phosphorylation by small molecule phosphodonors. *FEBS Lett* 1999, **457**:323-326.
31. Mayover TL, Halkides CJ, Stewart RC: Kinetic characterization of CheY phosphorylation reactions: comparison of P-CheA and small-molecule phosphodonors. *Biochemistry* 1999, **38**:2259-2271.
32. Klein AH, Shulla A, Reimann SA, Keating DH, Wolfe AJ: The intracellular concentration of acetyl phosphate in *Escherichia coli* is sufficient for direct phosphorylation of two-component response regulators. *J Bacteriol* 2007, **189**:5574-5581.
33. Barak R, Welch M, Yanovsky A, Osawa K, Eisenbach M: Acetyladenylate or its derivative acetylates the chemotaxis protein CheY *in vitro* and increases its activity at the flagellar switch. *Biochemistry* 1992, **31**:10099-10107.
34. Yan J, Barak R, Liarzi O, Shainskaya A, Eisenbach M: *In vivo* acetylation of CheY, a response regulator in chemotaxis of *Escherichia coli*. *J Mol Biol* 2008, **376**:1260-1271.
35. Matsubara M, Mizuno T: EnvZ-independent phosphotransfer signaling pathway of the OmpR-mediated osmoregulatory expression of OmpC and OmpF in *Escherichia coli*. *Biosci Biotechnol Biochem* 1999, **63**:408-414.
36. Anfora AT, Halladin DK, Haugen BJ, Welch RA: Uropathogenic *Escherichia coli* CFT073 is adapted to acetatogenic growth but does not require acetate during murine urinary tract infection. *Infect Immun* 2008, **76**:5760-5767.
37. McCleary W, Stock J: Acetyl phosphate and the activation of 2-component response regulators. *J Biol Chem* 1994, **269**:31567-31572.
38. Feng J, Atkinson MR, McCleary W, Stock JB, Wanner BL, Ninfa AJ: Role of phosphorylated metabolic intermediates in the regulation of glutamine synthetase synthesis in *Escherichia coli*. *J Bacteriol* 1992, **174**:6061-6070.
39. Mizrahi I, Biran D, Ron EZ: Involvement of the Pta-AckA pathway in protein folding and aggregation. *Res Microbiol* 2009, **160**:80-84.
40. Wolfe AJ, Chang D-E, Walker JD, Seitz-Partridge JE, Vidaurri MD, Lange CF, Prüß BM, Henk MC, Larkin JC, Conway T: Evidence that acetyl phosphate functions as a global signal during biofilm development. *Mol Microbiol* 2003, **48**:977-988.
41. Shi IY, Kuzminov A: A Defect in the Acetyl Coenzyme-Acetate Pathway Poisons Recombinational Repair-Deficient Mutants of *Escherichia coli*. *J Bacteriol* 2005, **187**:1266-1275.
42. Nyström T: The glucose-starvation stimulon of *Escherichia coli*: induced and repressed synthesis of enzymes of central metabolic pathways and role of acetyl phosphate in gene expression and starvation survival. *Mol Microbiol* 1994, **12**:833-843.
43. Postma E, Verduyn C, Scheffers Wa, Van Dijken JP: Enzymic analysis of the crabtree effect in glucose-limited chemostat cultures of *Saccharomyces cerevisiae*. *Appl Environ Microbiol* 1989, **55**:468-477.
44. Lin H, Castro NM, Bennett GN, San K: Acetyl-CoA synthetase overexpression in *Escherichia coli* demonstrates more efficient acetate assimilation and lower acetate accumulation: a potential tool in metabolic engineering. *Appl Microbiol Biotechnol* 2006, **71**:870-874.
45. Rosenzweig F, Adams J: Microbial Evolution in a Simple Unstructured Environment: Genetic Differentiation in *Escherichia coli*. *Genetics* 1994, **917**:903-917.
46. Treves DS, Manning S, Adams J: Repeated evolution of an acetate-crossfeeding polymorphism in long-term populations of *Escherichia coli*. *Mol Biol Evol* 1998, **15**:789-797.
47. Franchini AG, Egli T: Global gene expression in *Escherichia coli* K-12 during short-term and long-term adaptation to glucose-limited continuous culture conditions. *Microbiology* 2006, **152**:2111-2127.

48. Hardiman T, Lemuth K, Keller M, Reuss M, Siemannherzberg M: **Topology of the global regulatory network of carbon limitation in *Escherichia coli*.** *J Biotechnol* 2007, **132**:359-374.
49. Görke B, Stülke JR: **Carbon catabolite repression in bacteria: many ways to make the most out of nutrients.** *Nat Rev Microbiol* 2008, **6**:613-624.
50. Narang A: **Quantitative effect and regulatory function of cyclic adenosine 5'-phosphate in *Escherichia coli*.** *J Biosci* 2009, **34**:445-463.
51. Nahku R, Valgepea K, Lahtvee PJ, Erm S, Abner K, Adamberg K, Vilu R: **Specific growth rate dependent transcriptome profiling of *Escherichia coli* K12 MG1655 in accelerostat cultures.** *J Biotechnol* 2010, **145**:60-65.
52. Nanchen A, Schicker A, Revelles O, Sauer U: **Cyclic AMP-dependent catabolite repression is the dominant control mechanism of metabolic fluxes under glucose limitation in *Escherichia coli*.** *J Bacteriol* 2008, **190**:2323-2330.
53. Khankal R, Chin JW, Ghosh D, Cirino PC: **Transcriptional effects of CRP* expression in *Escherichia coli*.** *J Biol Eng* 2009, **3**:13.
54. Ishizuka H, Hanamura A, Inada T, Aiba H: **Mechanism of the down-regulation of cAMP receptor protein by glucose in *Escherichia coli*: role of autoregulation of the *crp* gene.** *EMBO J* 1994, **13**:3077-3082.
55. Sarkar D, Siddiquee KA, Araúz-Bravo MJ, Oba T, Shimizu K: **Effect of *cra* gene knockout together with *edd* and *iclR* genes knockout on the metabolism in *Escherichia coli*.** *Arch Microbiol* 2008, **190**:559-751.
56. Adamberg K, Lahtvee PJ, Valgepea K, Abner K, Vilu R: **Quasi steady state growth of *Lactococcus lactis* in glucose-limited acceleration stat (A-stat) cultures.** *Antonie van Leeuwenhoek* 2009, **95**:219-226.
57. Martens L, Hermjakob H, Jones P, Adamski M, Taylor C, States D, Gevaert K, Vandekerckhove J, Apweiler R: **PRIDE: the proteomics identifications database.** *Proteomics* 2005, **5**:3537-3545.
58. Barsnes H, Vizcaino JA, Eidhammer I, Martens L: **PRIDE Converter: making proteomics data-sharing easy.** *Nat Biotechnol* 2009, **27**:598-599.

doi:10.1186/1752-0509-4-166

Cite this article as: Valgepea et al.: Systems biology approach reveals that overflow metabolism of acetate in *Escherichia coli* is triggered by carbon catabolite repression of acetyl-CoA synthetase. *BMC Systems Biology* 2010 **4**:166.

Submit your next manuscript to BioMed Central and take full advantage of:

- Convenient online submission
- Thorough peer review
- No space constraints or color figure charges
- Immediate publication on acceptance
- Inclusion in PubMed, CAS, Scopus and Google Scholar
- Research which is freely available for redistribution

Submit your manuscript at
www.biomedcentral.com/submit



PUBLICATION III

Lahtvee PJ, Adamberg K, Arike L, Nahku R, Aller K, Vilu R

Multi-omics approach to study the growth efficiency and amino acid metabolism in *Lactococcus lactis* at various specific growth rates

Microbial Cell Factories, 10:12, (2011)

RESEARCH

Open Access

Multi-omics approach to study the growth efficiency and amino acid metabolism in *Lactococcus lactis* at various specific growth rates

Petri-Jaan Lahtvee^{1,2}, Kaarel Adamberg^{2,3}, Liisa Arike^{2,3}, Ranno Nahku^{1,2}, Kadri Aller^{1,2}, Raivo Vilu^{1,2*}

Abstract

Background: *Lactococcus lactis* is recognised as a safe (GRAS) microorganism and has hence gained interest in numerous biotechnological approaches. As it is fastidious for several amino acids, optimization of processes which involve this organism requires a thorough understanding of its metabolic regulations during multisubstrate growth.

Results: Using glucose limited continuous cultivations, specific growth rate dependent metabolism of *L. lactis* including utilization of amino acids was studied based on extracellular metabolome, global transcriptome and proteome analysis. A new growth medium was designed with reduced amino acid concentrations to increase precision of measurements of consumption of amino acids. Consumption patterns were calculated for all 20 amino acids and measured carbon balance showed good fit of the data at all growth rates studied. It was observed that metabolism of *L. lactis* became more efficient with rising specific growth rate in the range 0.10 - 0.60 h⁻¹, indicated by 30% increase in biomass yield based on glucose consumption, 50% increase in efficiency of nitrogen use for biomass synthesis, and 40% reduction in energy spilling. The latter was realized by decrease in the overall product formation and higher efficiency of incorporation of amino acids into biomass. *L. lactis* global transcriptome and proteome profiles showed good correlation supporting the general idea of transcription level control of bacterial metabolism, but the data indicated that substrate transport systems together with lower part of glycolysis in *L. lactis* were presumably under allosteric control.

Conclusions: The current study demonstrates advantages of the usage of strictly controlled continuous cultivation methods combined with multi-omics approach for quantitative understanding of amino acid and energy metabolism of *L. lactis* which is a valuable new knowledge for development of balanced growth media, gene manipulations for desired product formation etc. Moreover, collected dataset is an excellent input for developing metabolic models.

Background

Lactococcus (L.) lactis is the most intensively studied lactic acid bacterium and it has a great industrial importance. In addition to its wide usage in the dairy industry, *L. lactis* subsp. *lactis* IL1403 was the first lactic acid bacterium whose genome was sequenced [1], and it is extensively used for production of different metabolic products and recombinant proteins [reviews in [2-4]]. As this bacterium is generally recognised as safe (GRAS), there has been increasing interest in its use as

a live vector for mucosal delivery of therapeutic proteins, including nasal and gastrointestinal vaccines [5,6]. However, there exists a remarkable lack of knowledge about the peculiarities of *L. lactis* metabolic regulation, especially regarding amino acid metabolism. There are several defined media designed for *L. lactis* [7-9], however, these are unbalanced and concentrations of individual amino acids are quite high, making their consumption measurements inaccurate as utilization by the cells is small compared to the total content. Lack of reliable information on consumption patterns and regulation of amino acid metabolism hinders design of cheaper balanced complex media and optimization of bioprocesses.

* Correspondence: raivo@kbf.ee

¹Tallinn University of Technology, Department of Chemistry, Akadeemia tee 15, 12618 Tallinn, Estonia

Full list of author information is available at the end of the article

Systems biology approaches where 'omics' methods are combined with advanced cultivation methods, computational and mathematical models form a solid platform for elucidating quantitative peculiarities of metabolism and its regulation in microorganisms. Transcriptome and proteome expression in *L. lactis* have been measured and compared several times in various phases of batch cultivations [10,11]. A multi-omics study where *L. lactis* was cultivated at steady state conditions was carried out by Dressaire et al. [12,13]. They characterized *L. lactis* at the transcriptome level in isoleucine limited chemostat cultures, calculated translation efficiencies based on proteome and transcriptome levels, and showed that energy costs associated with protein turnover in cells are bigger at low growth rates in comparison with higher ones.

To provide more comprehensive knowledge about amino acid metabolism in *L. lactis* we developed a new medium, which allowed studying quantitative patterns of amino acid consumption. To further link amino acid metabolism with the overall physiological state of cells, growth rate dependent transcriptomes, proteomes and extracellular metabolomes were measured and studied together with carbon, nitrogen and ATP, redox balance analyses. *L. lactis* was cultivated in accelerostat (A-stat) continuous cultures as this method allows acquisition of vast amount of data on quasi steady state growing cells and precise determination of growth characteristics, especially investigation of dependences of growth characteristics on residual concentrations of growth limiting substrate (e.g. glucose) which determines the specific growth rate of cells (μ).

Results

L. lactis growth characteristics

L. lactis was cultivated in A-stat culture where after stabilisation in chemostat at dilution rate 0.10 h^{-1} , specific growth rate (μ) was smoothly increased until the maximal μ (μ_{max}) was reached at $0.59 \pm 0.02 \text{ h}^{-1}$ (average value of five independent experiments \pm standard deviation; Figure 1). To obtain higher precision in the determination of amino acid consumption patterns, concentrations of most amino acids in the growth medium were reduced *ca* 3 times compared to the chemically defined medium (CDM) [14], exceptions being arginine and glutamine, whose concentrations were increased in the medium to avoid amino group shortage during the growth (see Methods). The residual glucose concentration remained below detection limit ($<0.1 \text{ mM}$) between μ 0.10 h^{-1} and $0.59 \pm 0.02 \text{ h}^{-1}$ in all five independent experiments. It is important to note that constant protein content ($45 \pm 2\%$ of cell dry weight) and constant amino acid composition of the protein fraction was observed in the full range of μ from 0.10 to 0.55 h^{-1}

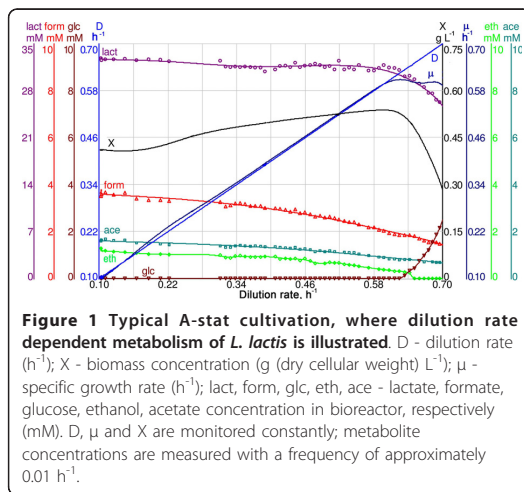


Figure 1 Typical A-stat cultivation, where dilution rate dependent metabolism of *L. lactis* is illustrated. D - dilution rate (h^{-1}); X - biomass concentration ($\text{g (dry cellular weight) L}^{-1}$); μ - specific growth rate (h^{-1}); lact, form, glc, eth, ace - lactate, formate, glucose, ethanol, acetate concentration in bioreactor, respectively (mM). D, μ and X are monitored constantly; metabolite concentrations are measured with a frequency of approximately 0.01 h^{-1} .

(Additional file 1, Table S1). RNA content increased from $6.5 \pm 1.0\%$ to $9.5 \pm 1.5\%$ in cell dry weight in between the latter μ values. The biomass yield per consumed carbon (Y_{XC}) increased from 0.13 ± 0.00 to $0.17 \pm 0.01 \text{ C-mol}_{\text{biomass}} \text{ C-mol}_{\text{carbon}}^{-1}$ when μ was raised from $0.20 \pm 0.02 \text{ h}^{-1}$ to $0.52 \pm 0.04 \text{ h}^{-1}$ (Additional file 2, Table S1). It was realized by decrease of by-product formation per biomass from 89.6 to $62.3 \text{ mmol gdw}^{-1}$ (sum of Y_{lact} , Y_{ace} and Y_{eth} , Additional file 2, Table S1). Corresponding yield of these by-products (lactate, acetate, ethanol) per consumed glucose decreased from 2.05 to $1.88 \text{ mol}_{\text{products}} \text{ mol}_{\text{glc}}^{-1}$, with lactate yield per consumed glucose $Y_{\text{lg}} = 1.83 \pm 0.03 \text{ mol}_{\text{lact}} \text{ mol}_{\text{glc}}^{-1}$ remaining constant. As by-product formation exceeded maximal possible yield (2 mol mol^{-1}) per consumed glucose at growth rates below 0.4 h^{-1} (Additional file 1, Table S2) it indicated that part of the amino acids should have been catabolised to pyruvate and eventually to by-products. The overall consumption of amino acids decreased from $12.5 \pm 0.5 \text{ mmol gdw}^{-1}$ to $9.3 \pm 0.3 \text{ mmol gdw}^{-1}$ with increasing μ (Additional file 2, Figure S1), exceeding two to three times that required for synthesis of proteins in biomass ($4.2 \pm 0.1 \text{ mmol gdw}^{-1}$, Additional file 1, Table S1), and constituting always $21 \pm 1\%$ (52 to $39 \text{ C-mmol gdw}^{-1}$) of all the total carbon utilised by cells throughout the μ range studied.

For proof of principle, a chemostat experiment was carried out at a dilution rate of 0.45 h^{-1} and the data obtained were compared with the data obtained at the same μ value in A-stat experiments. The measured substrate and product yields in chemostat culture had values in the range of presented standard deviations for A-stat data (Additional file 2, Table S2) which shows

that quasi steady state data from A-stat is comparable to chemostat.

Amino acid consumption profiles

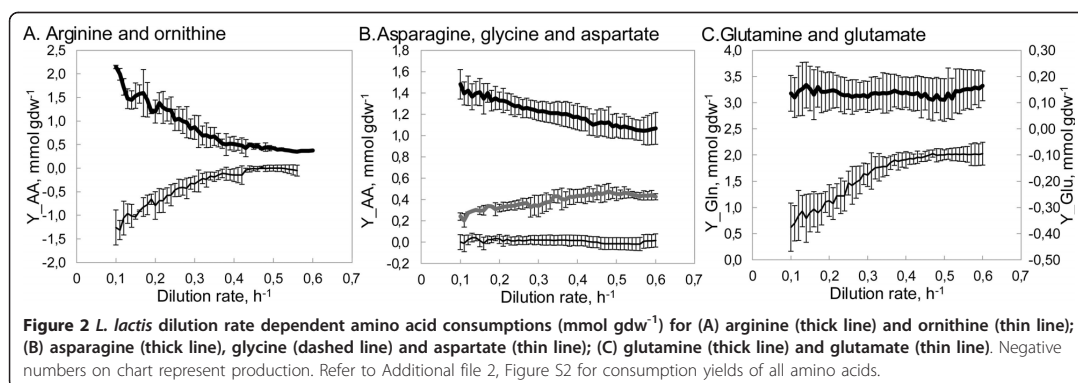
Based on amino acid concentrations in the cultivation broth, consumption patterns ($\text{mmol}_{\text{AA}} \text{gdw}^{-1}$) for all the 20 amino acids were calculated (Figure 2 and Additional file 2, Figure S2). The most abundantly consumed amino acid throughout the μ range studied was glutamine (Additional file 2, Figure S2). Asparagine, arginine, serine, threonine, alanine, leucine, isoleucine and cysteine were the next most intensively consumed amino acids which consumption exceeded notably the amounts necessary for biomass formation. Lysine, phenylalanine and valine were consumed in slightly higher amounts than needed for biomass production. Consumption of aspartate, histidine, and proline were in the range of measurement errors, hence, their consumption can be considered minimal or nonexistent. It has been shown that the latter amino acids are non-essential for the growth of *L. lactis* [8].

In more detail, specific growth rate dependent consumptions of asparagine, threonine and cysteine per biomass were constant in the μ range of 0.10 - 0.20 h^{-1} , but decreased 30 to 40% from $\mu = 0.20 \text{ h}^{-1}$ until μ_{max} value (Figure 2 and Additional file 2, Figure S2). Consumption of arginine decreased rapidly in the μ range of 0.10 - 0.35 h^{-1} from $2.15 \pm 0.04 \text{ mmol gdw}^{-1}$ and levelled at $0.44 \pm 0.07 \text{ mmol gdw}^{-1}$ at higher growth rates (Figure 2) - at an amount greater than necessary for biomass production ($0.20 \pm 0.02 \text{ mmol gdw}^{-1}$). Decreasing trends in the μ range 0.10 - 0.35 h^{-1} were observed for the production of ornithine and for the production of the only amino acid produced - glutamate. Glycine was the only amino acid which consumption increased during increasing μ (Figure 2), however, its consumption was always lower than its need for biomass formation. Consumption of other amino acids (Gln, Ile, His, Leu, Lys,

Met, Phe, Tyr, Trp, Val) did not change significantly throughout the studied μ range, indicating also a more efficient use of amino acids at higher μ values as growth yields based on carbon and nitrogen consumption increased.

Carbon, nitrogen and ATP balances

Carbon recovery which was calculated based on glucose and amino acid consumptions, product and biomass formation was $100 \pm 2\%$ over the entire μ range (Additional file 2, Figure S3). However, nitrogen recovery, calculated based on amino acid utilization and ornithine, glutamate and biomass formation, was $55 \pm 3\%$ (Additional file 2, Figure S3). Amino acids were the main nitrogen source in the medium, comprising more than 99% of the consumed nitrogen by the cultivated bacterium. Based on amino acid utilization, the total consumption of nitrogen decreased from 22 to 14 mmol gdw^{-1} between the μ range 0.10 - 0.59 $\pm 0.02 \text{ h}^{-1}$. On the basis of monomer composition, N-molar content in the biomass was found to be constant at 7.2 mmol gdw^{-1} during the studied μ range. Concomitantly, nitrogen incorporation into the biomass increased from 33 to 50% from total consumed nitrogen in amino acids with increasing μ . The rest of nitrogen (50-67%) could have been metabolised through arginine deiminase (ADI) pathway, by excreting other amino acids (glutamate, aspartate) or through deamination reactions (ammonium). Activity of the ADI pathway decreased in the μ range 0.10 - 0.35 h^{-1} and nitrogen excretion to ornithine and synthesis of exogenous NH_3 declined from 4.7 to 0.5 mmol gdw^{-1} (21 to 4% from total nitrogen consumed) in the above μ range. In addition, 0.4 to 0.06 mmol gdw^{-1} of nitrogen was excreted as glutamate and 0.1 mmol gdw^{-1} through transamination reactions with the formation of the following compounds detected and quantified by mass-spectrometry: 4-hydroxyphenylpyruvic acid, hydroxyphenyllactic acid, 2-hydroxy-3-methylbutyric acid, 2-hydroxyisocaproic acid and L-3-phenyllactic acid from tyrosine,



phenylalanine or branched chain amino acids (data not shown). The left-over of consumed nitrogen was 9.5 - 6.6 mmol gdw⁻¹ (contributing 44 - 48% from total nitrogen) in the μ range of 0.1 - 0.6 h⁻¹. This nitrogen must have been excreted as NH₃ if the excess of consumed amino acids not incorporated into protein fraction of biomass would have been converted to pyruvate. The latter assumption is supported by the fact that the carbon was fully recovered during the growth. Reduction of carbon and nitrogen wasting led to the increase of the biomass yields based on carbon (including glucose and amino acids) and nitrogen consumption 1.3 and 1.5 times, respectively (from 0.12 to 0.15 C-mol C-mol⁻¹ and from 0.33 to 0.50 N-mol N-mol⁻¹), in parallel with the increase of μ from 0.10 to 0.59 ± 0.02 h⁻¹.

Based on biomass monomer composition and the stoichiometry of ATP, NAD(P)H and central metabolites for monomer production, μ dependent ATP and NAD(P)H balance calculations were carried out (Additional file 1, Tables S3-S5). Calculations indicated that more ATP was produced than necessary for biomass formation. Presumably the ATP synthesized in excess was wasted in futile cycles. Calculated energy spilling was constant at 60 mmol ATP gdw⁻¹ in the range of the μ 0.10 - 0.15 h⁻¹ and decreased afterwards to 36 mmol gdw⁻¹ at μ_{\max} , indicating that the metabolism was the most efficient near μ_{\max} conditions (Additional file 1, Table S5). Similarly calculated NAD(P)H misbalance (spilling) decreased from 3.5 mmol gdw⁻¹ at low growth rates to 0 mmol gdw⁻¹ at specific growth rate >0.45 h⁻¹ (Additional file 1, Table S5). However, latter improvement of balance is inside the range of errors of lactate measurements (as lactate dehydrogenase is the main NAD regeneration reaction in lactic acid bacteria). Therefore a conclusion that redox balance was maintained throughout the studied growth conditions should be drawn.

Transcriptome and proteome response

Transcriptomes and proteomes at four different quasi steady state μ values (0.17, 0.24, 0.44, 0.52 h⁻¹) were compared to steady state $\mu = 0.10$ h⁻¹ (additional info in Methods). Changes in gene and protein expression levels for the most relevant reactions between μ 0.52 and 0.10 h⁻¹ are illustrated on Figure 3 and 4; a full list of measured gene and protein expression changes at various μ values can be found in Additional file 3. In this section we discuss changes of mRNA and protein expressions significant with P value ≤ 0.05 for μ 0.52 ± 0.03 h⁻¹ vs. 0.10 h⁻¹.

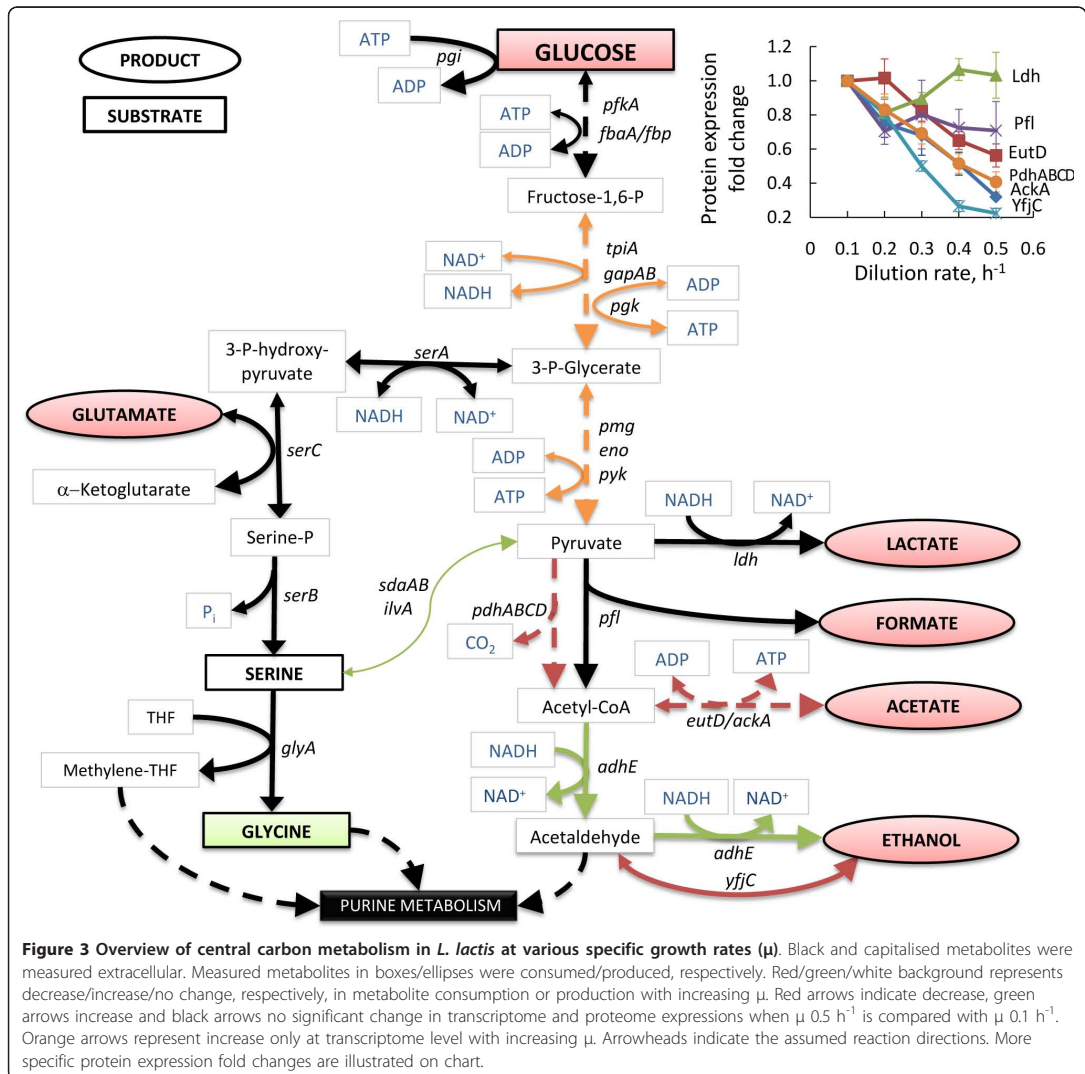
Mannose uptake genes *ptnAB*, which are responsible for glucose transport in *L. lactis*, and *ptsI* were up-regulated 2.1 to 4.3-fold at the transcriptome level at higher growth rates (above 0.44 h⁻¹). However, corresponding enzymes did not show any remarkable change in the same growth rate range as measured in the

proteome. Transporter genes for additional sugars (not present in our medium) like galactose (by *galE*) and cellobiose (by *ptcABC* and *yidB*) were 1.8 to 2.9-fold down-regulated at higher specific growth rates at the transcriptome level, whereas a 2.2- to 2.8-fold repression of *PtcAB* was measured for proteome. This down-regulation is known to be the consequence of carbon catabolite repression which is extensively studied also in other bacteria like *E. coli* and *B. subtilis* [15,16].

Expression in the upper part of glycolysis did not change significantly during increase of μ . However, the lower part of glycolysis (from *fbaA* to *eno*) was 1.8- to 4-times up-regulated at the transcriptome level, but only *Pmg* showed significant 1.6-fold up-regulation at the proteome level at the growth rates higher than 0.44 h⁻¹ (Figure 3). The pentose phosphate pathway showed a 1.3- to 2.0-fold down-regulation in genes *deoBC*, *rpiA*, *zwf*, *tkt*, *ywcC* (Additional file 3), which might be explained by a lower NADPH requirements at higher μ conditions. Despite the down-regulation of pentose phosphate pathway, genes encoding proteins involved in purine and pyrimidine metabolism were up-regulated. Moderate, 1.5- to 3.0-fold up-regulation both at the transcriptome and proteome level of the operon *PurA-BEFLMQ* was observed. With the increase of purine and pyrimidine metabolism, the need for amino group transfer from glutamine should have been also increased with rising specific growth rate. In agreement with this, expression of the genes in the first steps of purine and pyrimidine synthesis, *purF* increased and *carAB* remained constant respectively, with the increase of μ . High glutamine availability was maintained presumably by increased expression of glutamine transporter (*glnQP*) and glutamine synthetase (*glnA*).

Considering pyruvate metabolism, decreased acetate production was in accordance with the significant down-regulation of genes *eutD* and *ackA2* and their corresponding enzymes (see Figure 3). However, decreased production of formate and lactate seemed not to be regulated similarly with acetate - *Pfl* and *Ldh* showed no major changes neither in gene nor protein expression levels confirming that *Ldh* is regulated rather by the NADH/NAD⁺ ratio than by transcription and/or translation, as proposed in literature [17]. Although ethanol production decreased, *AdhE* expression increased 7.3- and 1.8-fold in transcriptome and proteome analysis, respectively. This might be related to the incorporation of ethanol formation pathway intermediate, acetaldehyde, to acetyl-CoA synthesis from deoxyribose. Pyruvate dehydrogenase subunits (*PdhABCD*) were 2- to 3-fold down-regulated at both levels (Figure 3).

It is well known, that *L. lactis* can direct part of the consumed (or *de novo* synthesised) serine into pyruvate by *sdaA* and *ilvA* - this flux could form up to 10% of overall



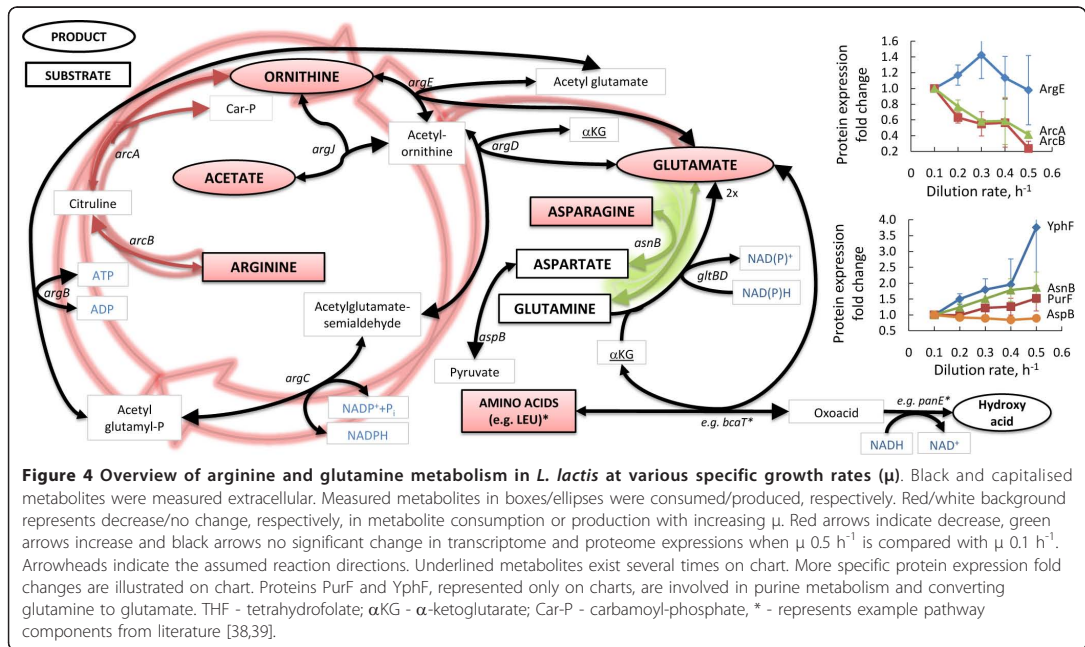
pyruvate flux [18]. In the current study, these noted genes were 1.4- to 2.2-fold up-regulated comparing $\mu = 0.50$ to $\mu = 0.10 \text{ h}^{-1}$. In concordance with the sharp decrease of arginine consumption from μ 0.10 h^{-1} up to μ 0.35 h^{-1} , the 2.3- to 4.5-fold decrease in protein expression of ArcAB, which converts arginine to ornithine, was observed during the increase of μ (Figure 4).

Discussion

Carbon balance and growth efficiency

Growth conditions have a strong influence on specific growth rate (μ), macromolecular composition of biomass

(i.e. ribosomal content) and cell size of microorganisms [18,19]. In this study, a gradual change to more efficient carbon metabolism with the increase of μ was observed for *L. lactis* (Figure 1). The first shift in *L. lactis* metabolism took place at μ 0.20 \pm 0.02 h^{-1} , when biomass yield (Y_{XC}) per consumed carbon started to increase. Thirty percent increase with the increase of μ from 0.10 to 0.60 h^{-1} was achieved by reduction of fermentation by-products synthesis (acetate, formate, ethanol). Concomitantly to the increase of biomass yield, calculated ATP balance showed decreased energy spilling. It has been postulated that higher energy spilling at lower μ conditions could be



caused by greater costs of turnover of macromolecules and sensory molecules, establishment of ion gradients across the cell membrane *etc* [20]. Dressaire et al. [12] calculated the degradation rates for proteins and found that protein median half-lives were *ca* 10-fold shorter at $\mu = 0.10$ h⁻¹ than at μ_{max} . As ATP is consumed during protein degradation [21] this non-growth related expenditure might form a higher proportion of the total energy synthesized at lower μ conditions than at higher growth rates.

Nitrogen metabolism

With the increase of specific growth rate from 0.10 to 0.60 h⁻¹ biomass yield Y_{XN} increased 1.5 times showing that cells used nitrogen more effectively for biomass production. The most important amino acid that plays role in the observed reduction of nitrogen wasting was arginine (arginine consumption decreased from 1.5 to 0.5 mmol gdw⁻¹ with increase of μ from 0.1 to 0.35 h⁻¹). Throughout the μ range studied, arginine consumption was 0.3 to 1.3 mmol gdw⁻¹ higher than spent for biomass synthesis and majority of the consumed arginine was transformed to ornithine (0.05 to 1.2 mmol gdw⁻¹), especially at lower specific growth rates, which indicates energy limitation of cells. However, not all arginine left over from calculated requirements for biosynthesis (0.1 to 0.25 mmol gdw⁻¹) was converted to ornithine. Based on annotated network of *L. lactis* there is no route for consumption of ornithine other than that leading to the

synthesis of glutamate (mediated by ArgCDJFG), which were reduced with increase of specific growth rates especially after 0.4 h⁻¹). Although the mechanisms of arginine overconsumption in addition to ornithine production are not known, correlation between ornithine production and glutamate synthesis was 0.99, which shows that these syntheses were most probably coupled. Production of glutamate has also been observed before, when both glutamine and glutamate were present in the cultivation medium [8,22].

Nitrogen wasting through glutamine metabolism was not decreased during the increase of specific growth rate. Glutamine, the most consumed amino acid (glutamine consumption covers 30 to 50% of total nitrogen consumed, at μ 0.10 and 0.60 h⁻¹, respectively), is used for synthesis of biomass proteins and it is the donor of amino groups in purine, pyrimidine and in aminosugar production pathways (glutamine and glutamate requirements for transamination reactions in aminosugar and nucleotide synthesis was in average 1.35 mmol gdw⁻¹). It should be noted that glutamine synthetase (*glnA*) was highly expressed (having array spot intensity values up to four times higher than these of average values of all genes) and increased with increase of μ in parallel to high consumption of the amino acid. Although we cannot argue over the direction of reactions on the basis of our experimental data, it could be assumed that maintenance of high intracellular concentrations of glutamine

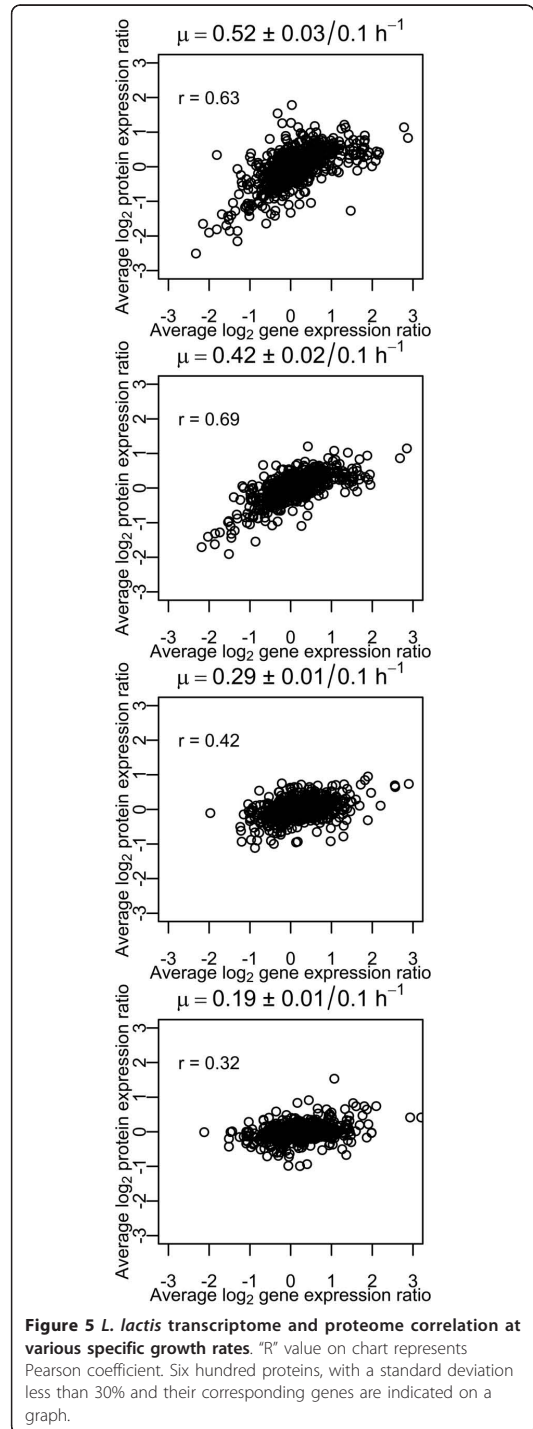
in the cells in the result of intense synthesis and consumption flows might be necessary to keep the transfer of amino group effective.

The third biggest part of nitrogen wasting could be associated with the consumption of asparagine, which was reduced from 1.4 to 1.1 mmol gdw⁻¹ with increase of μ from 0.10 to 0.60 h⁻¹. Asparagine and aspartate (which was not consumed and therefore should have been produced from asparagine) are required for syntheses of nucleotides (in average 0.35 mmol gdw⁻¹) and proteins (in average 0.4 mmol gdw⁻¹). It was shown that 0.35 to 0.65 mmol gdw⁻¹ of asparagine was not used for biosynthesis. Asparagine can be metabolised through asparaginase (*ansB*) - however its expression was in the range of threshold values in the mRNA array and corresponding protein was not detected. Instead of that the high expression (array spot intensity values up to seven times higher than these of average values of all genes) of asparagine synthetase (*asnB*), which expression even increased with increase of specific growth rate was observed. Similarly to glutamine it could be assumed that overconsumption of asparagine and high expression of the relevant synthesis genes might be necessary to keep the transfer of amino group effective. Energetically transport of asparagine in *L. lactis* is much more efficient than aspartate [23], moreover, asparagine is probably preferentially directed towards the production of aspartate [24,25]. Surplus of aspartate in its turn can be directed into pyruvate by AspB (Figure 4).

The role of other amino acids (other than glutamine, arginine and aspartate) in nitrogen wasting can be considered minimal as over-consumptions (amounts greater than necessary for biomass production) of these amino acids were below 0.2 mmol gdw⁻¹ (cysteine, serine, threonine) or 0.1 mmol gdw⁻¹ (all other not mentioned above).

Omics comparison

Good correlation with a Pearson coefficient up to 0.69 was observed between 600 measured protein and gene expression data (Figure 5). An interesting phenomenon was seen at μ values 0.52 \pm 0.03 h⁻¹ and 0.42 \pm 0.02 h⁻¹ compared to 0.10 h⁻¹: a large amount of genes up-regulated at the transcriptome level showed only small or no change at the proteome level (Figure 5). The vast majority of members in this group were related to ribosomal subunits (74% from all detected ribosomal proteins), as well as lower glycolysis (FbaA, GapB, Pfkfb3, Pfkfb4, Pfkfb5, Pfkfb6, Pfkfb7, Pfkfb8, Pfkfb9, Pfkfb10, Pfkfb11, Pfkfb12, Pfkfb13, Pfkfb14, Pfkfb15, Pfkfb16, Pfkfb17, Pfkfb18, Pfkfb19, Pfkfb20, Pfkfb21, Pfkfb22, Pfkfb23, Pfkfb24, Pfkfb25, Pfkfb26, Pfkfb27, Pfkfb28, Pfkfb29, Pfkfb30, Pfkfb31, Pfkfb32, Pfkfb33, Pfkfb34, Pfkfb35, Pfkfb36, Pfkfb37, Pfkfb38, Pfkfb39, Pfkfb40, Pfkfb41, Pfkfb42, Pfkfb43, Pfkfb44, Pfkfb45, Pfkfb46, Pfkfb47, Pfkfb48, Pfkfb49, Pfkfb50, Pfkfb51, Pfkfb52, Pfkfb53, Pfkfb54, Pfkfb55, Pfkfb56, Pfkfb57, Pfkfb58, Pfkfb59, Pfkfb60, Pfkfb61, Pfkfb62, Pfkfb63, Pfkfb64, Pfkfb65, Pfkfb66, Pfkfb67, Pfkfb68, Pfkfb69, Pfkfb70, Pfkfb71, Pfkfb72, Pfkfb73, Pfkfb74, Pfkfb75, Pfkfb76, Pfkfb77, Pfkfb78, Pfkfb79, Pfkfb80, Pfkfb81, Pfkfb82, Pfkfb83, Pfkfb84, Pfkfb85, Pfkfb86, Pfkfb87, Pfkfb88, Pfkfb89, Pfkfb90, Pfkfb91, Pfkfb92, Pfkfb93, Pfkfb94, Pfkfb95, Pfkfb96, Pfkfb97, Pfkfb98, Pfkfb99, Pfkfb100) and amino acid or peptide transport (BusAB, GlnPQ, GltPS, OptCD, PepCPX, PtnABD, PtsHI). Up-regulation at the transcriptome level and no significant change at proteome level during anaerobic growth of *L. lactis* in lower part of glycolysis have also been noticed before [11,12]. Despite the relatively good



correlation between the transcriptomic and proteomic data, several important regulations were observed only at transcriptome level. The data obtained indicated importance of taking into account the possibility of allosteric regulation, and carrying out measurements of fluxome in addition to transcriptome and proteome to fully characterize regulation of metabolic pathways.

By scanning the entire range of specific growth rates using A-stat experiments, it is possible to continuously monitor the steady state metabolism using on-line sensors or frequently collected samples for at-line analyses. Reproducibility of growth characteristics in A-stat were compared with chemostat at μ 0.45 h⁻¹. All measured substrate consumption and product formation yields (including amino acids) remained within mentioned standard deviation ranges indicating the accordance of quasi steady state and steady state data (Additional file 2, Table S2). Recently, similar comparisons at the global transcriptome level were conducted with *E. coli* achieving very good correlation with a Pearson coefficient up to 0.96 [26]. In both studies, it was shown that the A-stat cultivation technique allows precise monitoring the sequence of metabolic switch points.

Conclusions

Distinct ratios of glucose and amino acids in the growth media are very important for biomass yield optimization as carbon and nitrogen metabolism are tightly coupled in *L. lactis*. High biomass yields are crucial for producing vaccines using microorganisms and nutrient limitations can strongly affect achieving the desired results. As was shown in this study, some amino acids were consumed in large amounts (glutamine, asparagine, arginine) and more efficient growth might not be achieved by insufficient supply of these compounds. There have been several attempts to optimize the media for lactococci using a single omission technique [7,8], however, a systematic approach taking into account that amino acid requirements depend on environmental conditions (e.g. at various μ values) has not yet been fully realized as it is difficult using only batch cultivation. The current work combining systematic continuous cultivation approach with omics methods is therefore of high value for better media design, as well as for understanding principles of metabolism of the bacteria.

Using steady state cultivation methods and a systems biology approach for characterisation of *L. lactis* metabolism, it was possible to demonstrate a shift to more efficient metabolism at higher growth rates by increasing the biomass yield, change towards homolactic fermentation, and decreasing the flux through alternative energy generation pathways with lower efficiency than glycolysis e.g. acetate formation and the ADI pathway.

This study demonstrates the necessity of using strictly controlled continuous cultivation methods in combination with a multi-omics approach and element balance calculations to gain quantitative understanding of the regulation of complex global metabolic networks, important for strain dependent media optimisation or the design of efficient producer cells. However, questions about rationale of 2-3 times over-consumption of amino acids by cells and principles of properly balanced media remain to be answered in full in the future studies.

Methods

Microorganism and medium

The strain used throughout these experiments *Lactococcus lactis* subsp. *lactis* IL1403 was kindly provided by Dr. Ogier from INRA (Jouy-en-Josas, France). Inoculum was prepared using a lyophilized stock culture stored at -80°C which was pre-grown twice on the cultivation medium. Chemically defined medium with a reduced amino acid concentrations were developed especially for better detection of amino acids. Media contained 70% GIBCO™ F-12 Nutrient Mixture (Invitrogen Corporation, Carlsbad, CA) and 30% modified CDM (composition in [27]). This combination gave the best trade-off for growth yield and maximal growth rate. Composition of the final medium was as follows (mg L⁻¹): limiting substrate D-Glucose - 3500; L-Alanine - 78; L-Arginine - 185; L-Asparagine - 74; L-Aspartic acid - 72; L-Cysteine - 64; L-Glutamic acid - 70; L-Glutamine - 132; Glycine - 58; L-Histidine - 60; L-Isoleucine - 102; L-Leucine - 207; L-Lysine - 158; L-Methionine - 41; L-Phenylalanine - 86; L-Proline - 92; L-Serine - 163; L-Threonine - 76; L-Tryptophan - 16; L-Tyrosine - 29; L-Valine - 107; Biotin - 0.305; Choline chloride - 9.8; D-Pantothenate - 0.65; Folic Acid - 1.21; Niacinamide - 0.325; Pyridoxine hydrochloride - 0.642; Riboflavin - 0.326; Thiamine hydrochloride - 0.51; Vitamin B12 - 0.98; i-Inositol - 12.6; CaCl₂ - 28; CuSO₄ × 5H₂O - 0.272; FeSO₄ × 7H₂O - 0.71; MgCl₂ - 58; KCl - 157; NaCl - 5580; Na₂PO₄ - 99; ZnSO₄ × 7H₂O - 1; Hypoxanthine-Na - 3; Linoleic Acid - 0.1; Lipoic Acid - 0.1; Phenol Red - 0.8; Putrescine × 2HCl - 0.1; Na-Pyruvate - 77; Thymidine - 0.5.

A-stat cultivations

A-stat cultivations were carried out in a 1 L Biobundle bioreactor (Applikon, Schiedam, the Netherlands) controlled by an ADI1030 biocontroller (Applikon) and a cultivation control program "BioXpert NT" (Applikon) (detailed description in [28], with an addition of an *in situ* OD sensor (model TruCell2; Finesse, San Jose, CA)). Cultivations were carried out under anaerobic conditions (N₂-environment) with an agitation speed of 300 rpm at 34°C and pH 6.4. Five parallel A-stat experiments were carried out where after a batch phase,

constant dilution rate ($D = 0.1 \text{ h}^{-1}$) was initiated. Culture was stabilised until constant optical density and titration rate, pumping through at least 5 volumes of medium. After achieving steady state conditions, acceleration of dilution rate ($a = 0.01 \text{ h}^{-2}$) was started. Additionally, a steady state chemostat experiment was carried out at a dilution rate of 0.45 h^{-1} and results were compared with data collected from the A-stat experiment at the same dilution rate. Average yield and metabolic switch point values with their standard deviations were calculated based on five independent experiments, additionally taking into account chemostat experiment values at a dilution rate of 0.45 h^{-1} .

Analytical methods and growth characteristics

Biomass was constantly monitored by measuring the optical density at 600 nm; biomass dry weight was determined gravimetrically. Biomass correlation constant K was 0.372 ± 0.005 and was not specific growth rate dependent. Levels of glucose, lactate, formate, acetate and ethanol in the culture medium were measured with liquid chromatography (Alliance 2795 system, Waters Corp., Milford, MA), using a BioRad HPX-87H column (Hercules, CA) with isocratic elution of 5 mM H_2SO_4 at a flow rate of 0.6 mL min^{-1} and at 35°C . A refractive index detector (model 2414; Waters Corp.) was used for detection and quantification of substances. The detection limit for the analytical method was 0.1 mM. Samples from culture medium were centrifuged ($14,000 \times g$, 4 min); supernatants were collected and analyzed immediately or stored at -20°C until analysis. Free amino acid concentrations were determined from the same sample (analysing frequency *ca* 0.02 h^{-1}) with an amino acid analyzer (Acquity UPLC; Waters Corp.) according to the manufacturer's instructions. Empower software (Waters Corp.) was used for the data processing. For measuring amino acid concentrations in protein content, biomass was hydrolysed with 6 M HCl for 20 h at 120°C . From hydrolyte, amino acids were determined as free amino acids described above. Protein content from biomass dry cell weight was calculated based on amino acid analysis and, additionally, measured using the Lowry method [29], where bovine serum albumin was used as a standard. For measurement of DNA content in biomass genomic DNA was extracted and measured using instructions of RTP[®] Bacteria DNA Mini Kit (Invitac, Germany). Detailed protocol for fatty acid quantification is described in [30]. Growth characteristics μ , Y_{XS} , $Y_{\text{Substrate}}$, Y_{Product} were calculated as described previously [27,28]. For consumption calculations, measured medium concentrations were used.

Carbon, nitrogen and ATP balance calculations

For carbon balance calculations C-molar concentrations of measured substrates, products and biomass were used

(biomass C-molar concentration with a value $0.03625 \text{ C-mol gdw}^{-1}$ was calculated based on monomer composition). For nitrogen balance calculations N-molar amino acid consumptions, production of ornithine and glutamate, ADI pathway activity and biomass composition ($0.00725 \text{ N-mol gdw}^{-1}$) were taken into account.

For calculations of ATP and NAD(P)H balance measured biomass, amino acid, RNA, DNA and fatty acid contents were used. Other necessary data were adapted from literature [31]. Stoichiometry of ATP, NAD(P)H and central metabolites for monomer production were taken from the Kyoto Encyclopaedia of Genes and Genomes database <http://www.kegg.jp/>, with an assumption that amino acids were not synthesized. Specific calculations are presented in Additional file 1.

Gene expression profiling

Agilent's DNA microarrays (Santa Clara, CA) were designed in eArray web portal in $8 \times 15\text{K}$ format, containing 7 unique probes per target <https://earray.chem.agilent.com/earray/>. Target sequences for 2234 genes were downloaded from Kyoto Encyclopaedia of Genes and Genomes <ftp://ftp.genome.jp/pub/kegg/genes/organisms/lla/l.lactis.nuc>.

For microarray analysis, steady state chemostat culture of *L. lactis* IL1403 was used as reference ($D = 0.10 \text{ h}^{-1}$). Subsequent quasi steady state points from A-stat experiment at specific growth rates 0.52 ± 0.03 ; 0.42 ± 0.02 ; $0.29 \pm 0.01 \text{ h}^{-1}$ in biological duplicates and 0.17 h^{-1} were compared to the reference sample. Transcript change was considered significant if the P value between parallel experiments was less than 0.05.

Total RNA was extracted and quantified, cDNA synthesised and labelled as described previously [27], with minor modification: $11 \mu\text{g}$ of total RNA was used for cDNA synthesis. Hybridization, slide washing and scanning was performed using standard Agilent's reagents and hardware <http://www.chem.agilent.com>. Gene expression data was analyzed as described before [27], except global lowess normalization was used. Spots with intensities lower than 100 units in both channels and outliers among technical replicates (according [32]) were filtered. After filtering, seven technical replicates showed average standard deviation <10%. Gene (and protein) expression measurement results are shown in Additional file 3. DNA microarray data is also available at NCBI Gene Expression Omnibus (Reference series: GSE26536).

Protein expression profiling

For protein expression analysis, the steady state chemostat culture of *L. lactis* IL1403 was used as reference ($\mu = 0.10 \text{ h}^{-1}$). Quasi steady state points at $\mu = 0.20 \pm 0.01$, 0.30 ± 0.02 , 0.42 ± 0.01 and $0.50 \pm 0.01 \text{ h}^{-1}$ were

compared with the reference sample. Three biological replicates were analysed.

Samples intended for proteome analysis were collected, washed with PBS (0.137 M NaCl, 2.7 mM KCl, 10.0 mM Na₂HPO₄, 1.4 mM KH₂PO₄), flash frozen in liquid nitrogen and stored at -80°C prior to protein extraction.

Proteins were extracted in ice-cold SDS-buffer (100 mM Tris-HCl (pH 6.5), 1% SDS (w/v)). Cells were disrupted as a result of agitating the suspension with glass-beads at 4°C for 30 minutes. After centrifugation for 30 min at 4°C, the supernatant was collected and the protein concentration was determined by 2D Quant kit (Amersham Biosciences, Buckinghamshire, UK) and protein samples were stored at -80°C until further analysis.

Aliquots of 100 µg chloroform/MeOH chloroform precipitated proteins from each sample were processed for labeling with iTRAQ 4plex reagents (Applied Biosystems, Foster City, CA) according to manufacturer's instructions. Briefly, precipitated proteins were dissolved in 0.5 M triethylammonium bicarbonate (TEAB) and 0.1% SDS, disulfide bonds were reduced in 5 mM Tris-(2-carboxyethyl) phosphine (TCEP) for 1 h at 60°C, followed by blocking cysteine residues in 10 mM methyl methanethiosulfonate (MMTS) for 30 min at room temperature, before digestion with trypsin (1:40, enzyme to protein ratio) overnight at 37°C. For labeling, each iTRAQ reagent was dissolved in 70 µl of ethanol and added to the respective peptide mixture. After 1 h incubation at room temperature the reactions were stopped by adding 100 µl milliQ water and incubating for 30 min. All four samples were mixed together and ethanol was removed by drying in a vacuum concentrator (Model 5301, Eppendorf, Cambridgeshire, UK).

The combined peptide mixtures were separated into 10 fractions with a cation exchange cartridge system (Applied Biosystems, Foster City, CA) by different KH₂PO₄ concentrations (10-1000 mM) and cleaned by StageTips [33]. All fractions were analyzed twice by LC-MS/MS using an Agilent 1200 series nanoflow system (Agilent Technologies, Santa Clara, CA) connected to a Thermo Scientific LTQ Orbitrap mass-spectrometer (Thermo Electron, San Jose, CA) equipped with a nano-electrospray ion source (Proxeon, Odense, Denmark). Purified peptides were dissolved in 0.5% formic acid and loaded on self-packed fused silica emitter (150 mm × 0.075 mm; Proxeon) packed with Repropur-Sil C18-AQ 3 µm particles (Dr. Maisch, Germany) using a flow rate of 0.7 µl min⁻¹. Peptides were separated with a 180 min gradient from 3 - 40% B (A: 0.1% formic acid, B: 0.1% formic acid/80% acetonitrile) using a flow-rate of 200 nl min⁻¹ and sprayed directly into LTQ Orbitrap mass-spectrometer operated at 180°C capillary temperature and 2.4 kV spray voltage.

Mass spectrometry method combined HCD and CID spectrums as described in Köcher et al. [34]. Briefly, full mass spectra were acquired in profile mode, with mass range from *m/z* 300 to 1800 at resolving power of 60000 (FWHM). Up to four data-dependent MS/MS scans with CID and four scans with HCD tandem mass spectrometry experiment triggered from the same precursor ion were acquired in centroid mode for each FTMS full-scan spectrum. CID was carried out with a target signal value of 10 000 in the linear ion trap, collision energy of 35%, Q value of 0.25 and an activation time of 30 ms. HCD-generated ions were detected in the Orbitrap using the target signal value of 10 000, collision energy of 35% and an activation time of 40 ms. Each fragmented ion was dynamically excluded for 60s.

Raw files were extracted to .mgf files by MM File Conversion Tools <http://searcher.rrc.uic.edu/cgi-bin/mm-cgi/downloads.py>. Each .mgf file was converted to a QuantMerge file [34]. All files from the same sample were merged together. Data generated was searched against *L. lactis* IL1403 NCBI database (22092009) by MassMatrix search tool [35]. A reversed decoy database was used for false positives detection. In all cases, a peptide mass tolerance of 5 ppm was used and fragment ion masses were searched with a 0.6 Da mass window. Two missed cleavage sites for trypsin were allowed. Beta-methylthiolation of a cysteine was set as a fixed modification and oxidation of methionine as a variable modification. Quantification was set as iTRAQ and quantification statistics as arithmetic mean. Only proteins with confidence intervals of more than 95% were allowed for further data analysis (Additional file 3). Proteomic analysis raw data is available at the PRIDE database [36] <http://www.ebi.ac.uk/pride> under accession numbers 13105-13162 (username: review17185, password: wyd*b6_6). The data was converted using PRIDE Converter <http://code.google.com/p/pride-converter>[37]. Protein expression change was considered significant if the *P* value between parallel experiments was less than 0.05.

Additional material

Additional file 1: Specific growth rate dependent ATP and NAD(P)H balance calculations for A-stat experiments with *Lactococcus lactis* subsp. *lactis* IL1403.

Additional file 2: Supplementary figures and tables.

Additional file 3: Specific growth rate dependent mRNA and protein expression changes from A-stat experiments with *Lactococcus lactis* subsp. *lactis* IL1403. The expression fold change is given accordingly: sample at respective specific growth rate (quasi steady state) is divided by steady state chemostat sample (0.10 h⁻¹). Average log₂ gene and protein expression changes were calculated from "n" number of parallel A-stat experiments. In gene expression analysis spots with intensities lower than 100 units in both channels and outliers among technical replicates (according Rorabacher, 1991) were filtered. In

protein expression analysis, proteins identified with a confidence interval more the 95% and appearances in all mentioned parallels are presented.

Acknowledgements

The authors would like to thank Lauri Peil (University of Tartu) and Elina Pelonen (Turku University of Applied Sciences and Åbo Akademi) for their help in carrying out 'omics analysis. The financial support for this research was provided by the European Regional Development Fund project EU29994, and Ministry of Education, Estonia, through the grant SF01400908.

Author details

¹Tallinn University of Technology, Department of Chemistry, Akadeemia tee 15, 12618 Tallinn, Estonia. ²Competence Center of Food and Fermentation Technologies, Akadeemia tee 15b, 12618 Tallinn, Estonia. ³Tallinn University of Technology, Department of Food Processing, Ehitajate tee 5, 19086 Tallinn, Estonia.

Authors' contributions

PJL, KAd, RV designed experiments and conceived the project. PJL, KAd carried out experiments. PJL, RN, LA, KAd contributed in analytics and data analysis. KAd was responsible for mathematical calculations. PJL drafted the manuscript. KAd helped drafting the manuscript. RV, RN, LA edited the manuscript. All authors read and approved the final manuscript.

Competing interests

The authors declare that they have no competing interests.

Received: 13 July 2010 Accepted: 24 February 2011

Published: 24 February 2011

References

- Bolotin A, Wincker P, Mauger S, Jaillon O, Malmgren K, Weissenbach J, Ehrlich SD, Sorokin A: **The complete genome sequence of the lactic acid bacterium *Lactococcus lactis* ssp. *lactis* IL1403.** *Genome Research* 2001, **11**:731-53.
- Hughenoltz J, Sybesma W, Groot MN, Wisselink W, Ladero V, Burgess K, van Sinderen D, Piard JC, Eggink G, Smid EJ, Savoy G, Sesma F, Jansen T, Hols P, Kleerebezem M: **Metabolic engineering of lactic acid bacteria for the production of nutraceuticals.** *Antonie Van Leeuwenhoek* 2002, **82**:217-35.
- Kleerebezem M, Boels IC, Groot MN, Mierau I, Sybesma W, Hughenoltz J: **Metabolic engineering of *Lactococcus lactis*: the impact of genomics and metabolic modelling.** *J Biotechnol* 2002, **98**:199-213.
- Hughenoltz J: **The lactic acid bacterium as a cell factory for food ingredient production.** *Intern Dairy J* 2008, **18**:466-75.
- Morello E, Bermúdez-Humarán LG, Llull D, Solé V, Miraglio N, Langella P, Poquet I: ***Lactococcus lactis*, an efficient cell factory for recombinant protein production and secretion.** *J Mol Microbiol Biotechnol* 2008, **14**:48-58.
- Bermúdez-Humarán LG: ***Lactococcus lactis* as a live vector for mucosal delivery of therapeutic proteins.** *Human Vaccines* 2009, **5**:264-7.
- Jensen PR, Hammer K: **Minimal Requirements for Exponential Growth of *Lactococcus lactis*.** *Appl Environ Microbiol* 1993, **59**:4363-6.
- Novak L, Coccagn-Bousquet M, Lindley N, Loubiere P: **Metabolism and energetics of *Lactococcus lactis* during growth in complex or synthetic media.** *Appl Environ Microbiol* 1997, **63**:2665-70.
- Zhang G, Block DE: **Using highly efficient nonlinear experimental design methods for optimization of *Lactococcus lactis* fermentation in chemically defined media.** *Biotechnol Prog* 2009, **25**:1587-97.
- Larsen N, Boye M, Siegmundfeldt H, Jakobsen M: **Differential expression of proteins and genes in the lag phase of *Lactococcus lactis* subsp. *lactis* grown in synthetic medium and reconstituted skim milk.** *Appl Environ Microbiol* 2006, **72**:1173-9.
- Mazzoli R, Pessione E, Dufour M, Laroute V, Giuffrida M, Giunta C, Coccagn-Bousquet M, Loubiere P: **Glutamate-induced metabolic changes in *Lactococcus lactis* NCD0 2118 during GABA production: combined transcriptomic and proteomic analysis.** *Amino Acids* 2010, **3**:727-37.
- Dressaire C, Redon E, Milhem H, Besse P, Loubiere P, Coccagn-Bousquet M: **Growth rate regulated genes and their wide involvement in the *Lactococcus lactis* stress responses.** *BMC Genomics* 2008, **9**:343.
- Dressaire C, Gittion C, Loubiere P, Monnet V, Queinnee I, Coccagn-Bousquet M: **Transcriptome and proteome exploration to model translation efficiency and protein stability in *Lactococcus lactis*.** *PLoS Comput Biol* 2009, **5**:12.
- Poolman B, Konings WN: **Relation of growth of *Streptococcus lactis* and *Streptococcus cremoris* to amino acid transport.** *J Bacteriol* 1988, **170**:700-707.
- Görke B, Stülke J: **Carbon catabolite repression in bacteria: many ways to make the most out of nutrients.** *Nat Rev Microbiol* 2008, **6**:613-24.
- Titgemeyer F, Hillen W: **Global control of sugar metabolism: a gram-positive solution.** *Antonie Van Leeuwenhoek* 2002, **82**:59-71.
- Garrigues C, Loubiere P, Lindley ND, Coccagn-Bousquet M: **Control of the shift from homolactic acid to mixed-acid fermentation in *Lactococcus lactis*: predominant role of the NADH/NAD⁺ ratio.** *J Bacteriol* 1997, **179**:5282-7.
- Novak L, Loubiere P: **The metabolic network of *Lactococcus lactis*: Distribution of ¹⁴C-labeled substrates between catabolic and anabolic pathways.** *J Bacteriol* 2000, **182**:1136-1143.
- Molenaar D, van Berlo R, de Ridder D, Teusink B: **Shifts in growth strategies reflect tradeoffs in cellular economics.** *Mol Syst Biol* 2009, **5**:323.
- Russell JB: **The energy spilling reactions of bacteria and other organisms.** *J Mol Microbiol Biotechnol* 2007, **13**:1-11.
- Ogura T, Wilkinson AJ: **AAA+ superfamily ATPases: common structure - diverse function.** *Gen Cells* 2001, **6**:575-597.
- Smid EJ, Konings WN: **Relationship between utilization of proline and proline-containing peptides and growth of *Lactococcus lactis*.** *J Bacteriol* 1990, **172**:5286-92.
- Benthin S, Villadsen J: **Amino acid utilization by *Lactococcus lactis* subsp. *cremoris* FD1 during growth on yeast extract or casein peptone.** *J Appl Microbiol* 1996, **80**:65-72.
- Lapujade P, Coccagn-Bousquet M, Loubiere P: **Glutamate biosynthesis in *Lactococcus lactis* subsp. *lactis* NCD0 2118.** *Appl Environ Microbiol* 1998, **64**:2485-9.
- Konings WN, Poolman B, Driessen AJ: **Bioenergetics and solute transport in lactococci.** *Crit Rev Microbiol* 1989, **16**:419-76.
- Valgepea K, Adamberg K, Nahku R, Lahtvee PJ, Arike L, Vilu R: **Systems biology approach reveals that overflow metabolism of acetate in *Escherichia coli* is triggered by carbon catabolite repression of acetyl-CoA synthetase.** *BMC Syst Biol* 2010, **4**:166.
- Lahtvee PJ, Valgepea K, Nahku R, Abner K, Adamberg K, Vilu R: **Steady state growth space study of *Lactococcus lactis* in D-stat cultures.** *Antonie Van Leeuwenhoek* 2009, **96**:487-96.
- Adamberg K, Lahtvee PJ, Valgepea K, Abner K, Vilu R: **Quasi steady state growth of *Lactococcus lactis* in glucose-limited acceleration stat (A-stat) cultures.** *Antonie Van Leeuwenhoek* 2009, **95**:219-26.
- Lowry OH, Rosebrough NJ, Farr AL, Randall RJ: **Protein measurement with the Folin phenol reagent.** *J Biol Chem* 1951, **193**:265-75.
- Spitsmeister M, Adamberg K, Vilu R: **UPLC/MS based method for quantitative determination of fatty acid composition in Gram-negative and Gram-positive bacteria.** *J Microbiol Methods* 2010, **82**:288-95.
- Oliveira A, Nielsen J, Forster J: **Modeling *Lactococcus lactis* using a genome-scale flux model.** *BMC Microbiol* 2005, **5**:39.
- Rorabacher DB: **Statistical treatment for rejection of deviant values: critical values of Dixon's "Q" parameter and related subrange ratios at the 95% confidence level.** *Analyst Chem* 1991, **63**:139-146.
- Rappsilber J, Mann M, Ishihama Y: **Protocol for micro-purification, enrichment, pre-fractionation and storage of peptides for proteomics using StageTips.** *Nat Prot* 2007, **2**:1896-906.
- Köcher T, Pichler P, Schützbiel M, Stingl C, Kaul A, Teucher N, Hasenfuss G, Penninger JM, Mechtler K: **High precision quantitative proteomics using iTRAQ on an LTQ Orbitrap: a new mass spectrometric method combining the benefits of all.** *J Prot Res* 2009, **8**:4743-52.
- Xu H, Freitas MA: **MassMatrix: a database search program for rapid characterization of proteins and peptides from tandem mass spectrometry data.** *Proteom* 2009, **9**:1548-55.
- Martens L, Hermjakob H, Jones P, Adamski M, Taylor C, States D, Gevaert K, Vandekerckhove J, Apweiler R: **PRIDE: the proteomics identifications database.** *Proteomics* 2005, **5**:3537-3545.

37. Barsnes H, Vizcaíno JA, Eidhammer I, Martens L: **PRIDE Converter: making proteomics data-sharing easy.** *Nat Biotechnol* 2009, **27**:598-599.
38. Ganesan B, Dobrowolski P, Weimer BC: **Identification of the leucine-to-2-methylbutyric acid catabolic pathway of *Lactococcus lactis*.** *Appl Environ Microbiol* 2006, **72**:4264-73.
39. Chambellon E, Rijnen L, Lorquet F, Gitton C, van Hylckama Vlieg JET, Wouters JA, Yvon M: **The D-2-hydroxyacid dehydrogenase incorrectly annotated PanE is the sole reduction system for branched-chain 2-keto acids in *Lactococcus lactis*.** *J Bacteriol* 2009, **191**:873-81.

doi:10.1186/1475-2859-10-12

Cite this article as: Lahtvee *et al.*: Multi-omics approach to study the growth efficiency and amino acid metabolism in *Lactococcus lactis* at various specific growth rates. *Microbial Cell Factories* 2011 **10**:12.

**Submit your next manuscript to BioMed Central
and take full advantage of:**

- Convenient online submission
- Thorough peer review
- No space constraints or color figure charges
- Immediate publication on acceptance
- Inclusion in PubMed, CAS, Scopus and Google Scholar
- Research which is freely available for redistribution

Submit your manuscript at
www.biomedcentral.com/submit



PUBLICATION IV

Lahtvee PJ, Valgepea K, Nahku R, Abner K, Adamberg K, Vilu R

Steady state growth space study of *Lactococcus lactis* in D-stat cultures

Antonie Van Leeuwenhoek, 96(4):487-96, (2009)

Steady state growth space study of *Lactococcus lactis* in D-stat cultures

Petri-Jaan Lahtvee · Kaspar Valgepea · Ranno Nahku ·
Kristo Abner · Kaarel Adamberg · Raivo Vilu

Received: 19 March 2009 / Accepted: 24 June 2009 / Published online: 15 July 2009
© Springer Science+Business Media B.V. 2009

Abstract Growth space of *Lactococcus lactis* subsp. *lactis* IL1403 was studied at constant growth rate using D-stat cultivation technique. Starting from steady state conditions in a chemostat culture ($\mu = 0.2 \text{ h}^{-1}$), the pH and/or temperature were continuously changed in the range of 5.4–6.4 and 26–34°C, respectively, followed by the return to the initial environmental conditions. Based on substrate consumption and product formation yields and expression changes of 1,920 genes, it was shown that changes of physiological state were not

dependent on the direction of movement (from pH 6.3 to 5.4 or from 5.4 to 6.3), showing that quasi steady state values in D-stat corresponded to the steady state values in chemostats. Relative standard deviation of growth characteristics in triplicate D-stat experiments was below 10%. Continuing the experiment and reestablishing initial growth conditions revealed in average 7% difference (hysteresis) in growth characteristics when comparing chemostat steady state cultures prior and after the change of environmental conditions. Similarly, shifts were also seen at gene expression levels. The large amount of quantitatively reliable data obtained in this study provided a new insight into dynamic properties of bacterial physiology, and can be used for describing the growth space of microorganisms by modeling cell metabolism.

Electronic supplementary material The online version of this article (doi:10.1007/s10482-009-9363-2) contains supplementary material, which is available to authorized users.

P.-J. Lahtvee · K. Valgepea · R. Nahku ·
K. Abner · R. Vilu (✉)
Department of Chemistry, Tallinn University
of Technology, Akadeemia tee 15, 12618 Tallinn, Estonia
e-mail: raivo@kbfi.ee

P.-J. Lahtvee · K. Valgepea · R. Nahku ·
K. Abner · K. Adamberg · R. Vilu
Competence Centre of Food and Fermentation
Technology, Akadeemia tee 15b, 12618 Tallinn, Estonia

K. Adamberg
Department of Food Processing, Tallinn University
of Technology, Ehitajate tee 5, 19086 Tallinn, Estonia

Keywords Continuous culture · *Lactococcus lactis* · Acid stress · Growth space · Transcriptome

Introduction

We have entered the era of synthetic biology with high throughput DNA sequencing (genetic) and omics methods, which in principle should make comprehensive quantitative characterization of molecular physiology of cells possible. However, cultivation methods where cells are in defined physiological states (Hoskisson and Hobbs 2005) and thus quantitatively

reliable data on cell metabolism could be obtained, have found little use in practice. Until present, multidimensional growth space has been systematically determined, and studied in batch cultures (Le Marc et al. 2005, see also <http://www.bioprocessors.com/>). However, batch experiments do not supply information about the growth space dynamics. For obtaining data on dynamic properties of the bacteria, they have to be cultivated preferably in continuous cultures in defined physiological states. Defined physiological states could be most readily realized in chemostat cultures. In spite of that, chemostat has not been used in bacterial physiology studies as widely as expected because the method is quite complex, laborious and time-consuming.

Due to its industrial importance, *L. lactis* is one of the best-studied microorganisms. However, a limited number of studies about growth dynamics—especially about dynamics of change of physiological state of cell on the change of growth conditions, could be found in the literature. Effects of pH, oxygen and dilution rate on the growth of *L. lactis* in chemostat have been studied by Thomas et al. (1979), O’Sullivan and Condon (1999), Even et al. (2001, 2003), Jensen et al. (2001), Dressaire et al. (2008). Dressaire et al. have made the first attempt to characterize the growth of *L. lactis* at the whole genome level using global transcriptome profiling.

We have previously shown that A-stat (chemostat with smooth change of dilution rate) is reproducible, informative and efficient cultivation method for studying physiology of cells at different specific growth rates in (quasi) steady state (Adamberg et al. 2009), provided that the change of growth conditions does not disrupt the quasi steady state of growing cells. Results of the *L. lactis* D-stat cultivation experiments (Kasemets et al. 2003) with smooth change of pH and/or temperature are reported in this paper. The rates of pH and temperature change sufficient for maintaining the quasi steady state growth of the culture during the transitions were determined, and the results obtained showed that D-stat cultures are reproducible tools for scanning the growth space of growing cells. In addition to the more conventional growth characteristics (Y_{xs} , Y_{lact} etc.) measured, also changes in transcriptome patterns of *L. lactis* IL1403 were investigated in different growth conditions. To our knowledge, this is the first

attempt made to characterize quasi steady state growth in multidimensional growth space of *L. lactis*.

Materials and methods

Bacterial strain and culture medium

The cultivated strain *Lactococcus lactis* subsp. *lactis* IL1403 was kindly provided by Dr. Ogier from INRA (Jouy-en-Josas, France). Inoculum was prepared using a lyophilized stock culture stored at -80°C which was pre-grown twice on the cultivation medium. The composition of the cultivation medium used was as follows (g L^{-1}): limiting substrate glucose—5, alanine—0.24, arginine—0.125, asparagine—0.21, aspartate—0.21, cysteine—0.13, glutamate—0.2, glutamine—0.1, glycine—0.175, histidine—0.15, isoleucine—0.33, leucine—0.66, lysine—0.44, methionine—0.125, phenylalanine—0.275, proline—0.225, serine—0.52, threonine—0.225, tryptophan—0.05, tyrosine—0.08, valine—0.33, K_2HPO_4 —3, KH_2PO_4 —2.5, NaCl —2.9, $\text{MgSO}_4 \cdot 7\text{H}_2\text{O}$ —0.2, $\text{CaCl}_2 \cdot 2\text{H}_2\text{O}$ —0.05, $\text{MnSO}_4 \cdot \text{H}_2\text{O}$ —0.016, $\text{ZnSO}_4 \cdot 7\text{H}_2\text{O}$ —0.005, $\text{CoCl}_2 \cdot 5\text{H}_2\text{O}$ —0.003, $\text{CuSO}_4 \cdot 5\text{H}_2\text{O}$ —0.003, $(\text{NH}_4)_6\text{Mo}_7\text{O}_{24} \cdot 4\text{H}_2\text{O}$ —0.003, $\text{FeSO}_4 \cdot 4\text{H}_2\text{O}$ —0.0014, pyridoxine—0.002, biotin—0.001, folic acid—0.001, niacin—0.001, pantothenic acid—0.001, riboflavin—0.001 and thiamine—0.001.

Cultivation system

The D-stat cultivation system consisted of a 1.25 L Biobundle bioreactor (Applikon, Schiedam, the Netherlands) controlled by an ADI 1030 biocontroller (Applikon) and a cultivation control program “BioXpert NT” (Applikon). The system was equipped with pH, pO_2 and temperature sensors. Two variable speed pumps (feeding and out-flow) were controlled using “BioXpert NT” control software. The bioreactor was set on a balance, which output was used as the control variable to ensure constant culture volume (300 ± 1 mL). Similarly, the inflow was determined by measuring the mass of fresh culture medium added. Cultivations were carried out under anaerobic conditions (N_2 -environment) with an agitation speed of 300 rpm at 34°C and pH 6.4, unless otherwise stated.

pH of the culture was controlled using 2 M NaOH and temperature with a heating blanket.

D-stat cultivation

The D-stat cultivation technique has been previously described by Kasemets et al. (2003). The principle is similar to chemostat where the culture is initially “stabilized” in a steady state at a chosen dilution rate (*D*). After a steady state is obtained, smooth change(s) of environmental parameter(s) (e.g. pH, temperature, substrate concentration) is (are) started while keeping the dilution rate constant. In our experiments, 300 mL of cultivation medium was inoculated with 5 mL of an

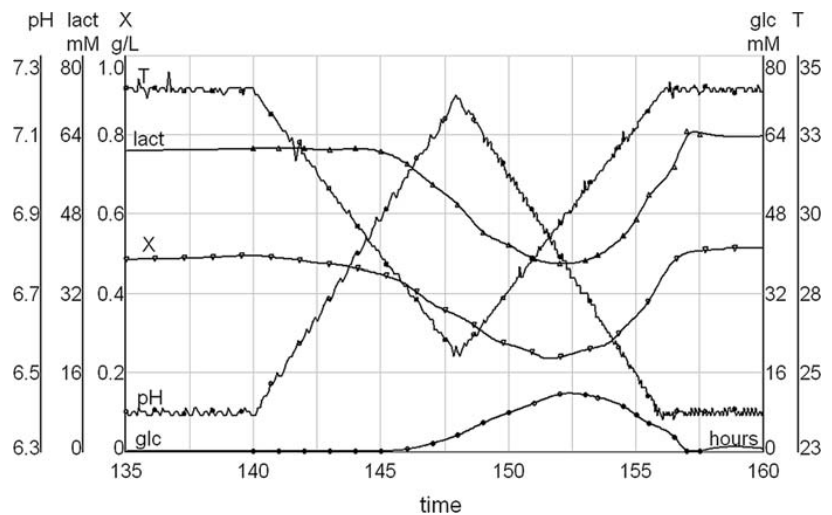
overnight grown culture. When optical density (OD₆₀₀) had reached 1.5–2, dilution rate was slowly increased up to the desired dilution rate where the culture was stabilized. Constant dilution rate *D* = 0.2 h⁻¹ was maintained throughout all experiments. After pumping through at least five working volumes of fresh medium for obtaining a steady state chemostat culture (OD = const.), smooth change of temperature and/or pH was switched on (Figs. 1, 3) at the changing rates presented in Table 1. After reaching the desired pH or temperature, the change of environmental conditions were reversed, and pH and/or temperature were changed back to the initial values, either immediately (Fig. 1) or after a period during which the

Table 1 Overview of *L. lactis* IL1403 D-stat experiments at dilution rate 0.2 h⁻¹

	Parameter(s) changed	Acceleration rate	Range	Units
Expt. 1	pH	0.1 U h ⁻¹	6.4–7.2–6.4	pH
	Temp.	1°C h ⁻¹	34–26–34	°C
Expt. 2	pH	0.1 U h ⁻¹	6.4–5.6–6.4	pH
	Temp.	1°C h ⁻¹	34–26–34	°C
Expt. 3	pH	0.025 U h ⁻¹	6.4–5.6–6.4	pH
	Temp.	0.25°C h ⁻¹	34–26–34	°C
Expt. 4	pH	0.02 U h ⁻¹	6.3–5.4–6.3	pH
Expt. 5	pH	0.0125 U h ⁻¹	6.1–5.4–6.1	pH
Expt. 6	pH	0.02–0.006 U h ^{-1(a)}	6.4–5.6–6.4	pH
Expt. 7	pH	0.02 U h ⁻¹	5.4–6.1–5.4	pH
Expt. 8	Temp.	0.25°C h ⁻¹	34–27–34	°C

^a Acceleration of pH was decreased gradually based on biomass formation and lactate production

Fig. 1 *Lactococcus lactis* IL1403 D-stat exp. 1 with simultaneous two-parameter change (pH and temperature). glc—glucose concentration in bioreactor (mM); lact—lactate concentration in bioreactor (mM); T—temperature (°C), X—biomass concentration in bioreactor (g L⁻¹)



culture was “stabilized” in chemostat (Fig. 2). Stability of the culture growth characteristics in chemostat was used to validate quasi steady state growth of the bacteria during the change of pH and/or temperature.

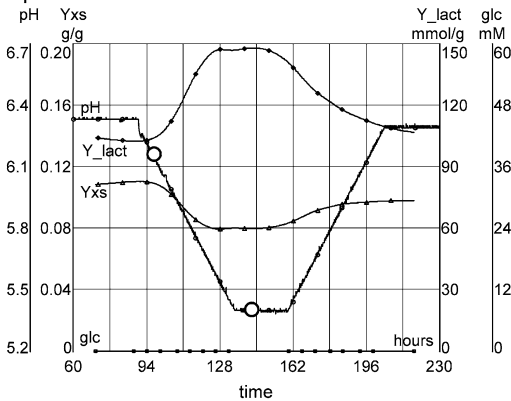
Analytical methods

The concentrations of organic acids (lactate, acetate and formate), ethanol and glucose in the culture media were analyzed by liquid chromatography (Alliance 2795 system, Waters Corp., Milford, MA), using a BioRad HPX-87H column (Hercules, CA) with isocratic elution of 0.005 M H₂SO₄ at a flow rate of 0.6 mL min⁻¹ and at 35°C. UV (210 nm; model 2487;

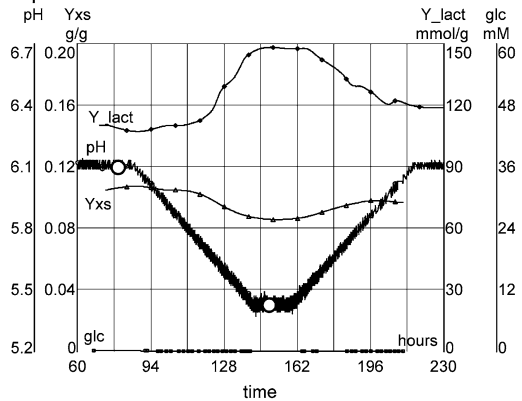
Waters Corp.) and refractive index (RI) detectors (model 2414; Waters Corp.) were used for detection and quantification of the substances. Detection limit for the analytical method was 0.1 mM. Samples from culture media were centrifuged (14,000g, 4 min), supernatants were collected and analyzed immediately or stored at -20°C until analysis. Amino acid concentrations were determined from the same sample with an amino acid analyzer (UPLC; Waters Corp.) according to the manufacturer’s instructions. Empower software (Waters Corp.) was used for the data processing.

Biomass concentration was calculated by measuring the optical density at 600 nm using a biomass

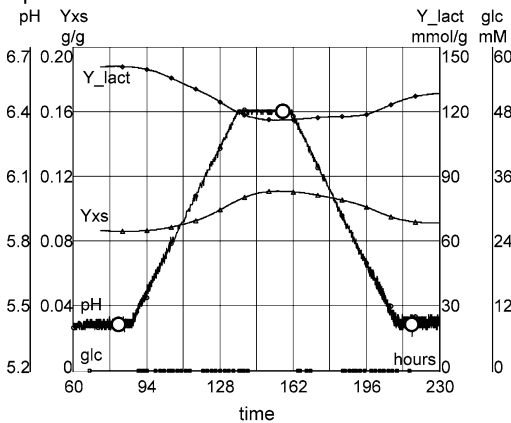
Exp. 4



Exp. 5



Exp. 7



Exp. 8

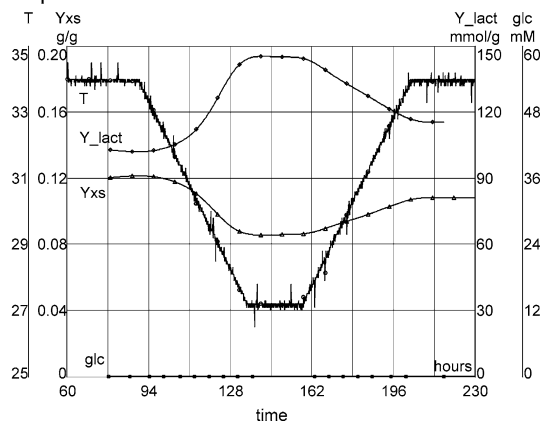


Fig. 2 *Lactococcus lactis* IL1403 D-stat experiments with the change of pH or temperature. Descriptions of the experiments can be seen in Table 1. Circles indicate sampling points for transcriptome analysis which in each experiment were

compared to one another. glc—glucose concentration in bioreactor (mM); Y_{lact}—lactate yield based on biomass production (mmol lact gdw⁻¹); T—temperature (°C); Y_{xs}—biomass yield based on glucose consumption (g gdw⁻¹)

conversion factor $K = 0.30 \pm 0.02 \text{ g L}^{-1} \text{ OD}_{600}^{-1}$ ($K = X/\text{OD}_{600}$, where X is in g dry weight [gdw] L^{-1}). Dry weight of bacteria was determined gravimetrically by centrifuging biomass from 15 mL of culture, washing it multiple times with distilled water and drying at 100°C for 24 h.

Global transcription profiling

Microarrays used in this study were purchased from Eurogentec (Seraing, Belgium) and contained 1,920 open reading frames (ORF) of *L. lactis* spotted in duplicates on standard 2.5 × 7.5 cm glass slides.

Samples of biomass were fixed with RNAprotect solution (QIAGEN, Valencia, CA)—the samples of culture media were mixed with RNAprotect solution (1:1 ratio), incubated for 5 min at room temperature and centrifuged for 10 min at 8,000g. Supernatant was discarded and the pellet stored at –80°C. Total RNA was extracted with RNeasy Mini Kit (QIAGEN) and genomic DNA was removed using RNase-Free DNase Set (QIAGEN). After addition of 500 μL lysozyme (10 mg lysozyme in 1 mL TE pH 8; Amresco Inc., Solon, OH), three freeze-thawing cycles were carried out followed by incubation at 37°C for 1 h. 20 μL of proteinase K solution (20 U proteinase K in 1 mL; Amresco Inc.) was added and incubated for 1 h at 37°C before RNA extraction.

cDNA was synthesized from 15 μg of total RNA at 46°C overnight using the following reagents per reaction: 1 μg random primers (Random decamers; Invitrogen, Carlsbad, CA), 6 μL five times concentrated first strand buffer (Invitrogen), 3 μL 0.1 M DTT (Invitrogen), 0.9 μL dNTPs (final concentrations: dATP 0.5 mM, dCTP 0.5 mM, dGTP 0.5 mM, dTTP 0.3 mM, aminoallyl-dUTP 0.2 mM), 1 μL RNase Inhibitor (Bioron, Ludwigshafen, Germany), 2 μL Superscript III (Invitrogen). RNA strands were hydrolyzed in the samples by adding 4.5 μL 1 M NaOH and incubating at 70°C for 10 min, after incubation the samples were neutralized with 4.5 μL 1 M HCl. cDNA was purified with MinElute PCR purification kit (QIAGEN) and labeled with Cy3 (CyTM3 Mono Reactive Dye Pack, Amersham, Buckinghamshire, UK) or Cy5 (CyTM5 Mono Reactive Dye Pack, Amersham). Staining was carried out in 10 μL of NaHCO₃ (pH 9) at room temperature in dark for 1 h and the samples were purified again with MinElute PCR purification kit. Subsequently, the following

hybridization master mix was used (per slide): 20 × SSC 16.3 μL, 100% formamide 32.5 μL, 10% SDS 0.65 μL. The hybridization was carried out at 42°C for 16 h.

Analysis of gene expression data

Microarray slides were scanned using an Agilent DNA Microarray Scanner (Santa Clara, CA). Spot intensities and corresponding background signals were quantified with Genepix Pro (version 6; Axon Instruments [http://www.moleculardevices.com/pages/software/gn_gene_pix_pro.html]). Spots which had a signal-to-noise ratio less than three or intensities of both, 635 and 532 nm channels lower than 500 units were filtered. Further analysis was carried out in R environment (version 2.6.1; R Development Core Team [<http://www.r-project.org/>]) using KTH package (KTH Microarray Center [<http://www.biotech.kth.se/molbio/microarray/dataanalysis/index.html>]). Flagged spots and background were extracted before “printTipLoess” normalization.

Calculation of growth characteristics

Growth characteristics of bacteria were calculated based on OD of the culture, total volume of medium pumped out from bioreactor (L) and lactate or glucose concentrations in culture medium (mol L^{-1}) as follows:

$$\mu = \{[d(V_{\text{out}})]/(V \times dt)\} + \{[d(\text{OD})]/(dt \times \text{OD})\}$$

$$Q_{\text{glc}} = \{[\Delta S_{\text{glc}} \times d(V_{\text{out}})]/(V \times \text{OD} \times K \times dt)\} - \{[d(\Delta S_{\text{glc}})]/(dt \times \text{OD} \times K)\}$$

$$Y_{\text{XS}} = \mu/Q_{\text{glc}}$$

$$Q_{\text{lact}} = \{[\text{lact} \times d(V_{\text{out}})]/(V \times \text{OD} \times K \times dt)\} - \{[d(\text{lact})]/(dt \times \text{OD} \times K)\}$$

$$Y_{\text{lact}} = Q_{\text{lact}}/\mu,$$

where μ is specific growth rate (h^{-1}); lact is concentration of produced lactic acid (mmol L^{-1}); Q_{glc} is specific glucose consumption rate ($\text{g glc gdw}^{-1} \text{h}^{-1}$ or $\text{mmol glc gdw}^{-1} \text{h}^{-1}$); ΔS_{glc} is amount of consumed glucose (g glc L^{-1} or mmol glc L^{-1}); Y_{XS} is biomass yield calculated on glucose consumption ($\text{gdw g glucose}^{-1}$); Q_{lact} is specific production rate of lactate ($\text{mmol lact gdw}^{-1} \text{h}^{-1}$); V is bioreactor volume (L); Y_{lact} is lactate yield based on biomass

production ($\text{mmol lact gdw}^{-1}$); OD is optical density at 600 nm; V_{OUT} is total volume of medium pumped out from bioreactor (L); K is biomass conversion factor (see above for equation) and t is running cultivation time (h).

Growth space visualization

3-D growth space was visualized using Datafit program (version 9.0; Oakdale Engineering [<http://www.curvefitting.com>]) with polynomial fit [$Y_{\text{XS}} = a + b/\text{pH} + c/\text{pH}^2 + d \times \ln T + e \times (T)^2$] and quasi steady state data points (the chosen regression represented our data points the best).

Results

D-stat cultivation experiments with continuous change of one parameter (pH or temperature) or simultaneous change of two parameters (pH and temperature) were carried out, and growth characteristics of *L. lactis* IL1403 in different pH and/or temperature conditions at dilution rate 0.2 h^{-1} were studied (see Table 1). Thus continuous moving in two-dimensional bacterial growth sub-space was performed. As can be seen on Figs. 1 and 2, environmental conditions were changed in D-stat experiments back and forth, where initial growth conditions were restored in the end of the experiments. Special attention was paid to make sure whether the initial physiological states (steady states) were reinstated after the back and forth change of growth conditions.

Experiments with two-parameter change (exp. 1, 2, 3 in Table 1; Fig. 1) showed a possibility for culture characteristics to return to their initial values after initial optimal growth conditions were reestablished. However, it has to be noted that the culture was not in quasi steady state throughout the whole experiment (see transient increase of residual glucose concentration on Fig. 1). This indicated that changing rates of pH and temperature, 0.1 U h^{-1} and 1°C h^{-1} respectively, were too fast to enable the culture to adapt to the changing environmental conditions, and maintain steady state growth in the glucose limited state. Hence, single parameter change experiments with slower changing rates (see Table 1) were carried out subsequently to make sure that the bacteria were in the

glucose limited quasi steady state during the full course of the experiments.

No glucose was observed in the culture media during the transition from the initial stabilization value of pH (pH 6.1–6.4) until pH 5.4–5.6 (exp. 4–6; Table 1), indicating maintenance of quasi steady state growth in these conditions (for exp. 4 and 5, see also Fig. 2). To prove the maintenance of the steady state, D-stat experiments were switched into chemostat at the lowest pH values and kept in constant environmental conditions for over five generations. Results obtained in latter chemostat showed that production rates of biomass and main growth by-products were maintained constant, varying only in the range of measurements error ($<5\%$) (Fig. 2). In addition, Y_{lact} and Y_{XS} values at pH 5.4 in exp. 7 (initial chemostat) and quasi steady state values at pH 5.4 in exp. 4 and 5 (after the first transition) were similar in the range of standard deviation. Furthermore, it was observed that growth characteristics were not dependent on the direction of pH movement (from pH 6.3 to 5.4 in exp. 4 or from 5.4 to 6.3 in exp. 7), showing that quasi steady state values in D-stat were identical to steady state values in chemostat. Hence, it can be assumed that the bacteria were in (quasi) steady state during the entire transition. Maintenance of quasi steady state growth during the change of temperature from 34 to 27°C was proved also in exp. 8.

Growth characteristics

For the comparison of four D-stat cultivations with pH changing rates below 0.02 U h^{-1} (quasi steady state growth; exp. 4–7), biomass yield per consumed glucose (Y_{XS}) and lactic acid yield per biomass produced (Y_{lact}) were calculated. Y_{XS} was $0.108 \pm 0.003 \text{ gdw g glucose}^{-1}$ at optimal pH, and decreased to $0.084 \pm 0.003 \text{ gdw g glucose}^{-1}$ at pH 5.4. Small relative standard deviation (6%) of the Y_{XS} values determined in four experiments showed very good reproducibility of D-stat method. The value of Y_{lact} decreased with the decrease of pH from $144 \pm 11 \text{ mmol gdw}^{-1}$ at optimal pH to $106 \pm 14 \text{ mmol gdw}^{-1}$ at pH 5.4 with the average standard deviation value of 9%. Similarly, changes in Y_{lact} and Y_{XS} were observed in the experiments with simultaneous pH and temperature change (exp. 1, 2, 3 in Table 1) as well. However, biomass yield (Y_{XS}) coefficients values at pH 5.6 and temperature 26°C were about 15% lower in

comparison with those observed in the case of only changing pH or temperature—see exp. 4–7. This can be explained by applying higher adaptive stress on the metabolism in the case of simultaneous pH and temperature change in double-parameter experiments than in the single-parameter experiments, and by the fact that changing rates used were higher ($a_{\text{pH}} = 0.025 \text{ U h}^{-1}$ and $a_{\text{T}} = 0.25^\circ\text{C h}^{-1}$) in the double-parameter experiments.

All described cultivations could be considered as homolactic—lactate production comprised more than 90% of all products observed, and the share of lactate slightly increased in higher stress conditions.

Transcriptome

To characterize the effects of changing pH on the physiological state of the bacteria more thoroughly, global transcriptome measurements were carried out at different quasi steady state growth conditions. Samples taken for comparison are shown in Fig. 2 and the list of measured genes which expression changed more than 1.8 times in different environmental conditions may be found in supplementary materials (<http://www.tftak.eu/?id=69>).

Forty-one genes which expression changed more than 1.8 times were observed as the result of the first pH change, i.e. as the result of moving away from the initial chemostat conditions in exp. 4, 5 and 7 (Fig. 2 exp. 4, 5 and 7). The most remarkable change at transcriptional level took place in arginine (urea cycle) metabolism, where expression of genes *arcA*, *arcC1*, *arcC2*, *arcD1*, *argE* and *argR* increased 2- to 6.25-fold on lowering the pH. When moving from acidic conditions to optimal pH values, expression levels of the same genes decreased (in exp. 7) as a response to the change of pH—independent of the movement direction in growth space. It must be noted that the concentration of arginine in the culture media was below the detection limit (0.01 mM) during the whole experiment. Citrate cycle genes *citC*, *citD* and *citE* were down-regulated when lowering the pH and up-regulated when the pH was returned to the initial value. Arginine and citrate formation pathways are well-known as taking part in the regulation of survival against acid stress by increasing internal pH or generating additional metabolic energy (Konings 2002). In the case of *lysQ*, which encodes a lysine/histidine specific transport permease protein (Vitreschak et al. 2004), a

significant fivefold up-/down-regulation was observed while pH was decreased/increased, respectively. As the overall consumption of lysine and histidine were less than the error of the measurement (5%), we can only assume that shifts in the expression of the genes responsible for lysine/histidine transport were necessary to adapt to the varying pH conditions. Moreover, based on homology analysis, genes *yxbE* and *yxbF*, which are known to encode universal stress proteins, were strongly up-regulated at lower pH conditions. All other detected major changes in transcriptomes concerned hypothetical or poorly studied proteins (see supplementary materials).

Hysteresis

As can be seen from Fig. 2, biomass concentration in chemostat in the beginning of the experiments and after the return to the initial conditions in the end of the experiments differed by $8 \pm 3\%$, indicating hysteresis in the physiological states of the culture. Production of lactate per biomass and glucose consumption per biomass was lower in the end of the experiments (exp. 4–8) by 6–13%, in comparison with the beginning of the experiments. Microarray analysis revealed that the expression levels of certain arginine and citrate metabolism genes—*arcA*, *arcC1*, *arcC2*, *arcD1*, *argE*, *argR* and *citC*, *citD*—changed during the first pH shift. However, instead of recovering their expression after moving back to initial environmental conditions, these genes remained expressed at the level attained during the first pH shift (exp. 7 in Fig. 2). See also supplementary materials for more information about transcription differences during the back and forth changes of the growth conditions (hysteresis).

It was shown in three additional parallel chemostat experiments with *L. lactis* that no changes, neither in biomass concentration, nor in the levels of main metabolites were observed at optimal growth conditions during 70 generations (data not shown). However, as mentioned above, after reducing of the changing rates used in the experiments 4–8 which led to the remarkable prolongation of the D-stat experiments, and the time while the bacteria were exposed to the changed environmental conditions (mild stress), hysteresis of the gene expression and growth parameters were observed in our experiments. Although significant, further characterization and

study of the hysteresis was out of the scope of the present study, and was postponed to the future.

Discussion

The results obtained showed that D-stat cultivation method made it possible to reproducibly scan relatively large growth space areas of *L. lactis* in reasonable time in quasi steady state at fixed dilution rate. 3D graph describing the dependence of biomass yield (based on glucose consumption) on temperature and pH for the bacteria is shown on Fig. 3. The differences between modelled surface and actual data points were less than 10%. The region of the optimal growth conditions in the studied range is indicated by the lightest area on the surface on Fig. 3. Simultaneous change of pH and temperature led to a more noticeable change of growth parameters in comparison with a single parameter change, as expected.

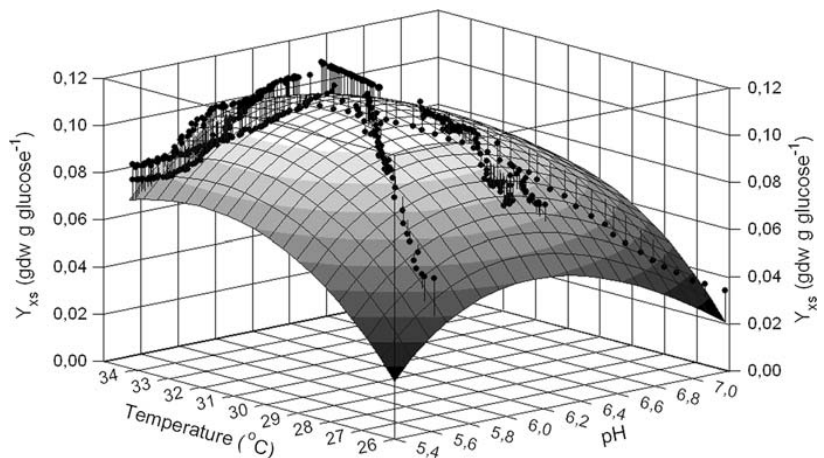
Important issues in planning and carrying out D-stat (changestat) experiments are duration of cultivation experiments, range of growth conditions scanned and choice of changing rates, which should enable to maintain quasi steady state. Duration of the cultivation experiments might be a crucial factor in prolonged experiments. It has been shown previously that extended chemostats (100–1,000 generations) could be used for studying culture adaptation and selecting mutated strains with special characteristics (Francis and Hansche 1973; Maharjan et al. 2007). The observation that bacteria can be found in

different physiological states in the same environmental conditions before and after applying mild stress in D-stat experiments during 60 generations was made in the present study. The data obtained in our experiments indicated that the changed environmental conditions applied in the D-stat experiments might lead to the onset of the adaptive mechanisms in shorter time than in the constant environmental conditions in chemostat.

The hysteresis of physiological states of the D-stat cultures observed seemed to be phenomenologically similar to the temporary application of the sub-lethal stress after which the vitality of microorganisms have been improved and maintained even after the cessation of stress conditions (Sánchez et al. 2007). Even though sub-lethal stress is still not sufficiently studied at molecular level, three general hypotheses for the explanation of this phenomenon have been formulated: (1) some stress response proteins are expressed in stress conditions and maintained expression of these genes leads to the increase of the survival even long after the cessation of the stress; (2) mutations take place during the sub-lethal stress, or (3) some mutated sub-populations could survive with more ease than the main population. Taking into account these possibilities, more detailed analysis of stress and hysteresis should be carried out in the future, investigating especially possible mutations—e.g. sequencing genomes of the culture during the cultivation.

Another important factor in carrying out changestat experiments is the changing rate of environmental parameters. It has been previously shown that the

Fig. 3 *Lactococcus lactis* IL1403 quasi steady state growth surface describing the dependence of biomass yield (based on glucose consumption) on temperature and pH for the bacteria. The surface is based on all D-stat experiments. Y_{xs} —biomass yield calculated on glucose consumption ($\text{gdw g glucose}^{-1}$). Black dots represent quasi steady state data points from exp. 1–8



farther the culture is moved from optimal growth conditions, the lower changing rates have to be applied in order to maintain quasi steady state (Adamberg et al. 2009; O'Sullivan and Condon 1999; van der Sluis et al. 2001). Therefore, identification of physiological parameters, which would indicate the (forthcoming) loss of quasi steady state, is a critical issue in carrying out changestat experiments in practice, especially when developing and applying adaptive algorithms. The most suitable indicators of physiological states are the parameters, which could be measured online—e.g. optical density, titration rate, gas production rate etc. In addition, substrate consumption and product formation can be used. Indeed, it has been shown that online measurements of carbon dioxide evolution could be successfully used for the elucidation of the response of the metabolism to the change of the growth conditions (Vemuri et al. 2006). Additionally, indicator molecules of overflow metabolism (acetate, ethanol) in microorganisms having respirofermentative growth like *E. coli* and yeast could be used for adaptive control (Jobé et al. 2003). However, the changes of these metabolic characteristics can also be a “normal” quasi steady state physiological response of the cell metabolism to the change of the environmental conditions. Therefore, the most reliable, though time-consuming way to check the maintenance of steady state growth in changestat experiments is the “chemostat control”, i.e. halting the changing rate and continuing the experiment in chemostat. If all physiological parameters (production or consumption rates of metabolites per biomass etc.) remain constant, it can be concluded that the changestat (D-stat, etc.) culture was in a quasi steady state before the acceleration was stopped. This kind of control was also routinely used in our experiments.

A method for scanning the growth space of microorganism was tested in this paper. Use of D-stat cultivation method allowed obtaining a large amount of steady state data in multidimensional quasi steady state growth space of *L. lactis* in reasonable time and effort. It was possible to study reproducibly and quantitatively adaptive responses of growth characteristics as well as gene expression at transcriptome level while changing the pH and temperature in D-stat cultures.

Acknowledgments We thank Sten Erm for useful discussions. The financial support for this research was provided by the

Enterprise Estonia project EU22704, and Ministry of Education, Estonia, through the grant SF0140090s08.

References

- Adamberg K, Lahtvee P, Valgepea K, Abner K, Vilu R (2009) Quasi steady state growth of *Lactococcus lactis* in glucose-limited acceleration stat (A-stat) cultures. *Antonie Van Leeuwenhoek* 95(3):219–226
- Dressaire C, Redon E, Milhem H, Besse P, Loubière P, Coccain-Bousquet M (2008) Growth rate regulated genes and their wide involvement in the *Lactococcus lactis* stress responses. *BMC Genomics* 9:343
- Even S, Lindley ND, Coccain-Bousquet M (2001) Molecular physiology of sugar catabolism in *Lactococcus lactis* IL1403. *J Bacteriol* 183(13):3817–3824
- Even S, Lindley ND, Coccain-Bousquet M (2003) Transcriptional, translational and metabolic regulation of glycolysis in *Lactococcus lactis* subsp. *cremoris* MG 1363 grown in continuous acidic cultures. *Microbiology* 149(Pt 7):1935–1944
- Francis JC, Hansche PE (1973) Directed evolution of metabolic pathways in microbial populations II. A repeatable adaptation in *Saccharomyces cerevisiae*. *Genetics* 74(2):259–265
- Hoskisson PA, Hobbs G (2005) Continuous culture—making a comeback? *Microbiology* 151(10):3153–3159
- Jensen NBS, Melchiorson CR, Jokumsen KV, Villadsen J (2001) Metabolic behavior of *Lactococcus lactis* MG1363 in microaerobic continuous cultivation at a low dilution rate. *Appl Environ Microbiol* 67(6):2677–2682
- Jobé AM, Herwig C, Surzyn M, Walker B, Marison I, von Stockar U (2003) Generally applicable fed-batch culture concept based on the detection of metabolic state by online balancing. *Biotechnol Bioeng* 82(6):627–639
- Kasemets K, Drews M, Nisamedtinov I, Adamberg K, Paalme T (2003) Modification of A-stat for the characterization of microorganisms. *J Microbiol Methods* 55(1):187–200
- Konings WN (2002) The cell membrane and the struggle for life of lactic acid bacteria. *Antonie Van Leeuwenhoek* 82(1–4):3–27
- Le Marc Y, Pin C, Baranyi J (2005) Methods to determine the growth domain in a multidimensional environmental space. *Int J Food Microbiol* 100(1–3):3–12
- Maharjan RP, Seeto S, Ferenci T (2007) Divergence and redundancy of transport and metabolic rate-yield strategies in a single *Escherichia coli* population. *J Bacteriol* 189(6):2350–2358
- O'Sullivan E, Condon S (1999) Relationship between acid tolerance, cytoplasmic pH, and ATP and H⁺-ATPase levels in chemostat cultures of *Lactococcus lactis*. *Appl Environ Microbiol* 65(6):2287–2293
- Sánchez B, Champomier-Verges M, Collado MDC, Anglade P, Baraige F, Sanz Y, de los Reyes-Gavilán CG, Margolles A, Zagorec M (2007) Low-pH adaptation and the acid tolerance response of *Bifidobacterium longum* biotype longum. *Appl Environ Microbiol* 73(20):6450–6459
- Thomas TD, Ellwood DC, Longyear VM (1979) Change from homo- to heterolactic fermentation by *Streptococcus*

- lactis* resulting from glucose limitation in anaerobic chemostat cultures. *J Bacteriol* 138(1):109–117
- van der Sluis C, Westerink BH, Dijkstal MM, Castelein SJ, van Boxtel AJ, Giuseppin ML, Tramper J, Wijffels RH (2001) Estimation of steady-state culture characteristics during acceleration-stats with yeasts. *Biotechnol Bioeng* 75(3): 267–275
- Vemuri GN, Altman E, Sangurdekar DP, Khodursky AB, Eiteman MA (2006) Overflow metabolism in *Escherichia coli* during steady-state growth: transcriptional regulation and effect of the redox ratio. *Appl Environ Microbiol* 72(5):3653–3661
- Vitreschak AG, Lyubetskaya EV, Shirshin MA, Gelfand MS, Lyubetsky VA (2004) Attenuation regulation of amino acid biosynthetic operons in proteobacteria: comparative genomics analysis. *FEMS Microbiol Lett* 234(2):357–370

Nahku R, Peebo K, Valgepea K, Barrick JE, Adamberg K, Vilu R

Stock culture heterogeneity rather than new mutational variation complicates short-term cell physiology studies of *Escherichia coli* K-12 MG1655 in continuous culture

Microbiology, 157(Pt 9):2604-2610

Stock culture heterogeneity rather than new mutational variation complicates short-term cell physiology studies of *Escherichia coli* K-12 MG1655 in continuous culture

Ranno Nahku,^{1,2} Karl Peebo,^{1,2} Kaspar Valgepea,^{1,2} Jeffrey E. Barrick,³ Karel Adamberg^{2,4} and Raivo Vilu^{1,2}

Correspondence
Raivo Vilu
raivo@kbfi.ee

¹Tallinn University of Technology, Department of Chemistry, Akadeemia tee 15, 12618 Tallinn, Estonia

²Competence Centre of Food and Fermentation Technologies, Akadeemia tee 15b, 12618 Tallinn, Estonia

³The University of Texas at Austin, Department of Chemistry and Biochemistry, Institute for Cellular and Molecular Biology, Austin, TX 78712, USA

⁴Tallinn University of Technology, Department of Food Processing, Ehitajate tee 5, 19086 Tallinn, Estonia

Nutrient-limited continuous cultures in chemostats have been used to study microbial cell physiology for over 60 years. Genome instability and genetic heterogeneity are possible uncontrolled factors in continuous cultivation experiments. We investigated these issues by using high-throughput (HT) DNA sequencing to characterize samples from different phases of a glucose-limited accelerostat (A-stat) experiment with *Escherichia coli* K-12 MG1655 and a duration regularly used in cell physiology studies (20 generations of continuous cultivation). Seven consensus mutations from the reference sequence and five subpopulations characterized by different mutations were detected in the HT-sequenced samples. This genetic heterogeneity was confirmed to result from the stock culture by Sanger sequencing. All the subpopulations in which allele frequencies increased (*betA*, *cspG/cspH*, *glyA*) during the experiment were also present at the end of replicate A-stats, indicating that no new subpopulations emerged during our experiments. The fact that ~31 % of the cells in our initial cultures obtained directly from a culture stock centre were mutants raises concerns that even if cultivations are started from single colonies, there is a significant chance of picking a mutant clone with an altered phenotype. Our results show that current HT DNA sequencing technology allows accurate subpopulation analysis and demonstrates that a glucose-limited *E. coli* K-12 MG1655 A-stat experiment with a duration of tens of generations is suitable for studying cell physiology and collecting quantitative data for metabolic modelling without interference from new mutations.

Received 20 April 2011
Revised 15 June 2011
Accepted 21 June 2011

INTRODUCTION

Nutrient-limited continuous culture has been used to study the cell physiology of micro-organisms for over 60 years (Monod, 1950; Novick & Szilard, 1950a). The main advantage of continuous cultivation methods (e.g. chemostat) over batch cultivation is the fact that in the former it is possible to maintain constant environmental conditions, and

Abbreviations: A-stat, accelerostat; *D*, dilution rate; DAACS, dicarboxylate/amino acid, cation symporter; HT, high-throughput; IS, insertion sequence; SNP, single nucleotide polymorphism.

Supplementary Methods, six supplementary figures and two supplementary tables are available with the online version of this paper.

therefore to force cells to grow at desired specific growth rates and in strictly defined physiological states. This control allows the acquisition of coherent quantitative steady-state data for metabolic modelling. Accelerostats (A-stats) enable the collection of a vast amount of quantitative data within a large range of specific growth rates in a single experiment (Paalme *et al.*, 1995). An A-stat experiment starts as a chemostat, but after reaching steady state, a smooth change of dilution rate (*D*) is applied (Fig. 1). A typical change in *D* is relatively slow (0.01 h^{-2}), which allows cells to adapt to the changing conditions and still maintain a stable physiological state equivalent to steady state: a quasi-steady state. Chemostats (at steady state) and A-stats (at

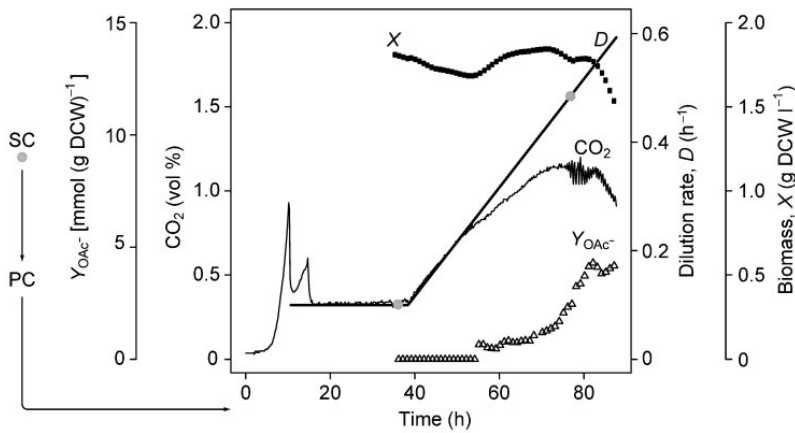


Fig. 1. Overview of *E. coli* K-12 MG1655 A-stat experiment in which samples for HT DNA sequencing were taken. Grey dots denote sampling points for HT DNA sequencing: stock culture and two samples at $D=0.11$ and 0.48 h^{-1} . The numbers of generations between the sampling points were as follows: stock culture and $D=0.11\text{ h}^{-1}$, 18 generations (including four generations of continuous culture); $D=0.11$ and 0.48 h^{-1} , 16 generations. The glucose concentration remained below the detection limit (120 mg l^{-1}) until the maximal specific growth rate was achieved. SC, stock culture; PC, pre-culture; X, dry cell weight (DCW) per litre; D, dilution rate; Y_{OAc^-} , acetate production per gram dry cell weight; CO_2 , carbon dioxide volumetric percentage in the gas outflow. This A-stat experiment is the same as that reported in Fig. 1 of Valgepea *et al.* (2010).

quasi-steady state) have been shown to yield quantitatively comparable results in terms of their main growth characteristics (e.g. biomass yield, substrate consumption and product accumulation rates) in experiments using *Escherichia coli* K-12 MG1655 (Valgepea *et al.*, 2010) and *Lactococcus lactis* IL1403 (Lahtvee *et al.*, 2011) over a range of specific growth rates ($0.10\text{--}0.51\text{ h}^{-1}$).

Quantitative data collected from continuous cultivation methods are often used for metabolic modelling. Because DNA sequences encode the metabolic network of the cell, it is essential to know if and when the genomes of cells are changing during these experiments. In fact, chemostats were initially introduced to study evolution and selection in a constant environment. Fitter clones are known to rapidly arise in some cases (Helling *et al.*, 1987; Novick & Szilard, 1950b), introducing an uncontrolled dynamic factor that reduces the quantitative reliability of steady-state data. Although Egli and colleagues have shown that evolution and selection can be reproducible at the phenotypic level in large (10^{11} cells) chemostat populations (Wick *et al.*, 2001, 2002), other studies have detected significant genotypic variation among similarly evolved cultures (Notley-McRobb & Ferenci, 1999a, b; Maharjan *et al.*, 2006). Therefore, checking the stability of the genome of the cultured strain and monitoring the genetic homogeneity of the whole population over time in continuous cultures are vital for understanding when genetic heterogeneity and evolution interfere with steady-state physiology measurements of growing cells.

Flaws in stock culture handling are one possible source of genetic heterogeneity in cell physiology studies. Indeed, heterogeneity in stab agar cultures has been reported during long-term storage of *E. coli* K-12 W3110 at room temperature (Jishage & Ishihama, 1997; Naas *et al.*, 1994, 1995). Considerably fewer mutations are expected when cell cultures are stored in the frozen state, in which no metabolic activity is possible. Nevertheless, genetic differences, including loss of genes and variation in growth phenotype on various carbon sources, have been detected in *E. coli* K-12 MG1655 strains acquired from different stock centres and laboratories (Soupene *et al.*, 2003). What is more, variation in motility has been observed between *E. coli* K-12 strain derivatives (including MG1655), whereby increased motility is found to be caused by insertion sequence (IS)-mediated activation of *flhD*, a regulator of flagellar gene transcription (Barker *et al.*, 2004). Presumably, periodic subculturing contributes to this heterogeneity.

Genetic heterogeneity may also arise during continuous cultivation experiments as the result of spontaneous mutations. Information about which genes are possible targets for beneficial mutations is available from continuous cultivation experiments that are much longer than 'routine' cell physiology studies. Long-term evolution of *E. coli* in glucose-limited chemostats has been studied quite intensively during the last decade (Adams, 2004; Ferenci, 2008). As might be expected, mutations that increase glucose transport capabilities are common in glucose-limited chemostats (Helling *et al.*, 1987; Manch *et al.*, 1999;

Wick *et al.*, 2001, 2002). These mutations are observed in prolonged continuous cultivation experiments that exceed the number of generations necessary for cell physiology studies by at least an order of magnitude. Therefore, to study cell physiology properly in continuous culture, or any other cultivation system, it is important to find out how long a genetically uniform culture can be maintained.

Generally, pumping through five working volumes in a chemostat is assumed to be enough to reach steady state (50 h and seven generations at $D=0.1\text{ h}^{-1}$). The presence of a true steady state at this point has been questioned, based on how rapidly fitter clones may arise (Ferenci, 2008). Indeed, mutations in the stress-induced sigma factor *rpoS* have been detected in *E. coli* K-12 BW2952 cultures growing in glucose-limited chemostats at $D=0.1\text{ h}^{-1}$ after only 24–72 h (three to 10 generations) of cultivation (Notley-McRobb *et al.*, 2003). However, the appearance of *rpoS* mutations appears to be strain-dependent. None were detected in *E. coli* K-12 MG1655 after 96 h (14 generations) at $D=0.1\text{ h}^{-1}$ (King *et al.*, 2004), making it difficult to generalize about how long a genetically uniform culture of *E. coli* K-12 can be maintained. Moreover, it is plausible that MG1655 acquires mutations other than those in *rpoS* during glucose-limited continuous cultivation experiments.

Recent advances in DNA sequencing technologies (Mardis, 2008) have made it possible to routinely determine the full genome sequences of micro-organisms and to generate high-coverage datasets for analysing genetic diversity within communities (Barrick & Lenski, 2009). High-throughput (HT) DNA sequencing was used in the present work to examine genome stability and genetic heterogeneity during a short-term continuous cultivation experiment (A-stat, 20 generations of continuous cultivation) of *E. coli* K-12 MG1655. We found that *E. coli* K-12 MG1655 is suitable for studying cell physiology using glucose-limited A-stat experiments with a duration of up to 20 generations of continuous cultivation without interference from new, spontaneous mutations. However, we found that substantial genetic heterogeneity and mutational diversity existed in bacterial cultures from stock centres, which underscores the importance of using HT DNA sequencing to verify genome integrity in any experiment.

METHODS

Strains and preparation of stock culture. *E. coli* K-12 MG1655 [λ^- F⁻ *rph-1 Fmr^r*; Deutsche Sammlung von Mikroorganismen und Zellkulturen (DSMZ), DSM no. 18039] was used in all A-stat experiments. The strain ordered from DSMZ was originally obtained from the Coli Genetic Stock Center (CGSC) and has the collection number CGSC 6300. This strain was used for validation of consensus mutations and subpopulations. Additionally, *E. coli* K-12 MG1655 strain (reference no. C 438-01), obtained from Statens Serum Institute (SSI), was used for comparison of K-12 MG1655 strains from two different stock centres. This strain also originated from CGSC; however, SSI obtained the *E. coli* K-12 MG1655 strain through a collaborator, and therefore it is possible that this stock is a subculture of the original CGSC sample (Karen A. Krogfelt, personal communication).

The stock culture used to start the A-stat experiment was prepared by inoculating directly from the stab agar culture obtained from DSMZ into Luria–Bertani (LB) medium and cultivating aerobically until the late exponential growth phase (around 10 generations). The cells were then washed, suspended in defined minimal medium containing 1.2% (*v/v*) glycerol, divided into aliquots, lyophilized, and stored at $-80\text{ }^{\circ}\text{C}$. A single stock aliquot was used to inoculate each A-stat cultivation experiment.

Medium and cultivation conditions. A detailed description of the medium, cultivation conditions and growth characteristics in these A-stat experiments has been reported previously (Valgepea *et al.*, 2010). In short, defined minimal medium with 4.5 g α -D-glucose l^{-1} , a temperature of 37 $^{\circ}\text{C}$, pH 7, an agitation speed of 800 r.p.m. and aerobic conditions (air flow rate 150 ml min^{-1}) were used in all experiments. After the culture had been stabilized under chemostat conditions at $D=0.10\text{ h}^{-1}$ to achieve steady state, a continuous increase in D with an acceleration rate of 0.01 h^{-2} was applied.

Genomic DNA extraction. An aliquot of the lyophilized stock culture (4.2×10^6 cells) and two whole-population samples (not single colonies) acquired at $D=0.11\text{ h}^{-1}$ (8.4×10^9 cells) and 0.48 h^{-1} (3.0×10^9 cells) from one A-stat experiment were chosen for DNA extraction and subsequent HT DNA sequencing analysis. Genomic DNA for resequencing and mutation validation was extracted using the RTP Bacteria DNA Mini kit (Invitex) following the manufacturer's protocol.

Illumina whole-genome resequencing. Whole-genome resequencing was performed by GATC Biotech using an Illumina Genome Analyzer II instrument. A single-end library was prepared from each genomic DNA sample and sequenced using the manufacturer's standard protocols. FASTQ read files were generated by Sequencing Control software (version 2.6) with Real-time Analysis (version 1.6.32) and GA Pipeline (version 1.5.1). Raw read data have been deposited in the National Center for Biotechnology Information (NCBI) Sequence Read Archive (accession no. SRP006176).

Genome sequence data analysis. Sequencing reads were compared with the *E. coli* K-12 MG1655 reference genome (accession no. U00096.2) using the *breseq* analysis pipeline (Barrick *et al.*, 2009; Woods *et al.*, 2011) (version 1.00rc7). Source code for *breseq* is freely available online (<http://barricklab.org/twiki/bin/view/Lab/Tools/BacterialGenomeResequencing>). The online documentation describes the methods used to predict consensus point mutations, small indels, large deletions and new sequence junctions. Specific settings for this study are provided in Supplementary Methods.

Mutation validation with Sanger sequencing. Predicted mutations were validated by performing PCR followed by Sanger sequencing. Sanger sequencing was performed by the Estonian Biocentre using an Applied Biosystems 3730xl DNA analyser and the BigDye Terminator v3.1 Cycle Sequencing kit (Applied Biosystems). Subpopulations with base substitutions were confirmed by Sanger sequencing PCR products from mixed population samples (Supplementary Figs S1–S5). The Supplementary Methods fully describe the PCR protocol and subpopulation analysis.

RESULTS AND DISCUSSION

Mismatches from the *E. coli* K-12 MG1655 reference genome

The genome stability and genetic heterogeneity of *E. coli* K-12 MG1655 routinely used in our laboratory were studied

during 20 generations of continuous cultivation in a glucose-limited A-stat experiment. Fig. 1 illustrates the time-course of one A-stat experiment, showing when samples were collected for HT DNA sequencing.

Seven differences from the *E. coli* K-12 MG1655 reference genome (GenBank accession no. U00096.2) were found at a 100 % frequency in all three sequenced samples (Table 1). Most of these consensus mutations were single nucleotide polymorphisms (SNPs). In addition, two relatively large deletions were detected. First, an *IS1* was deleted from the regulatory region of *flhDC* (DNA-binding transcriptional dual regulator that controls gene expression of flagella genes). Second, a 111 bp deletion from the repetitive sequence region between genes *gltP* [glutamate and aspartate dicarboxylate/amino acid:cation symporter (DAACS)-family transporter] and *yjcO* (conserved protein) was found. Mutations that improve glucose uptake, for instance in *ptsG* of the glucose phosphotransferase system, or the stress-induced sigma factor *rpoS*, might be expected during continuous cultivation based on results in similar chemostat environments (Kinnersley *et al.*, 2009; Notley-McRobb & Ferenci, 1999a, b; Notley-McRobb *et al.*, 2003; Wick *et al.*, 2001, 2002). However, we did not detect the emergence of either of these mutations.

Detection of mutations in all samples could point to errors in the reference genome sequence as well as to problems of handling of cultures in stock centres. To address the latter possibility, we sequenced these regions in an *E. coli* K-12 MG1655 strain that was ordered from another stock centre (SSI). The presence of identical mutations in MG1655 strains of different origins would suggest errors in the reference genome, whereas variations in the mutations present would indicate problems in strain handling. We found that six out of seven mutations detected in the MG1655 strain obtained from the DSMZ collection (Table 1) were also present in the SSI strain. In addition, most of the consensus mutations found in the current study have been reported before in HT DNA sequencing studies of *E. coli* K-12 MG1655 strains acquired from other sources (Conrad *et al.*, 2009; Harris *et al.*, 2009; Lee & Palsson, 2010). Together, these observations suggest that most of the discrepancies are actually sequencing errors in the reference genome. On the other hand, our results also

demonstrate that the two *E. coli* K-12 MG1655 strains investigated were not exactly the same in different stock centres (only the SSI strain had the *IS1* insertion in the *flhDC* regulon). This observation highlights a problem that may arise during strain handling. The population bottleneck caused by picking a single colony before subculturing is particularly prone to fixing a new mutation in the resultant sample.

Search for evolution during the A-stat experiment

Next, we turned our attention to the dynamics of mutations that appeared to be polymorphic in the population, that is, only present in a subset of individuals. Using the HT DNA sequencing data with 111-fold average genome coverage we predicted mutations present in subpopulations (Methods, Table 2). Only a few of these appeared to be present in more than 5 % of the whole population by the end of the experiment, and all were present in fewer than 20 % of all samples (Supplementary Table S1). A problem in analysing subpopulations with a low frequency using HT DNA sequencing data is that one has to distinguish true subpopulations from false positives caused by sequencing errors with nontrivial biases. Hence, additional validation with Sanger sequencing was performed for high-scoring predictions (Methods, Supplementary Table S1). Three high-scoring subpopulations (*betA*, *cspH/cspG*, *glyA*) in which allele frequencies increased during the experiment were validated from the sample taken at $D=0.48 \text{ h}^{-1}$ (Supplementary Figs S1–S3). Two of the three mutations (*betA*, *cspH/cspG*) were also detected in the stock culture (Fig. 2). The only subpopulation that was not detected with HT DNA sequencing from the stock culture, and therefore might have arisen during the experiment, was an SNP in *glyA*. However, the presence of a *glyA* population in the stock culture was verified by colony screening (see below), proving that all of these subpopulations were also present in the stock culture at detectable frequencies.

To further confirm that the detected heterogeneity did not arise during the cultivation experiment or result from differences between stock culture aliquots, the occurrence of subpopulations in two additional A-stat experiments (started from separate aliquots of the same stock culture)

Table 1. Consensus mutations in all HT-sequenced samples

Gene(s) affected	Genome position	Mutation	Annotation	Function(s) of related gene(s)
<i>ylbE_1</i>	547 694	A→G	Pseudogene	Predicted protein
<i>ylbE_1</i>	547 835	+G	Pseudogene	Predicted protein
<i>flhD/uspC</i>	Δ1 976 527–1 977 302	<i>IS1</i> deletion	Intergenic	Subunit of flagella regulator (FlhD ₂ C ₂)/universal stress protein
<i>rrlD</i>	3 422 257–3 422 259	ATC→CAT	Non-coding	23S rRNA
<i>ppiCl/yjyFO</i>	3 957 957	C→T	Intergenic	Peptidyl-prolyl <i>cis-trans</i> isomerase C/conserved protein
<i>gltPl/yjcO</i>	4 294 291	T→C	Intergenic	Glutamate and aspartate DAACS transporter/conserved protein
<i>gltPl/yjcO</i>	Δ4 294 305–4 294 415	Δ111 bp	Intergenic	Glutamate and aspartate DAACS transporter/conserved protein

Table 2. Mutations present in subpopulations in the HT-sequenced samples

Experimentally validated subpopulations are shown. See Supplementary Table S1 for complete information about all high-scoring subpopulations predicted from the HT DNA sequencing data.

Gene(s) affected	Genome position*	Mutation	Annotation	Function(s) of related gene(s)
<i>yahE</i>	335 361	T→C	F71F (TTT→TTC)	Predicted protein
<i>dppD</i>	3 701 283	G→A	L197L (CTG→TTG)	ATP-binding component of the dipeptide ABC transporter
<i>cspH/cspG</i>	1 050 465	T→A	Intergenic	Stress protein, member of the CspA family/cold-shock protein
<i>glyA</i>	2 683 035	G→A	H165H (CAC→CAT)	Serine hydroxymethyltransferase
<i>betA</i>	326 446	C→T	G9D (GGT→GAT)	Choline dehydrogenase
<i>yadL</i>	152 081–152 084	IS5 insertion	Coding region	Gene of predicted chaperone–usher fimbrial operon
<i>flhD/uspC</i>	1 977 510–1 977 513	IS5 insertion	Intergenic	Subunit of flagella regulator (FlhD ₂ C ₂)/universal stress protein

*Positions of IS5 insertions give the target site nucleotides that were duplicated upon insertion of the new IS copy. Both new IS5 copies were inserted in the forward (+) orientation in the genome.

was investigated. If there was the same (reproducible) subpopulation distribution at the end of A-stat experiments, one could conclude that the mutations discovered were the consequence of selection acting on existing variation, i.e. the set of mutations already present in the stock culture at detectable levels. Indeed, it was found that all the subpopulations with SNPs that had increasing allele frequencies (*betA*, *cspH/cspG*, *glyA*) were reproducibly present in all three replicate A-stat experiments (Supplementary Figs S1–S3). This observation further supports the hypothesis that the above-mentioned subpopulations were already present in the stock culture. Therefore, we conclude that the current 20-generation continuous cultivation duration of *E. coli* K-12 MG1655 in the glucose-limited A-stat was short enough to avoid the emergence of new subpopulations, making it suitable for studying cell physiology and collecting quantitative data

for metabolic modelling without interference from new spontaneous mutations.

Heterogeneity of the stock culture

After confirming that the stock culture was not uniform, we further investigated the predicted subpopulations. The following subpopulations were predicted (frequencies ranging between 6.5 and 17.0% in stock culture) and validated: *dppD*, *allD*, *recB*, *yahE* (Supplementary Table S1). It was found that the putative mutations in *allD* and *recB* with low overall scores (see Supplementary Table S1 legend for description) were false positives (Supplementary Fig. S6), whereas high-scoring predictions in *dppD* and *yahE* were genuine (Supplementary Figs S4–S5). In addition, two IS-related mutations, namely IS5 insertions in the *flhD* regulon (*flhD/uspC*) and in *yadL*, were detected in the HT DNA

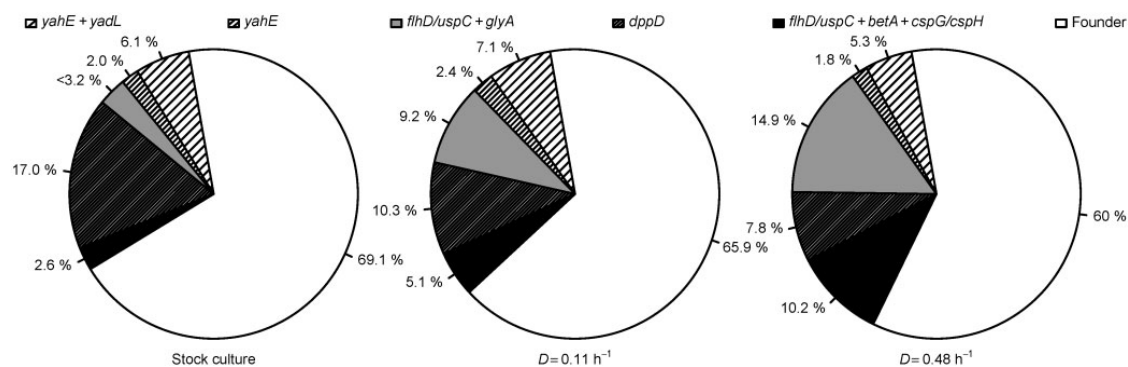


Fig. 2. Population heterogeneity in the *E. coli* K-12 MG1655 A-stat experiment. All the subpopulations shown here were verified with Sanger sequencing. In the stock culture, the mutation in *glyA* was not detected with HT DNA sequencing; therefore, the frequency for this sample was estimated from genome coverage at the position where a *glyA* mutation was detected in other samples. See Table 2 for details of mutations.

sequencing data (Supplementary Methods) and verified to have frequencies below 10% (data not shown).

We next investigated whether any of these mutations existed in combination in the same cells. Four mutations had increasing allele frequencies during the experiment: *betA*, *cspH/cspG*, *glyA* and *flhD/uspC*. IS elements in the regulatory region of *flhD* that lead to increased motility are common in *E. coli* (Barker *et al.*, 2004). Therefore, we screened colonies acquired from the stock culture used in the A-stat experiments for increased motility, as described by Barker *et al.* (2004). Out of the 42 investigated clones, four turned out to be motile and contained the IS5 insertion described above (data not shown). All the motile colonies were screened for *betA*, *cspH/cspG* or *glyA* mutations. Two clones had the *betA* and *cspH/cspG* SNPs, and the other two contained the *glyA* mutation (data not shown). Next, we hypothesized that mutations in *yahE* and *yadL* might also exist in the same subpopulation, as the frequencies of both alleles remained constant during the course of the experiment (Supplementary Table S1). Screening of stock culture clones revealed that all but one clone isolated with the mutation in *yahE* also contained the IS5 insertion in *yadL*.

The fact that the mutation in *yahE* was synonymous made it seem likely that the single *yahE* mutant clone without *yadL* harboured additional mutations. Therefore, we tested it for the presence of a *yhdJ/yhdU* (predicted methyltransferase/predicted membrane protein) mutation, because it was the only predicted mutation with considerable reliability (high overall score) and a change in allele frequency similar to that of *yahE* in the A-stat experiment (Supplementary Table S1). It turned out that the *yhdJ/yhdU* mutation was not present in the *yahE* clone (data not shown). However, given its low frequency in the population, we cannot exclude the possibility that an undetected mutation may be present in this genetic background. After resolving the genetic linkage between the most common mutations in the population, we conclude that roughly 31% of our stock culture contained at least one mutation relative to the majority genotype.

Conclusions

Our HT DNA sequencing data and detailed validation strategy enabled us to find all the mutations that appeared at appreciable frequencies during a continuous culture experiment. Sequencing of the stock culture gave, first of all, an overview of genetic heterogeneity in the stab agar received from one stock centre. We found that mutant genotypes made up roughly 31% of our stock culture grown directly from this stab. Since the stock culture was prepared by growth through only about 10 generations in our laboratory, it is unlikely that this heterogeneity was due to new spontaneous mutations. No subpopulation emerging from a single cell could reach a detectable frequency in this short time if growth was the only competitive process. Therefore, we conclude that the mutants had to be already

present in the stab agar at relatively high frequencies, due to either growth in the stab or heterogeneity in the original stock culture.

Even if our A-stat experiments had been initiated from single colonies, there would have been a large chance of picking a mutant clone. With three replicate experiments, there would have been a 67% chance that at least one replicate would have begun with a mutation relative to the majority genotype. This surprising heterogeneity shows the importance of sequencing the genome of a culture at the start of a microbial physiology study, especially if the phenotypic data from the experiment are to be used in comparisons between different research groups or for metabolic modelling.

Taking into account the apparent differences in evolvability between *E. coli* K-12 MG1655 used in the current study and *E. coli* K-12 BW2952, where the latter apparently has mutations available in the short term that are much more beneficial in this glucose-limited environment (Notley-McRobb *et al.*, 2003), it seems essential to evaluate the genome stability of every strain or species that is to be used for cell physiology studies in continuous cultures. Our results show that the current HT DNA sequencing technology is suitable and even necessary for accurate subpopulation analysis. We also demonstrate specifically that *E. coli* K-12 MG1655 has sufficient genome stability to be used in glucose-limited A-stat experiments with a duration of up to 20 generations of continuous cultivation for studying cell physiology, without mutations that occur in the course of adaptive evolution arising during the experiment.

ACKNOWLEDGEMENTS

This research was supported by EU project EU29994, Estonian targeted and science foundation projects SF0140090s08 and G8165, the US National Institutes of Health (R00 GM087550 to J.E.B.), and the US National Science Foundation BEACON Center for the Study of Evolution in Action (DBI-0939454 to J.E.B.).

REFERENCES

- Adams, J. (2004). Microbial evolution in laboratory environments. *Res Microbiol* **155**, 311–318.
- Barker, C. S., Prüss, B. M. & Matsumura, P. (2004). Increased motility of *Escherichia coli* by insertion sequence element integration into the regulatory region of the *flhD* operon. *J Bacteriol* **186**, 7529–7537.
- Barrick, J. E. & Lenski, R. E. (2009). Genome-wide mutational diversity in an evolving population of *Escherichia coli*. *Cold Spring Harb Symp Quant Biol* **74**, 119–129.
- Barrick, J. E., Yu, D. S., Yoon, S. H., Jeong, H., Oh, T. K., Schneider, D., Lenski, R. E. & Kim, J. F. (2009). Genome evolution and adaptation in a long-term experiment with *Escherichia coli*. *Nature* **461**, 1243–1247.
- Conrad, T. M., Joyce, A. R., Applebee, M. K., Barrett, C. L., Xie, B., Gao, Y. & Palsson, B. Ø. (2009). Whole-genome resequencing of *Escherichia coli* K-12 MG1655 undergoing short-term laboratory evolution in lactate minimal media reveals flexible selection of adaptive mutations. *Genome Biol* **10**, R118.

- Ferenci, T. (2008).** Bacterial physiology, regulation and mutational adaptation in a chemostat environment. *Adv Microb Physiol* **53**, 169–229.
- Harris, D. R., Pollock, S. V., Wood, E. A., Goiffon, R. J., Klingele, A. J., Cabot, E. L., Schackwitz, W., Martin, J., Eggington, J. & other authors (2009).** Directed evolution of ionizing radiation resistance in *Escherichia coli*. *J Bacteriol* **191**, 5240–5252.
- Helling, R. B., Vargas, C. N. & Adams, J. (1987).** Evolution of *Escherichia coli* during growth in a constant environment. *Genetics* **116**, 349–358.
- Jishage, M. & Ishihama, A. (1997).** Variation in RNA polymerase sigma subunit composition within different stocks of *Escherichia coli* W3110. *J Bacteriol* **179**, 959–963.
- King, T., Ishihama, A., Kori, A. & Ferenci, T. (2004).** A regulatory trade-off as a source of strain variation in the species *Escherichia coli*. *J Bacteriol* **186**, 5614–5620.
- Kinnersley, M. A., Holben, W. E. & Rosenzweig, F. (2009).** *E. unibius plurum*: genomic analysis of an experimentally evolved polymorphism in *Escherichia coli*. *PLoS Genet* **5**, e1000713.
- Lahtvee, P.-J., Adamberg, K., Arike, L., Nahku, R., Aller, K. & Vilu, R. (2011).** Multi-omics approach to study the growth efficiency and amino acid metabolism in *Lactococcus lactis* at various specific growth rates. *Microb Cell Fact* **10**, 12.
- Lee, D.-H. & Palsson, B. Ø. (2010).** Adaptive evolution of *Escherichia coli* K-12 MG1655 during growth on a nonnative carbon source, L-1,2-propanediol. *Appl Environ Microbiol* **76**, 4158–4168.
- Maharjan, R., Seeto, S., Notley-McRobb, L. & Ferenci, T. (2006).** Clonal adaptive radiation in a constant environment. *Science* **313**, 514–517.
- Manch, K., Notley-McRobb, L. & Ferenci, T. (1999).** Mutational adaptation of *Escherichia coli* to glucose limitation involves distinct evolutionary pathways in aerobic and oxygen-limited environments. *Genetics* **153**, 5–12.
- Mardis, E. R. (2008).** Next-generation DNA sequencing methods. *Annu Rev Genomics Hum Genet* **9**, 387–402.
- Monod, J. (1950).** La technique de culture continue, theorie et applications. *Ann Inst Pasteur (Paris)* **79**, 390–410.
- Naas, T., Blot, M., Fitch, W. M. & Arber, W. (1994).** Insertion sequence-related genetic variation in resting *Escherichia coli* K-12. *Genetics* **136**, 721–730.
- Naas, T., Blot, M., Fitch, W. M. & Arber, W. (1995).** Dynamics of IS-related genetic rearrangements in resting *Escherichia coli* K-12. *Mol Biol Evol* **12**, 198–207.
- Notley-McRobb, L. & Ferenci, T. (1999a).** Adaptive *mgl*-regulatory mutations and genetic diversity evolving in glucose-limited *Escherichia coli* populations. *Environ Microbiol* **1**, 33–43.
- Notley-McRobb, L. & Ferenci, T. (1999b).** The generation of multiple co-existing *mal*-regulatory mutations through polygenic evolution in glucose-limited populations of *Escherichia coli*. *Environ Microbiol* **1**, 45–52.
- Notley-McRobb, L., Seeto, S. & Ferenci, T. (2003).** The influence of cellular physiology on the initiation of mutational pathways in *Escherichia coli* populations. *Proc Biol Sci* **270**, 843–848.
- Novick, A. & Szilard, L. (1950a).** Description of the chemostat. *Science* **112**, 715–716.
- Novick, A. & Szilard, L. (1950b).** Experiments with the chemostat on spontaneous mutations of bacteria. *Proc Natl Acad Sci U S A* **36**, 708–719.
- Paalme, T., Kahru, A., Elken, R., Vanatalu, K., Tiismaa, K. & Vilu, R. (1995).** The computer-controlled continuous culture of *Escherichia coli* with smooth change of dilution rate. *J Microbiol Methods* **24**, 145–153.
- Soupepe, E., van Heeswijk, W. C., Plumbridge, J., Stewart, V., Bertenthal, D., Lee, H., Prasad, G., Paliy, O., Charennoppakul, P. & Kustu, S. (2003).** Physiological studies of *Escherichia coli* strain MG1655: growth defects and apparent cross-regulation of gene expression. *J Bacteriol* **185**, 5611–5626.
- Valgepea, K., Adamberg, K., Nahku, R., Lahtvee, P.-J., Arike, L. & Vilu, R. (2010).** Systems biology approach reveals that overflow metabolism of acetate in *Escherichia coli* is triggered by carbon catabolite repression of acetyl-CoA synthetase. *BMC Syst Biol* **4**, 166.
- Wick, L. M., Quadroni, M. & Egli, T. (2001).** Short- and long-term changes in proteome composition and kinetic properties in a culture of *Escherichia coli* during transition from glucose-excess to glucose-limited growth conditions in continuous culture and vice versa. *Environ Microbiol* **3**, 588–599.
- Wick, L. M., Weilenmann, H. & Egli, T. (2002).** The apparent clock-like evolution of *Escherichia coli* in glucose-limited chemostats is reproducible at large but not at small population sizes and can be explained with Monod kinetics. *Microbiology* **148**, 2889–2902.
- Woods, R. J., Barrick, J. E., Cooper, T. F., Shrestha, U., Kauth, M. R. & Lenski, R. E. (2011).** Second-order selection for evolvability in a large *Escherichia coli* population. *Science* **331**, 1433–1436.

Edited by: S. D. Bentley

RECENT DISSERTATIONS DEFENDED AT TUT
IN NATURAL AND EXACT SCIENCES

- B71 **Cecilia Sarmiento.** *Suppressors of RNA Silencing in Plants.* 2008.
- B72 **Vilja Mardla.** *Inhibition of Platelet Aggregation with Combination of Antiplatelet Agents.* 2008.
- B73 **Maie Bachmann.** *Effect of Modulated Microwave Radiation on Human Resting Electroencephalographic Signal.* 2008.
- B74 **Dan H÷ivonen.** *Terahertz Spectroscopy of Low-Dimensional Spin Systems.* 2008.
- B75 **Ly Villo.** *Stereoselective Chemoenzymatic Synthesis of Deoxy Sugar Esters Involving Candida antarctica Lipase B.* 2008.
- B76 **Johan Anton.** *Technology of Integrated Photoelasticity for Residual Stress Measurement in Glass Articles of Axisymmetric Shape.* 2008.
- B77 **Olga Volobujeva.** *SEM Study of Selenization of Different Thin Metallic Films.* 2008.
- B78 **Artur Jõgi.** *Synthesis of 4'-Substituted 2,3'-dideoxynucleoside Analogues.* 2008.
- B79 **Mario Kadastik.** *Doubly Charged Higgs Boson Decays and Implications on Neutrino Physics.* 2008.
- B80 **Fernando Pérez-Caballero.** *Carbon Aerogels from 5-Methylresorcinol-Formaldehyde Gels.* 2008.
- B81 **Sirje Vaask.** *The Comparability, Reproducibility and Validity of Estonian Food Consumption Surveys.* 2008.
- B82 **Anna Menaker.** *Electrosynthesized Conducting Polymers, Polypyrrole and Poly(3,4-ethylenedioxythiophene), for Molecular Imprinting.* 2009.
- B83 **Lauri Ilison.** *Solitons and Solitary Waves in Hierarchical Korteweg-de Vries Type Systems.* 2009.
- B84 **Kaia Ernits.** *Study of In₂S₃ and ZnS Thin Films Deposited by Ultrasonic Spray Pyrolysis and Chemical Deposition.* 2009.
- B85 **Veljo Sinivee.** *Portable Spectrometer for Ionizing Radiation "Gammamapper".* 2009.
- B86 **Jüri Virkepu.** *On Lagrange Formalism for Lie Theory and Operadic Harmonic Oscillator in Low Dimensions.* 2009.
- B87 **Marko Piirsoo.** *Deciphering Molecular Basis of Schwann Cell Development.* 2009.
- B88 **Kati Helmja.** *Determination of Phenolic Compounds and Their Antioxidative Capability in Plant Extracts.* 2010.
- B89 **Merike Sõmera.** *Sobemoviruses: Genomic Organization, Potential for Recombination and Necessity of P1 in Systemic Infection.* 2010.
- B90 **Kristjan Laes.** *Preparation and Impedance Spectroscopy of Hybrid Structures Based on CuIn₃Se₅ Photoabsorber.* 2010.
- B91 **Kristin Lippur.** *Asymmetric Synthesis of 2,2'-Bimorpholine and its 5,5'-Substituted Derivatives.* 2010.
- B92 **Merike Luman.** *Dialysis Dose and Nutrition Assessment by an Optical Method.* 2010.
- B93 **Mihhail Berezovski.** *Numerical Simulation of Wave Propagation in Heterogeneous and Microstructured Materials.* 2010.
- B94 **Tamara Aid-Pavlidis.** *Structure and Regulation of BDNF Gene.* 2010.
- B95 **Olga Bragina.** *The Role of Sonic Hedgehog Pathway in Neuro- and Tumorigenesis.* 2010.
- B96 **Merle Randrüüt.** *Wave Propagation in Microstructured Solids: Solitary and Periodic Waves.* 2010.
- B97 **Marju Laars.** *Asymmetric Organocatalytic Michael and Aldol Reactions Mediated by Cyclic Amines.* 2010.
- B98 **Maarja Grossberg.** *Optical Properties of Multinary Semiconductor Compounds for Photovoltaic Applications.* 2010.
- B99 **Alla Maloverjan.** *Vertebrate Homologues of Drosophila Fused Kinase and Their Role in Sonic Hedgehog Signalling Pathway.* 2010.
- B100 **Priit Pruunsild.** *Neuronal Activity-Dependent Transcription Factors and Regulation of Human BDNF Gene.* 2010.
- B101 **Tatjana Knjazeva.** *New Approaches in Capillary Electrophoresis for Separation and Study of Proteins.* 2011.
- B102 **Atanas Katerski.** *Chemical Composition of Sprayed Copper Indium Disulfide Films for Nanostructured Solar Cells.* 2011.
- B103 **Kristi Timmo.** *Formation of Properties of CuInSe₂ and Cu₂ZnSn(S,Se)₄ Monograin Powders Synthesized in Molten KI.* 2011.

- B104 **Kert Tamm.** *Wave Propagation and Interaction in Mindlin-Type Microstructured Solids: Numerical Simulation.* 2011.
- B105 **Adrian Popp.** *Ordovician Proetid Trilobites in Baltoscandia and Germany.* 2011.
- B106 **Ove Pärn.** *Sea Ice Deformation Events in the Gulf of Finland and Their Impact on Shipping.* 2011.
- B107 **Germo Väli.** *Numerical Experiments on Matter Transport in the Baltic Sea.* 2011.
- B108 **Andrus Seiman.** *Point-of-Care Analyser Based on Capillary Electrophoresis.* 2011.
- B109 **Olga Katargina.** *Tick-Borne Pathogens Circulating in Estonia (Tick-Borne Encephalitis Virus, Anaplasma phagocytophilum, Babesia Species): Their Prevalence and Genetic Characterization.* 2011.
- B110 **Ingrid Sumeri.** *The Study of Probiotic Bacteria in Human Gastrointestinal Tract Simulator.* 2011.
- B111 **Kairit Zovo.** *Functional Characterization of Cellular Copper Proteome.* 2011.
- B112 **Natalja Makarytsheva.** *Analysis of Organic Species in Sediments and Soil by High Performance Separation Methods.* 2011.
- B113 **Monika Mortimer.** *Evaluation of the Biological Effects of Engineered Nanoparticles on Unicellular Pro- and Eukaryotic Organisms.* 2011.
- B114 **Kersti Tepp.** *Molecular System Bioenergetics of Cardiac Cells: Quantitative Analysis of Structure-Function Relationship.* 2011.
- B115 **Anna-Liisa Peikolainen.** *Organic Aerogels Based on 5-Methylresorcinol.* 2011.
- B116 **Leeli Amon.** *Palaeoecological Reconstruction of Late-Glacial Vegetation Dynamics in Eastern Baltic Area: A View Based on Plant Macrofossil Analysis.* 2011.
- B117 **Tanel Peets.** *Dispersion Analysis of Wave Motion in Microstructured Solids.* 2011.
- B118 **Liina Kaupmees.** *Selenization of Molybdenum as Contact Material in Solar Cells.* 2011.
- B119 **Allan Olsper.** *Properties of VPg and Coat Protein of Sobemoviruses.* 2011.
- B120 **Kadri Koppel.** *Food Category Appraisal Using Sensory Methods.* 2011.
- B121 **Jelena Gorbatšova.** *Development of Methods for CE Analysis of Plant Phenolics and Vitamins.* 2011.
- B122 **Karin Viipsi.** *Impact of EDTA and Humic Substances on the Removal of Cd and Zn from Aqueous Solutions by Apatite.* 2012.
- B123 **David W. Schryer.** *Metabolic Flux Analysis of Compartmentalized Systems using Dynamic Isotopologue Modeling.* 2012.
- B124 **Ardo Illaste.** *Analysis of Molecular Movements in Cardiac Myocytes.* 2012.
- B125 **Indrek Reile.** *3-Alkylcyclopentane-1,2-Diones in Asymmetric Oxidation and Alkylation Reactions.* 2012.
- B126 **Tatjana Tamberg.** *Some Classes of Finite 2-Groups and Their Endomorphism Semigroups.* 2012.
- B127 **Taavi Liblik.** *Variability of Thermohaline Structure in the Gulf of Finland in Summer.* 2012.
- B128 **Priidik Lagemaa.** *Operational Forecasting in Estonian Marine Waters.* 2012.
- B129 **Andrei Errapart.** *Photoelastic Tomography in Linear and Non-linear Approximation.* 2012.
- B130 **Külliki Krabbi.** *Biochemical Diagnosis of Classical Galactosemia and Mucopolysaccharidoses in Estonia.* 2012.
- B131 **Kristel Kaseleht.** *Identification of Aroma Compounds in Food using SPME-GC/MS and GC-Olfactometry.* 2012.
- B132 **Kristel Kodar.** *Immunoglobulin G Glycosylation Profiling in Patients with Gastric Cancer.* 2012.
- B133 **Kai Rosin.** *Solar Radiation and Wind as Agents of the Formation of the Radiation Regime in Water Bodies.* 2012.
- B134 **Ann Tiiman.** *Interactions of Alzheimer's Amyloid-Beta Peptides with Zn(II) and Cu(II) Ions.* 2012.
- B135 **Olga Gavrilova.** *Application and Elaboration of Accounting Approaches for Sustainable Development.* 2012.
- B136 **Olesja Bondarenko.** *Development of Bacterial Biosensors and Human Stem Cell-Based In Vitro Assays for the Toxicological Profiling of Synthetic Nanoparticles.* 2012.